

Percolation in the Poisson Boolean model with convex grains



Inaugural-Dissertation

zur

Erlangung des Doktorgrades

der Mathematisch-Naturwissenschaftlichen Fakultät

der Universität zu Köln

vorgelegt von

Marilyn Korfhage

(geb. Düsterbeck)

aus Köln

angenommen im Jahr 2025

Begutachtung:

Prof. Dr. Peter Mörters

JProf. Dr. Anna Gusakova

Abstract

In this thesis we study the Poisson Boolean model where the grains are random convex bodies with a rotation-invariant distribution, i.e. we have a Poisson Boolean model where the locations of the vertices are distributed in \mathbb{R}^d according to a Poisson process. The vertices are then given by i.i.d. copies of a random convex body attached to the individual locations. The random convex bodies are called the grains of the vertices.

We say that a grain distribution is *dense* if the union of the grains covers the entire space and *robust* if the union of the grains has an unbounded connected component irrespective of the intensity of the underlying Poisson process. If the grains are balls of random radius, then density and robustness are equivalent, but in general this is not the case. In this work we are dealing with the Poisson Boolean model where convex bodies are rotation-invariant distributed and have regularly varying diameters with indices $-\alpha_1 \geq \dots \geq -\alpha_d$ where $\alpha_k > 0$ for all $k \in \{1, \dots, d\}$. We show in this model that in any dimension $d \geq 2$ there are parameter regimes for the indices such that the grain distribution is robust but not dense. We give on the one hand some universal criteria for density and robustness of a grain distribution and on the other hand also some special criteria on the grain distribution being robust. In addition to that we prove non-robustness for a generalisation of a 2-dimensional ellipses model.

We further investigate the behaviour of the chemical distance in the robust but not dense regime. We will see in this work that the universal criterium for a grain distribution being robust is the existence of some $k \in \{1, \dots, d\}$ such that $\alpha_k < \min\{2k, d\}$. To avoid that this connected component covers the entire \mathbb{R}^d almost surely we also require $\alpha_k > k$ for all $k \in \{1, \dots, d\}$. We show that under these assumptions, the chemical distance of two far apart vertices \mathbf{x} and \mathbf{y} behaves like $c \log \log |x - y|$ as $|x - y| \rightarrow \infty$, with an explicit and very surprising constant c that depends only on the model parameters. We furthermore show that if there exists k such that $\alpha_k \leq k$, the chemical distance is smaller than $c \log \log |x - y|$ for all $c > 0$ and that if $\alpha_k \geq \min\{2k, d\}$ for all k , the chemical distance is bigger than $c \log \log |x - y|$ for all $c > 0$.

Contents

1. Introduction	1
1.1 Motivation	1
1.1.1 Spatial random graphs	2
1.1.2 Properties of geometric random graphs	5
1.1.3 Summary of established results	8
1.2 Structure	12
2. Modell and Behaviour	15
2.1 Framework and behaviours of the model	15
2.1.1 Definitions and result on total covering of the space . . .	15
2.1.2 Results on robustness and non-robustness	20
2.2 Proofs on the behaviour of the model	21
2.2.1 Criteria for density	22
2.2.2 Universal criteria for robustness	24
2.2.3 Specific criteria for robustness	31
2.2.4 Specific criteria for non-robustness	33
3. Chemical distance	54
3.1 Main results on the chemical distance	54
3.2 Proof of the lower bound	56
3.3 Proof of the upper bound	62
4. Examples	81
5. Possible future work	89
A. Further calculation	92
A.1 Existence of a box inside a convex body K	92
A.2 Results are independent of the choice of diameters	97
A.3 Proof of the inequality of (2.8)	99

A.4	Intersection probability for $\mathcal{A}_1(\mathbf{0}, \mathbf{y})$ - $\mathcal{A}_5(\mathbf{0}, \mathbf{y})$	102
A.5	Intersection probability for $\mathcal{A}_6(\mathbf{0}, \mathbf{y})$ - $\mathcal{A}_8(\mathbf{0}, \mathbf{y})$	104
A.6	Continuity of the percolation probability	106
B. List of Notation		108
Bibliography		111

Chapter 1

Introduction

1.1 Motivation

The area of networks and random graphs has a lot of real-world applications and is an important topic in research. For us, graphs consist of vertices and edges between pairs of vertices, representing a connection between the pairs. This simple structure allows for the modelling of many complex systems. In social networks like Facebook, the vertices represent the users and edges their friendship. Another example is the structure of the world wide web. For that the vertices are the websites and edges represents the links between them. In this example one could add more information by introducing directed edges. A directed edge then goes for example from one website to another if it includes a hyperlink to the other page. If both sites link to each other we have an edge which is undirected. Beyond the internet, networks also play a role in other fields. In neurobiology, for instance, vertices are the neurons and edges are given between two neurons if they interact directly. Graphs can also be used to study infection chains, where vertices are the infected individuals and edges indicate disease transmission. In such example one have on the one hand direction of an edge, i.e. if one person has infected the other, and on the other hand we can depict the chronological sequences of disease transmission by a time component. A further example are air-traffic routes, where vertices are the countries and two vertices are connected by an edge if and only if there exists a direct flight between these two counties.

We see that various types of graphs can be studied: spatially embedded graphs (e.g. countries and corresponding flights) and non-spatial graphs (e.g. world wide web with links). But we can also add some temporal developments

in a graph, such as the spread of diseases. Alternatively, stationary networks without a time component can be analysed.

In this thesis, we are interested in spatially embedded graphs that do not involve a temporal component and have no direction on the edges, i.e. we just know if two vertices are connected or not and have no additional information about that. Therefore, we focus next only on examples with these characteristics before proceeding to interesting properties and some results related to them.

1.1.1 Spatial random graphs

In this thesis we are interested in graphs $\mathcal{G} := (\mathcal{V}, \mathcal{E})$ with \mathcal{V} is the vertex set and \mathcal{E} is the edge set which is a subset of (unordered) pairs of vertices. We use the convention that $(u, v) \in \mathcal{E}$, that the vertices $u, v \in \mathcal{V}$ are connected via an (unoriented) edge. We are interested in spatially embedded graphs. For that we can for example look at $\mathcal{V} \subset \mathbb{Z}^d$, i.e. looking at lattice graphs or $\mathcal{V} \subset \mathbb{R}^d$, i.e. some continuum percolation models. In the following we give some example.

Bernoulli bond percolation

One model, which was often studied and is of interest is $\mathcal{G} = (\mathcal{V}, \mathcal{E})$ with $\mathcal{V} = \mathbb{Z}^d$ for $d \geq 1$. In this model we say that two vertices are neighbours if and only if the Euclidean distance between them is 1 and first start with all edges between the neighbours. Looking now at two vertices that are neighbours, we fix $p \in (0, 1)$ as a retention parameter and have a coin flip for every edge so that we keep independent from each other edges an edge with probability p and remove it with probability $1 - p$. This model was first introduced by Broadbent and Hammersley in [6] and is called *Bernoulli bond percolation*; as edges are also referred to in this model as bonds and we have for every edge an i.i.d. Bernoulli random variable with Parameter p that decides whether we keep or remove it. If we keep an edge we say that this edge is open. One can find an extensive introduction to this model in the book of Grimmett [29].

The Bernoulli bond percolation model is a discrete model where, as described, positions of the vertices are given deterministically as the elements of \mathbb{Z}^d . It is a model with limitations that make it less than ideal for modelling phenomena where more randomness is present. For other examples like chains of infections, neuronal networks and a lot of more, it is important to use ad-

ditional of randomness in space that place vertices not on lattices but in a more flexible way. For this, one can look at continuum models that allow to have vertices with locations in \mathbb{R}^d like in the random connection model or the Poisson Boolean model in \mathbb{R}^d . Both models have been frequently analysed and we briefly introduce them here.

Stationary marked random connection model in \mathbb{R}^d

For the *random connection model* we use a point process that places points randomly on a measurable space $(\mathbb{X}, \mathcal{B})$, where \mathbb{X} is a complete separable metric space and \mathcal{B} is its Borel- σ -algebra. We focus here on the models which are generated via a Poisson point process ξ with a σ -finite intensity measure ν . A *Poisson point process* with intensity measure ν satisfies the following properties for all sets $A, A_1, \dots, A_n \in \mathcal{X}$ and $n \in \mathbb{N}$:

- $\xi(A)$ is Poisson distributed with parameter $\nu(A)$,
- if the sets A_1, \dots, A_n are pairwise disjoint, then $\xi(A_1), \dots, \xi(A_n)$ are independent.

These properties are discussed for instance in the book of Last and Penrose [40].

To define connections between points $x, y \in \xi$, we use a connection function, which is a measurable and symmetric function $\zeta : \mathbb{X} \times \mathbb{X} \rightarrow [0, 1]$. Given such a function, an edge between x and y is placed with probability $\zeta(x, y)$. This type of model has been studied for example in [42, 9], while the general framework was first introduced by Penrose [47].

Since the general random connection model includes a broad class of processes, we focus on a particular subclass: the *stationary marked random connection model in \mathbb{R}^d* driven by a spatial Poisson point process, which is for example described in the work of Chebunin and Last [9].

In particular, we are interested in the case where \mathbb{R}^d is the space for the locations of the vertices and the connection structure depends on additional marks. In this setting, we consider therefore a product space $\mathbb{X} = \mathbb{R}^d \times \mathbb{M}$, where \mathbb{M} denotes the mark space, and each point in the process is assigned a mark in \mathbb{M} . The intensity measure ν is then given by $u\lambda \otimes \mu$, where $u > 0$, λ is the d -dimensional Lebesgue measure on \mathbb{R}^d , and μ is a probability measure on \mathbb{M} . This construction yields a stationary random connection model, as the intensity of the points in the process is a multiple of the Lebesgue measure

(see e.g. [40, 9]). We therefore have that the process fulfils

$$T_x \xi \stackrel{d}{=} \xi,$$

for T_x a translation by $x \in \mathbb{R}^d$, i.e. the distribution of the process does not change under translations (cf. [40]). We also have that this kind of process is ergodic, i.e. the process is degenerate on translation invariant measurable sets (see e.g. [40, 9]).

In this thesis the main interest is on the Poisson Boolean model which is a special case of the stationary marked random connection model. The marks will be the before mentioned grains.

Poisson Boolean model in \mathbb{R}^d

The *Poisson Boolean model* in \mathbb{R}^d is studied in many works. We start with a homogeneous Poisson Point process \mathcal{P} in \mathbb{R}^d . For every $x \in \mathcal{P}$ we want to attach in some \tilde{C}_x , an i.i.d. copy of a random mark $C \subset \mathbb{R}^d$, which we call the grain at x , and shift it by x , i.e.

$$C_x := x + \tilde{C}_x.$$

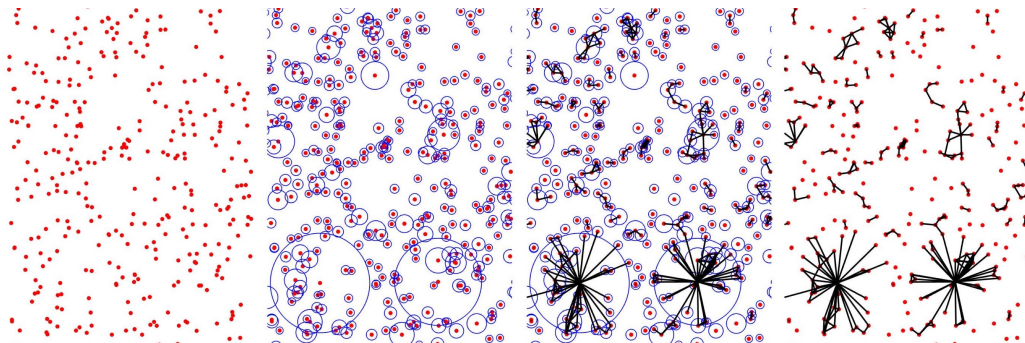
There are several studies of the Poisson Boolean model, see for example the work of Meester and Roy [45] for an introduction, or Hug et al. [36]. Note that the underlying point process has intensity measure $u\lambda$ with $u > 0$ and again λ is the d -dimensional Lebesgue measure.

Let C be a random or deterministic ball, i.e. we have a random or fixed radius and the corresponding ball has its center in the origin. \tilde{C}_x is then an i.i.d. copy of C and C_x is a ball centered in x . This choice of grains is the typical model that has been studied in different works [31, 45, 40, 22].

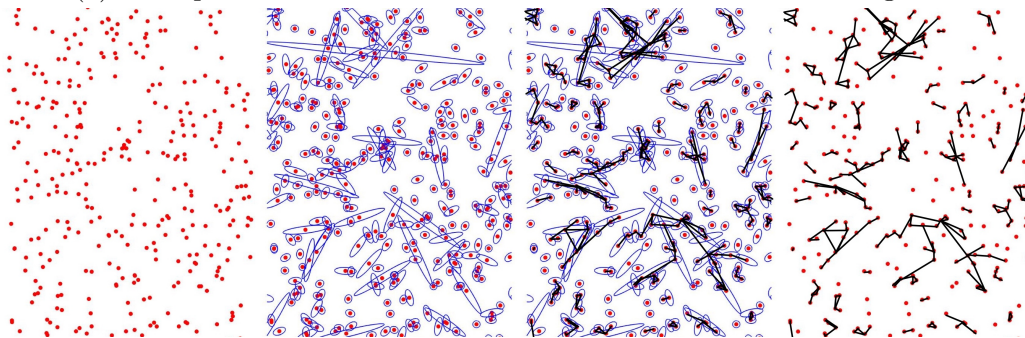
Looking now at the case $d = 2$ and letting C be an ellipse with heavy tailed distributed major axis and a fixed minor axis with length one, we get the model which was studied in [53, 34]. Related, one can also consider “sticks” instead of ellipses. Two works on these are [49, 7]. We also mention some work with more general shapes, namely general convex shapes, as in [50, 23].

Note that depending on the literature and the object of interest in the Poisson Boolean model, one can find the name *Booelan model* when focusing on the covering of the process, i.e. the union of the grains (see e.g. [45, 40, 41]) or the *Gilbert graph* associated to the Boolean model (see e.g. [20, 16, 40, 48]). For the Gilbert graph, the vertices are given via the points driven by the

Poisson point processes including its grains. The grains are relevant for the connection probability, and we say that two vertices are connected by an edge if and only if the corresponding grains are intersecting, but then do not affect the resulting graph otherwise. An illustration of the Boolean model including the corresponding graph can be seen in Figure 1.1.



(a) Example in \mathbb{R}^2 for the Poisson Boolean model with balls as grains.



(b) Example in \mathbb{R}^2 for the Poisson Boolean model with ellipses as grains.

Figure 1.1: Example in \mathbb{R}^2 for the Poisson Boolean model with convex grains. From left to right: Points placed by the Poisson point process, covering of the process by the random marks, edges constructed via the corresponding marks and on the right side the Gilbert graph.

1.1.2 Properties of geometric random graphs

After introducing some examples for spatially embedded graphs, we provide some definitions and corresponding motivations in order to describe the behaviour and properties of the graphs.

Percolation The concept of *percolation* is interesting for example in theory of probability and physics and has a lot of real world connections. One can observe percolation in the real world for example when we look at the spread of a fire in a forest and look at the event that when the fire starts from one side of the forest that it reaches the other side of it. The same principle is

seen when looking at a big stone which is porose, when dropping water on it and looking at the event that the stone gets wet in the middle resp. the water percolates through the stone so that the other side of it is wet. This kind of phenomena, i.e. having some “path” that goes from one side of a medium to another, is called percolation. Both examples and more can be found in the book of Grimmett [29]

If we want to formalise the concept of percolation, a natural concept in graph theory is to ask whether there exists an infinite cluster, that is, whether there a self avoiding infinite path can be found. To answer this question, we first have to define a path. We already established that two vertices $x, y \in \mathcal{V}$ are connected (directly) if $(x, y) \in \mathcal{E}$, that is the edge (x, y) exists. We denote this by $x \sim y$.

We say that a *path* between x and y exists if and only if there exist vertices $x_1, x_2, \dots, x_n \in \mathcal{V}$ such that $x \sim x_1$, $x_i \sim x_{i+1}$ for $i \in \{1, \dots, n-1\}$, and $x_n \sim y$, with $n \in \mathbb{N}$. More precisely we say there exists a path of length n that connects x and y . We denote this by $x \overset{n}{\sim} y$. If there exists a path of infinite length somewhere in the graph, for which none of the vertices appear more than once, we say that the model percolates. In the literature, this is also often referred to as the model being supercritical or having a supercritical phase. When all paths are finite, the terminology subcritical or subcritical phase (cf. [45, 29]) is used.

When studying the Poisson Boolean model, percolation can also be understood in terms of coverage, rather than in terms of the graph. In this case, we ask whether an unbounded connected component exists, where a connected component is defined as a maximal union of intersecting grains.

Once we know that the model percolates, we can further study the percolation probability, which is the probability that a point of the process lies in the unbounded connected component or in the infinite cluster, which is the same as asking if the vertex is connected to an infinite path. This probability typically depends on some of the model parameters. Similarly the existence of an unbounded connected component or infinite path itself also depends on these parameters. In the case of Bernoulli bond percolation, for example, it depends on the retention probability p and the dimension d . Similarly, for the Poisson Boolean model, both the dimension and the choice of grain distributions play a crucial role.

Beyond the question of the existence of an unbounded connected components, we are also interested in whether the unbounded connected component

(or path) is, in some sense, trivial or non-trivial. For instance, we ask whether all vertices are connected to each other or in terms of coverage if the entire space is covered almost surely. In addition to that it is also interesting to look at the uniqueness of such an unbounded connected component resp. infinite cluster.

Looking at the triviality of the unbounded connected component, i.e. whether all vertices are connected or the entire space is covered, the question is also closely related to the degree of a typical vertex. If the grains of the vertices are for example of infinite size in expectation in the Poisson Boolean model, this leads to a total covering of space and all points being connected to each other, so the degree becomes infinite. Such a setting is generally not of interest, as it does not realistically model connectivity observed in real-world situations. We are therefore more interested in non-trivial cases where such full connectivity or complete coverage does not occur.

Chemical distance A key topic in percolation theory and, more broadly, the study of geometrically embedded random graphs is the relationship between the Euclidean distance of two points and their graph distance, commonly referred to as the chemical distance. The chemical distance is defined as the length of the minimal path connecting two vertices. The chemical distance is not only an interesting concept in theory, but also a relevant measure in real-world situations. First, let us give some examples in non-spatial graphs that show why the minimum length of a path connecting two nodes might be interesting. Consider a graph in which vertices are represented as actors and an edge exists between them if they have appeared in the same film. The so-called Kevin Bacon number indicates the minimum number of edges connecting an actor to Kevin Bacon. A similar concept is the Erdős number, where mathematicians are connected by an edge if they have co-authored a paper. Since Paul Erdős wrote over 1500 papers and had more than 500 co-authors, the Erdős number serves as an equivalent to the Kevin Bacon number in this academic collaboration graph. Both examples can be found in the book of Durrett [13] and are examples for the observation of the *small-world* effect that was described in the social experiment that was of interest for Milgram. He looked at the question of how many intermediaries one needs so that two randomly chosen Americans can get in touch with each other. Surprisingly this number was on average equal five (cf. [46]).

It is of course also possible to embed both examples spatially if we use

the birthplace or similar as the location for the individuals. Another example is the spread of diseases, which has become a highly relevant topic in recent years. Here, the chemical distance can describe how many transmission steps are needed for a disease to spread from one side of the world to the other. Looking now at the chemical distance in percolation theory, we have that this is an interesting property when there exists an infinite path or an unbounded connected component. For that, when points belong to the unbounded connected component and are sufficiently far apart in Euclidean space, the aim is to understand how the Euclidean distance of these points affects in the chemical distance. One can observe different type of behaviours. There exist models in which the chemical distance is of linear order of the Euclidean distance. One can also study models where distance scales as a power of the logarithm (cf. [4]) or even as an iterated logarithm of the Euclidean distance. When the latter occurs, the graph is said to be *ultrasmall*. This phenomenon has been observed, for example, in geometric random graphs with long edges and scale-free degree distribution as in the work of Gracar et al. [24].

Besides the results concerning some Poisson Boolean models and the Bernoulli bond percolation there exist a lot of other works about chemical distance. There is research about chemical distances extended to models incorporating long-range interactions, such as random interlacements (Černý and Popov [8]), its vacant set, and the Gaussian free field (Drewitz et al. [14]).

In the following we focus on the models from above and summarise some results.

1.1.3 Summary of established results

We start with the Bernoulli bond percolation and summarise some important results for it which can be found for example in [29]. For this model it is known that there exists for every dimension $d \geq 2$ a critical retention parameter $p_c(d) \in (0, 1)$ such that the model is supercritical if $p > p_c(d)$ and subcritical if $p < p_c(d)$. For $d = 2$ it is known that $p_c(2) = \frac{1}{2}$. For all other dimensions $d > 2$, the exact value of $p_c(d)$ is not known. There exists inequalities and asymptotic estimates for $p_c(d)$ for large dimensions. It is known for example that $p_c(d) \geq \frac{1}{2d-1}$ and $p_c(d) \sim \frac{1}{2d}$ (cf. [29]).

Let us now have a closer look at the percolation probability. There are a few results and conjectures concerning its behaviour for p close to $p_c(d)$ with $p > p_c(d)$. It is conjectured that there exists a critical exponent β , depending on the dimension, such that the percolation probability behaves

like $(p - p_c(d))^\beta$. For d larger than 19, this has already been confirmed in the work by Hara and Slade in [33] for $\beta = 1$. For small dimensions the question remains open. More results on the critical percolation probability can be also found in for example [21]. It is also known that the percolation probability is continuous for $p > p_c(d)$, as shown in the work of Aizenman and Pisztora [1]. Moreover it is proven in the supercritical phase that the infinite cluster is unique, which can be also found in [1].

For the chemical distance in Bernoulli bond percolation in the supercritical regime, it is known that it grows linearly with the Euclidean distance (cf. [2]). Further results concerning the chemical distance can be found in [18, 19, 11].

To conclude, note that instead of Bernoulli bond percolation, where edges are removed with probability $1 - p$ and retained with probability p , one may also consider Bernoulli site percolation, where the retention parameter p determines whether a vertex is retained or removed. Corresponding results have also been established in that context. Some works and introduction on the Bernoulli bond percolation can be found in [29, 10, 21].

We state next a few results on random connection models driven by a Poisson point process in \mathbb{R}^d . Chebunin and Last show in [9] that under certain condition the unbounded connected component, if it exists, is unique. The relevant condition is irreducibility, which states that the probability that any two vertices $x, y \in \xi$ are connected is strictly positive.

There is also research by Last et al. [42], where general properties of functions of marked random connection models driven by a Poisson point process are studied. Here, “marked” includes also the setting of the stationary marked random connection model, as it only refers to the random connection modes where each vertex is assigned a random mark from some mark space.

There is also a work by Gracar et al. [28], where a phase transition for percolation in the weight-dependent random connection models is studied. The connection probability between two vertices depends in their model on weights of the vertices as well as on their spatial distance. They identify conditions depending on the model parameters so that a phase transition occurs, i.e. a nontrivial critical intensity is given.

Further contribution is the work of Meester et al. [44], where conditions are provided under which one can determine the behaviour of the critical intensity of the Poisson point process as $d \rightarrow \infty$ for the random connection model.

There are certainly many more results that could be mentioned here. How-

ever, each of them requires specific additional assumptions, and no general results can be stated for the stationary marked random connection model driven by a Poisson point process with respect to the percolation probability and the chemical distance, as the behaviour of the models can vary significantly. This will become evident in the following part, where we turn to various results concerning the Poisson Boolean model.

Finally, we present therefore results for the Poisson Boolean model with various choices of grains. This not only illustrates how differently the models behave depending on the type of grains one chooses, but also provides the motivation for the topic of this thesis.

We start here with the work of Gou  r   where he looks at the set K as the grain which is compact, convex, symmetric, and a subset of \mathbb{R}^d . In addition to that he assumes that the Lebesgue measure of K is equal 1 (see [23]). He studies the asymptotic behaviour of the percolation probability and the critical intensity in two different settings. One of the settings considers attaching convex bodies to the points of a point process, where the bodies are scaled by a factor of $1/2$. In this context, it is shown that the percolation probability for all λ as the underlying intensity, converges as $d \rightarrow \infty$ to the survival probability of a Galton–Watson process with $\text{Poisson}(\lambda)$ offspring distribution. Furthermore, it is proven that the critical intensity converges to 1. In the second setting, the scaling factor of the convex body is chosen randomly from two values. One of the scaling factors is a parameter $\rho \in (1, 2)$. Depending on ρ , the intensity λ of the Poisson point process is chosen, where λ is also a function of a further parameter, namely β . For $d \rightarrow \infty$, the asymptotic behaviour of the percolation probability and the critical intensity is then established depending on β and ρ . For further details on the second setting see [23].

In addition to that there exists a result on the critical intensity depending on the shape of the convex body. Roy showed in [50] that for the Poisson Boolean model the critical intensity with convex shapes of volume one is minimal when using triangles or regular polytopes; for all other shapes, the critical intensity is higher.

We now look at so called stick percolation. As mentioned previously, the works [49, 7] deal with this model, where Roy [49] treats the 2-dimensional case and Broman [7] deals with the more general case $d \geq 2$. In [49], bounded sticks, i.e. lines through a vertex of bounded length are studied, which all are uniformly rotated. Specifically, the critical intensity with respect to the

percolation probability is investigated and it is shown to coincide with other terms of criticality, such as the one where the expected number of sticks in the cluster of the origin is infinite. In [7], sticks of length L and width 1 are considered. The asymptotic behaviour of the critical intensity as $L \rightarrow \infty$ is studied. Two different distributions of the rotation of the stick are considered, including uniform rotation. In both cases, boundaries for the critical intensity is given which shows that it is non-trivial (bigger than zero) and finite.

We now look at the classical case, i.e. with balls as grains. In this model we first consider the existence of an unbounded connected component. It is well known that such a component exists the expected volume of the ball is infinite (cf. [31, 45, 22]). It is also known that this unbounded connected component almost surely covers the whole space \mathbb{R}^d . Due to [9] it is clear that this is unique as well for the choice of all other grains, where irreducibility is satisfied, as Poisson Boolean models with grains are also stationary marked random connection models. It is also known that the percolation probability is continuous for $u \neq u_c$ as u is the intensity of the underlying point process and u_c is the critical intensity. The proof of it can be found in [45, 51].

Considering the critical intensity of the Poisson Boolean model, one can find a result for $d = 2$ with constant radius (radius equal to one) in the book of Meester and Roy [45]. There, a lower and an upper bound for the critical intensity are proven, which implies that it is neither trivial (equals zero) nor infinite. For $d \geq 2$ and bounded radii, it is shown in [45] that the critical intensity is non-trivial and finite. From this we can surmise that the same holds for arbitrary radius distributions with finite d th moment of the radius. Hence, a supercritical phase exists. However, more general conditions or an explicit formula for the critical intensity are not known.

We now consider ellipses percolation. Teixeira and Ungaretti introduced this model in [53]. There and in the work of Hilário and Ungaretti [34] several fundamental properties of this model are identified. On the one hand, they showed under which conditions the 2-dimensional ellipse model, with a fixed minor axis and a heavy-tailed distributed major axis covers the entire space [53]. This is the case, as in the model with balls as grains, when the expected volume of the grain is infinite. Furthermore, they identify a parameter regime for the tail exponent α in which an unbounded connected component exists that does not cover the entire \mathbb{R}^d . This occurs, except in boundary cases, when the tail parameter is such that the first moment of the volume is finite, but the second moment is infinite, i.e. $\alpha \in (1, 2)$. For $\alpha \geq 2$, the model has a subcritical

phase, so there exists some non-trivial critical intensity such that the model does not percolate if the intensity is smaller than this critical one. These results can be found in [53]. In [34], the chemical distance is analysed. The authors show that the chemical distance exhibits double logarithmic behaviour with respect to euclidean distance. Although the exact constant in front of the logarithmic term is not given, they give upper and lower bounds for it, which depend on the tail parameter α . In this work, we confirm the log log behaviour of the chemical distance and determine the precise value of the corresponding constant.

These results on the Poisson Boolean model, especially the last two models, are the main motivation for this thesis. In the classical model with balls as grains, it is known that total covering of the space and the existence of an unbounded connected component independently from the intensity u are equivalent. However, in the 2-dimensional case with ellipses as grains, this equivalence does not hold. There exists a regime for the tail parameter α in which an unbounded connected component exists independently of the intensity u of the Poisson point process, while the space is not almost surely covered. We therefore ask ourselves whether we can find grain distributions in all dimensions $d \geq 2$ such that this property of the unbounded connected component holds, i.e. such that this is not equivalent to total covering occurs. For that, one has to make clear what is required for the grain so that one can find such distributions. We know that the radius of a ball describes the grain completely in the sense that having the center, the distance from this to the boundary of the ball is in every direction the same. For ellipses this is clearly not the case. In contrast it is possible to get ellipses that are very long but thin as in the above mentioned model. This makes the orientation in this model crucial. In our work we define diameters so that one can control the shape of a grain and also determine the orientation of a grain.

1.2 Structure

In this section we give an overview of the structure of this thesis. In addition to that we explain which part of the results and proofs are based on which paper and describe my contribution to them.

Chapter 2 gives the detailed definition of the model and its behaviour, including terminology (a grain distribution being dense, robust and non-robust), in

order to describe this. More precisely you can find in Section 2.1 the formal definition of the model we are interested in and a definition of a sequence of diameters so that one has some control of the shape and size of the grains. In addition to that one can find the result concerning the behaviour of the grain distribution being dense, robust and non-robust. For density and robustness we state some universal criteria. In addition to that we provide some special criteria for robustness that extend the universal criteria for particular kinds of grain distribution. Moreover we prove criteria on the non-robustness for a generalisation of 2-dimensional ellipses model introduced by Teixeira and Ungaretti in [53]. In Section 2.2 one can find the proofs of the results on the behaviour. All results, definitions and proofs from Chapter 2 are based on the work [25].

Chapter 3 is based on the work [26]. Here, we present the results on the chemical distance for far apart vertices and the proofs on it. In Section 3.1 we state the main result on the chemical distance and discuss the nature of the constant that appears there. In Section 3.2 we give the proof of the lower bound of the chemical distance while the proof of the upper bound can be found in Section 3.3.

In Chapter 4 we discuss examples and state their properties given by our results from Chapter 2 and Chapter 3. We consider also a further example, where we have parameters such that with strong positive correlations between diameters, we get a robust grain distribution, but get non-robustness with the same parameters if we change the grain distribution. All these examples and results for them are taken from [25, 26].

Finally, in Chapter 5 we round this thesis up by discussing briefly some possible future research directions.

In the appendix of this thesis, one can find results on bounds of intersection probabilities and some geometrical tools. Some but not all, are taken from [26].

This thesis includes the work of the following two arXiv preprints.

[25] Gracar, P., Korfhage, M. and Mörters, P. (2024) **Robustness in the Poisson Boolean model with convex grains.**

Preprint arXiv:2410.13366

[26] Gracar, P. and Korfhage, M. (2025) **Chemical distance in the Poisson Boolean model with regularly varying diameters.**

Preprint arXiv:2503.18577

My contribution is essential in both preprints and is as follows. In the [25], I took part in all group discussions and worked out ideas that were jointly developed there and made the main contribution to filling in the technical details. The proof of the density of a grain distribution and connection to all other properties were developed together. The idea of the proof of the universal criteria for the robustness was developed in group discussions after I set the ground for the definition of the model. The calculations were then made by my own with the help of the group discussions with both co-authors. The preprint was then written primarily by me, and polished by my coauthors.

The idea for the second paper was initially developed in collaboration with Peter Gracar and Peter Mörters, when we first discussed the 2-dimensional ellipses model of Teixeira and Ungaretti from [53] and the results from [34]. We were interested in refining the result of [34] by finding the exact factor in front of the log log term. The idea of the truncated moment method came up in this discussion. In addition to that in discussions with Peter Gracar the use of a sprinkling argument as in [24] was suggested. Subsequently, I did a substantial part of the work on my own and then discussed the results with Peter Gracar and carried out revisions together with him. The paper was then written up and I wrote up a significant part of the proofs of the bounds for the chemical distance. Together with my coauthor we corrected mistakes, made the paper complete with introduction, motivation and discussion of the result and rewrote proofs to be precise and formally correct.

This thesis is written in sciebo Overleaf version: 3.5.13 | Integration version: 2.1.0 from the university of cologne. Figures, which are mostly also used in the preprints were all generated on my own with Matlab (Version 24.2.0.2863752 (R2024b) Update 5).

Chapter 2

Poisson Boolean model with regularly varying diameters and its behaviour

2.1 Framework and behaviours of the model

In this section we first start with the formal definition of the Poisson Boolean model with convex grains and give some definition to describe properties of the model. These include the definition of grain distribution being *dense*, *robust* and *non-robust* to give some terminology on the behaviour of the model. After that we state our result about this model for grain distributions being not dense. More precisely we state equivalent conditions on total covering of the space. We give then the definition of a decreasing sequence of diameters in order to describe the size and shape of a convex body and state in addition to that our main results concerning the behaviour of the Poisson Boolean model with convex grains that has some given marginal distribution on the diameters. Note that, except for a few changes, the following chapter is taken from [25].

2.1.1 Definitions and result on total covering of the space

As described in the previous chapter we take a homogeneous Poisson point process \mathcal{P} in \mathbb{R}^d of dimension $d \geq 2$ with positive intensity u and mark every point x of \mathcal{P} with an independent copy \tilde{C}_x of a random convex body $C \subset \mathbb{R}^d$. We assume that the distribution of C is rotation invariant about the origin. We will write $\text{Vol}(C)$ for the Lebesgue measure, i.e. the volume of the convex

body C . We denote

$$C_x := x + \tilde{C}_x = \{y \in \mathbb{R}^d : y - x \in \tilde{C}_x\},$$

and following [31] let \mathcal{C} be the union of the convex bodies $(C_x)_{x \in \mathcal{P}}$, i.e.

$$\mathcal{C} := \bigcup_{x \in \mathcal{P}} C_x.$$

The set \mathcal{C} is called the *Poisson Boolean model* with convex grain C and intensity u . As described in Chapter 1, there is also a natural graph $\mathcal{G} = (\mathcal{P}, \mathcal{E})$ associated with this model, where the points of the Poisson process \mathcal{P} constitute the vertex set and there is an (unoriented) edge connecting distinct points $x, y \in \mathcal{P}$ if and only if $C_x \cap C_y \neq \emptyset$.

There is little interest in the Boolean model if $\mathcal{C} = \mathbb{R}^d$ and we call the grain distribution *dense* if this is the case almost surely, for any Poisson intensity $u > 0$. Otherwise it is called *sparse*. We now give a few equivalent characterisations of a grain distribution being sparse. For that define

- M_0 as the number of grains containing the origin,

$$M_0 := \sum_{x \in \mathcal{P}} \mathbb{1}_{0 \in C_x}.$$

- N_x as the degree of the vertex $x \in \mathcal{P}$ in the graph \mathcal{G} ,

$$N_x := \sum_{\substack{y \in \mathcal{P} \\ y \neq x}} \mathbb{1}_{C_x \cap C_y \neq \emptyset}$$

- N_A as the degree of the set $A \in \mathcal{B}(\mathbb{R}^d)$,

$$N_A := \sum_{x \in \mathcal{P}} \mathbb{1}_{A \cap C_x \neq \emptyset}.$$

With that we get $N_x = N_{C_x}$ for $x \in \mathcal{P}$. Note that $\mathcal{B}(\mathbb{R}^d)$ is the Borel- σ -algebra regarding to \mathbb{R}^d .

Proposition 2.1. *Let \mathcal{P} be a homogeneous Poisson point process in \mathbb{R}^d and mark the points with independent random convex bodies $C \subset \mathbb{R}^d$ containing a ball of fixed radius. Let \mathcal{P}_0 be the Palm version of the*

marked Poisson point process, and denote its law by \mathbb{P}_0 and by \mathbb{E}_0 the corresponding expectation. The statement

$$\mathbb{E}[\text{Vol}(C)] < \infty \tag{2.1}$$

and the following statements are equivalent:

- | | | |
|--|--|---|
| (a) $\mathbb{P}(\mathcal{C} = \mathbb{R}^d) < 1$ | (b) $\mathbb{P}(\mathcal{C} = \mathbb{R}^d) = 0$ | (c) $\mathbb{P}(0 \in \mathcal{C}) < 1$ |
| (d) $\mathbb{E}_0[N_0] < \infty$ | (e) $\mathbb{P}_0(N_0 = \infty) < 1$ | (f) $\mathbb{P}_0(N_0 = \infty) = 0$ |
| (g) $\mathbb{E}[M_0] < \infty$ | (h) $\mathbb{P}(M_0 = \infty) < 1$ | (i) $\mathbb{P}(M_0 = \infty) = 0$ |

Remark: Statement (2.1) is only about the grain distribution and therefore does not depend on the Poisson intensity u . Hence all other statements are independent of u as well. The statements (a), (b) and (c) are about the random sets \mathcal{C} , the statements (g), (h) and (i) about the covering and (d), (e), (f) about the corresponding random graph. Recall that the grain distribution is sparse if one, and hence all, of the conditions in Proposition 2.1 hold for one, and hence all, values of $u > 0$.

We say that the grain distribution is *robust* if, for all $u > 0$, the set \mathcal{C} has an unbounded component, i.e. a component of infinite volume. This is easily seen to be equivalent to the fact that, for every intensity $u > 0$, the graph \mathcal{G} percolates, or in the Palm version there is a positive probability that there exists an infinite self-avoiding path in \mathcal{G} starting at the origin. Conversely, the grain distribution is *non-robust* if there exists $u_c > 0$ such that for all $0 < u < u_c$ every component of \mathcal{C} is bounded.

In the case that C is a centred ball of random radius, recall that Gou  r   [22] has shown that non-robustness is equivalent to sparseness, i.e. to the statements in Proposition 2.1. Recall also that this is however not true in the case of general convex grains. Remember that Teixeira and Ungaretti [53] have shown that for grains in \mathbb{R}^2 which are ellipses with a major axis of heavy tailed random length with index $-2 < \alpha < -1$ and a minor axis of unit length, for every $u > 0$, we have $\mathcal{C} \neq \mathbb{R}^2$ even though \mathcal{C} has an unbounded component, almost surely. We are therefore interested in some general result on robustness for every dimension.

Our main result gives *universal criteria* that ensure that the grain distribution is robust, independently of how the diameters (defined below) are

correlated. We also show that there exist robust grain distributions that do not satisfy the universal criteria, but instead satisfy *specific criteria*, which also put restrictions on the correlation structure of the diameters. Finally, we provide a (trivial) universal criterion and a specific criterion for a grain distribution to be non-robust. The latter applies in particular to a generalisation of the ellipses percolation model in [53].

Definition 2.1.1. Let $K \subset \mathbb{R}^d$ be a convex body, i.e. a compact convex set with nonempty interior. The *first diameter*, or just *diameter* of K , is defined as

$$D_K^{(1)} := \text{diam}(K) = \max\{|x - y| : x, y \in K\}.$$

Let $p_K^{(1)}$ be the orientation of $D_K^{(1)}$, i.e. $p_K^{(1)} = \frac{x-y}{|x-y|}$ where x, y are any (measurable) choice of maximizers in the definition of the diameter $D_K^{(1)}$. We define the *second diameter* as

$$D_K^{(2)} := \text{diam}\left(P_{H_{p_K^{(1)}}}(K)\right),$$

where $P_H(B)$ is the orthogonal projection of $B \subset \mathbb{R}^d$ onto the linear subspace $H \subset \mathbb{R}^d$, and where $H_{p_K^{(1)}}$ is the hyperplane perpendicular to $p_K^{(1)}$. Denote the orientation of $D_K^{(2)}$ by $p_K^{(2)} \in H_{p_K^{(1)}}$ and let $H_{p_K^{(2)}}$ be the hyperplane in $H_{p_K^{(1)}}$ perpendicular to $p_K^{(2)}$.

Iterating this procedure, given $H_{p_K^{(i)}}$ for some $2 \leq i < d$, the $(i+1)$ st diameter is

$$D_K^{(i+1)} := \text{diam}\left(P_{H_{p_K^{(i)}}}(K)\right)$$

and we denote by $p_K^{(i+1)}$ its orientation. By construction we have $D_K^{(i+1)} \leq D_K^{(i)}$ for all $i \in \{1, \dots, d-1\}$. Note that an illustration of this construction of diameters and some example for diameters in \mathbb{R}^3 is given in Figure 2.1. Although the sequence of diameters $D_K^{(1)}, \dots, D_K^{(d)}$ thus defined involves the non-unique choice of orientations, our results do not depend on any of these choices as the following assumption on the grain distribution holds true by any choice of these diameters. The proof of this claim is given in Section A.2.

We assume for our grain distribution that the tails of the random variables $D_C^{(i)}$ are regularly varying with index $-\alpha_i$, i.e.

$$\lim_{r \rightarrow \infty} \frac{\mathbb{P}(D_C^{(i)} \geq cr)}{\mathbb{P}(D_C^{(i)} \geq r)} = c^{-\alpha_i} \text{ for all } c > 1.$$

We include the case of bounded diameters $D_C^{(i)}$, in which case we put $\alpha_i = \infty$.

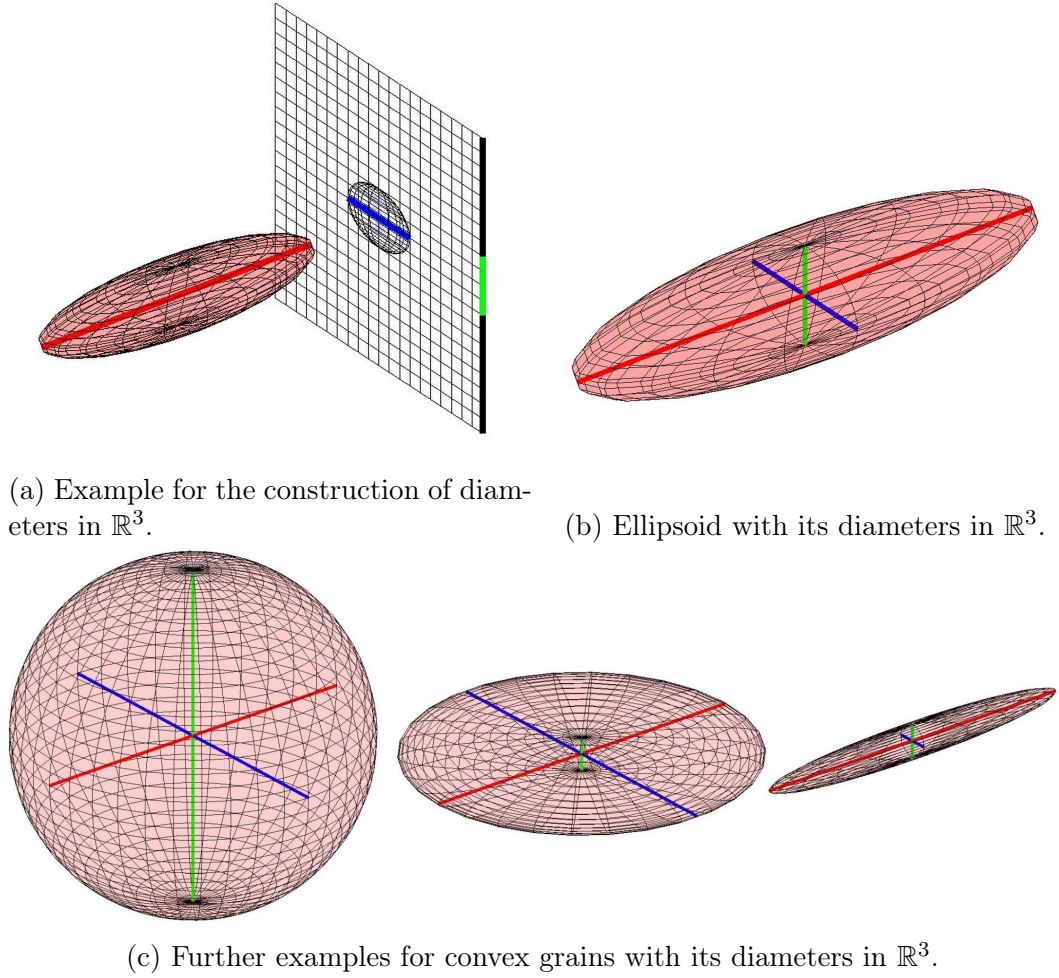


Figure 2.1: Example in \mathbb{R}^3 for the construction of the diameters for an ellipsoid. In pink the ellipsoid with the red line as the first diameter, the ellipses on the grid in picture (a) as the orthogonal projection of the ellipsoid onto the hyperplane, given as the grid, the blue line as the second diameter and in green the orthogonal projection of the set onto the hyperplane and the third diameter.

Note that, by definition, $\alpha_1 \leq \alpha_2 \leq \dots \leq \alpha_d$. Theorem 2.2 gives sufficient conditions for a grain distribution to be robust, either universally or provided the diameters are sufficiently strongly correlated. Theorem 2.3 gives a sufficient condition for non-robustness for grain distributions in d dimensions with k ‘large’ diameters and $d - k$ diameters of bounded diameters length. This includes a higher dimensional generalisation of the two-dimensional ellipses model studied in [53].

2.1.2 Results on robustness and non-robustness

Theorem 2.2. *In the Poisson Boolean model given by a d -dimensional random convex body C with rotation invariant distribution, containing a ball of fixed radius such that, for all $1 \leq k \leq d$, the k th diameter $D_C^{(k)}$ has regularly varying tail with index $-\alpha_k$, we have that the grain distribution is robust if*

(a) *there exists $1 \leq k \leq d$ such that $\alpha_k < \min\{2k, d\}$.*

Additionally, if there exist a random variable D which is regularly varying with index $-\alpha$ for $\alpha > 0$ and there exist $1 = \gamma_1 \geq \gamma_2 \geq \dots \geq \gamma_d \geq 0$ such that $D^{(k)} = D^{\gamma_k}$ for all $k \in \{1, \dots, d\}$, we have that the grain distribution is robust if either of the following two conditions holds:

(a) *$\exists k > \lfloor d/2 \rfloor$ such that $\alpha < d\gamma_k$, or*

(b) *$\exists k \leq \lfloor d/2 \rfloor$ such that $\alpha < 2k\gamma_k + \sum_{j=k+1}^{d-k} \gamma_j$.*

Note that the two criteria denoted (a) agree. Next, we consider a large class of grain distributions for which non-robustness can be shown under sufficient conditions on the tail exponents of the convex grains.

Theorem 2.3. *In the Poisson Boolean model given by a d -dimensional random convex body C with rotation invariant distribution, if diameters fulfil $D^{(1)} = D^{(k)}$ for some fixed $k \in \{1, \dots, d-1\}$ with $D^{(k)}$ is regularly varying with index $-\alpha_k$ and $D^{(j)} \leq M$ almost surely for some deterministic $M \in (0, \infty)$, for $j \in \{k+1, \dots, d\}$, the grain distribution is non-robust if*

(c) *$\text{Vol}(C) \in \mathcal{L}^2$ and $\alpha_k > 2k$.*

Also, the grain distribution is non-robust for the Poisson Boolean model if $D_C^{(1)} \in \mathcal{L}^d$.

Remarks:

- The first half of Theorem 2.2 only refers to the individual tail probabilities of the diameters. In particular, no further assumption is made on the *joint distribution* of the diameters $D_C^{(1)}, \dots, D_C^{(d)}$.

- The condition $\text{Vol}(C) \in \mathcal{L}^2$ of Theorem 2.3 implies that $\alpha_k \geq 2k$ for fixed $1 \leq k \leq d$ and $D_C^{(1)} \in \mathcal{L}^d$ implies $\alpha_1 \geq d$. Note however that $\alpha_k > 2k$ does not imply that $\text{Vol}(C) \in \mathcal{L}^2$.
- The universal condition in Theorem 2.2 implies $\text{Vol}(C) \notin \mathcal{L}^2$ and $D_C^{(k)} \notin \mathcal{L}^d$ (and in particular also $D_C^{(1)} \notin \mathcal{L}^d$), while the non-robustness condition in Theorem 2.3 implies $\text{Vol}(C) \in \mathcal{L}^2$ or $D_C^{(1)} \in \mathcal{L}^d$. One might be tempted to conjecture that these weaker conditions are sufficient in the specific model stated in Theorem 2.3. However, it turns out that this is not the case, as [53] provides an example of a non-robust grain distribution in \mathbb{R}^2 with $\text{Vol}(C) \notin \mathcal{L}^2$ and $D_C^{(1)} \notin \mathcal{L}^d$.
- Note that in Theorem 2.3 we omit the case $k = d$ as this is the case of the Poisson Boolean model with grains given by balls, which is non-robust when $D^{(1)} \in \mathcal{L}^d$; this was shown in [22].
- One might hope that we could find a more general result for a grain distribution being non-robust, similar to the universal criterion in Theorem 2.2. This is likely not possible without having more information on the diameter distribution beyond the trivial case of $\alpha_1 > d$ as in Chapter 4 we present in the last example some parameter regime where we see that it can be crucial to know more about the correlation structure of the diameters to that the grain distribution is robust or non-robust.

2.2 Proofs on the behaviour of the model

In order to prove our result we first formalise our setup. Denote by \mathcal{C}^d the space of convex bodies in \mathbb{R}^d with the Hausdorff metric. Recall that we assume that, for some fixed $\epsilon > 0$, the ϵ -interior of C is nonempty almost surely. We assume that \mathbb{P}_C is a law on $\mathcal{C}^d \times \mathbb{R}^d$ such that, for \mathbb{P}_C -almost every (C, m) the point m is in the ϵ -interior of C . We further assume that \mathbb{P}_C is invariant under simultaneous rotations of C and m about the origin. We now define the Poisson-Boolean base model, which we use in our proofs.

Definition 2.2.1. The *Poisson-Boolean base model* is the Poisson point process on

$$\mathcal{S} := \mathbb{R}^d \times (\mathcal{C}^d \times \mathbb{R}^d)$$

with intensity

$$u \lambda \otimes \mathbb{P}_C$$

where λ is the Lebesgue measure. The corresponding point process is denoted by \mathcal{X} . We call any $\mathbf{x} \in \mathcal{X}$ a *vertex* and its first component $x \in \mathbb{R}^d$ its *location*. By \mathcal{P} we denote the Poisson point process of locations. The second component is denoted by (\tilde{C}_x, m_x) and \tilde{C}_x is called the *grain at x* . We denote its diameters by $D_x^{(1)}, \dots, D_x^{(d)}$ and the corresponding directions by $p_x^{(1)}, \dots, p_x^{(d)}$.

Then we set

$$C_x := x + \tilde{C}_x$$

and define

$$\mathcal{C} := \bigcup_{x \in \mathcal{P}} C_x,$$

which is a representation of the *Poisson-Boolean model*. When considering two vertices $\mathbf{x}, \mathbf{y} \in \mathcal{X}$, we say they are connected by an edge, if and only if the sets C_x and C_y intersect. Recall, that we denote this by writing $\mathbf{x} \sim \mathbf{y}$. If \mathbf{x} and \mathbf{y} are connected through n edges recall that we write $\mathbf{x} \stackrel{n}{\sim} \mathbf{y}$ and say \mathbf{x} and \mathbf{y} are connected by a path of length exactly n .

2.2.1 Criteria for density

In all our proofs we use the notation $B_\varepsilon(x) := \{y \in \mathbb{R}^d : |y - x| \leq \varepsilon\}$. We also write $\eta K := \{\eta x : x \in K\}$ for the *blow-up* of the set $K \subset \mathbb{R}^d$ about the origin by a factor $\eta > 0$. Let $(e_i)_{i \in \{1, \dots, d\}}$ be the canonical basis of \mathbb{R}^d and for $\vartheta \in \mathbb{S}^{d-1}$ let rot_ϑ be an arbitrary but fixed rotation such that $\text{rot}_\vartheta(e_1) = \vartheta$. Throughout the proofs we use $c \in (0, \infty)$ as a generic constant which may change its value at every inequality, but is always finite and may depend on d, k, α_k and on $\varepsilon > 0$ appearing in the Potter bounds only. It depends also on $\epsilon > 0$ while ϵ is the radius of the ball which is completely included in C .

Proof of Proposition 2.1. This proof does not require rotation invariance. By the mapping theorem, see e.g. Theorem 5.1 in [40], the point process given by the points $x + m_x, x \in \mathcal{P}$ is again a homogeneous Poisson point process. We may therefore assume, without loss of generality, that there is a fixed $\epsilon > 0$ such that $B_\epsilon(x) \subset C_x$ for all $x \in \mathcal{P}$.

$(a) \Leftrightarrow (b)$ is clear by ergodicity. $(1) \Rightarrow (a)$ follows because, by Section 2 of [31], we have $\mathbb{P}(\text{Vol}(\mathbb{R}^d \setminus \mathcal{C}) = 0) = 1$ if and only if $\mathbb{E}[\text{Vol}(C)] = \infty$. To also get $\neg(1) \Rightarrow \neg(a)$ from this statement we apply it to ηC , for some fixed $0 < \eta < 1$,

and get that $\mathbb{E}[\text{Vol}(C)] = \infty$ implies $\mathbb{E}[\text{Vol}(\eta C)] = \eta^d \mathbb{E}[\text{Vol}(C)] = \infty$ and hence

$$\mathbb{P}\left(\text{Vol}\left(\mathbb{R}^d \setminus \bigcup_{x \in \mathcal{P}} (\eta C)_x\right) = 0\right) = 1,$$

This event implies $\bigcup_{x \in \mathcal{P}} C_x = \mathbb{R}^d$. Indeed, if $y \notin \bigcup_{x \in \mathcal{P}} (\eta C)_x$ there exists a sequence of points $(x_n)_n$ in \mathcal{P} such that the distance of y and $(\eta C)_{x_n}$ goes to zero. If we replace $(\eta C)_{x_n}$ by C_{x_n} , the distance to y is reduced by at least the fixed amount $\epsilon(1 - \eta) > 0$, because $\text{Dist}(x, \eta C) \geq \text{Dist}(x, C) + \text{Dist}(\partial C, \partial \eta C)$ and $\text{Dist}(\partial C, \partial \eta C) \geq (1 - \eta)\epsilon$, where $\text{dist}(A, B)$ is the standard Hausdorff distance for $A, B \subset \mathbb{R}^d$. Hence there exists n with $y \in C_{x_n}$. This completes the proof of $(a) \Leftrightarrow (1)$.

The implication $(c) \Rightarrow (a)$ is immediate from $\{\mathcal{C} = \mathbb{R}^d\} \subset \{0 \in \mathcal{C}\}$.

To show that $(1) \Leftrightarrow (g)$ we use Campbell's theorem to calculate

$$\mathbb{E}[M_0] = u \int \mathbb{P}(0 \in x + C) d\lambda(x) = u \int \mathbb{P}(x \in C) d\lambda(x) = u \mathbb{E}[\text{Vol}(C)],$$

which readily implies the equivalence.

To show that $(d) \Rightarrow (1)$ observe that under the Palm distribution $\mathcal{P}(C_0 \setminus \{0\}) = k$ implies that $N_0 \geq k$. Hence $\mathbb{E}_0[N_0] \geq \mathbb{E}_0[\mathcal{P}(C_0) - 1] = u \mathbb{E}[\lambda(C)]$, from which the implication follows. For the implication $(1) \Rightarrow (d)$ we enlarge the sets C_x , for each $x \in \mathcal{P}$, to become rectangles R_x taken as the sum of x and the cartesian product of the intervals $[-D_x^{(i)}, D_x^{(i)}]$ with respect to the orthonormal basis given by the directions $p_{C_x}^{(i)}$. The enlargement increases the volume of the sets by no more than a constant factor. Indeed, if R is the rectangle constructed from C we have $\text{Vol}(R) = 2^d \prod D^{(i)}$. As the convex hull of the points, which define the length and orientation of the diameter, is contained in C we can lower bound its volume iteratively via the formula of the volume of hyperpyramids (see e.g. [38]) and get

$$\text{Vol}(R) \leq (2^d \cdot d!) \text{Vol}(C).$$

We write \tilde{N}_A and \tilde{N}_0 for the degrees defined like N_A and N_0 but with respect to the enlarged sets.

By assumption we have $x + [-\epsilon/\sqrt{d}, \epsilon/\sqrt{d}]^d \subset R_x$. As $C_x \subset R_x$ we have $N_0 \leq \tilde{N}_0$ and we can bound the expected degree of the origin from above,

$$\mathbb{E}_0[N_0] \leq \mathbb{E}_0[\tilde{N}_0] \leq \mathbb{E}_0\left[\sum_{x \in (\epsilon/\sqrt{d})\mathbb{Z}^d} \mathbb{1}_{R_0}(x) \tilde{N}_{B_\epsilon(x)}\right],$$

where in the second inequality we use that $[-\epsilon/\sqrt{d}, \epsilon/\sqrt{d}]^d \subset R_0$ and hence balls of radius ϵ centred in the points of $(\epsilon/\sqrt{d})\mathbb{Z}^d \cap R_0$ cover R_0 . Now $\mathbb{1}_{R_0}(x)$ and $\tilde{N}_{B_\epsilon(x)} - \mathbb{1}_{R_0 \cap B_\epsilon(x) \neq \emptyset}$ are independent and we get an upper bound of

$$\mathbb{E}_0[N_0] \leq \mathbb{E}_0[\#((\epsilon/\sqrt{d})\mathbb{Z}^d \cap R_0)] \mathbb{E}[\tilde{N}_{B_\epsilon(0)} + 1].$$

By [17] there exists a constant $c(d, \epsilon)$ which only depends on the dimension and ϵ such that the number of lattice points in K can be bounded from above by $c(d, \epsilon)\text{Vol}(K)$. Looking now at the last factor we use

$$\mathbb{E}[\tilde{N}_{B_\epsilon(0)}] = u \int \mathbb{P}_0(B_\epsilon(0) \cap (x + R) \neq \emptyset) dx = u \int \mathbb{P}(B_\epsilon(x) \cap R \neq \emptyset) dx.$$

As $\{B_\epsilon(x) \cap R \neq \emptyset\} \subset \{x \in 2R\}$ we can bound the previous term from above by

$$u\mathbb{E}[\text{Vol}(2R)] = u2^d \mathbb{E}[\text{Vol}(R)] \leq u2^{2d} \cdot d! \mathbb{E}[\text{Vol}(C)].$$

Hence we get that $\mathbb{E}_0[N_0]$ is finite if $\mathbb{E}[\text{Vol}(C)]$ is finite.

The equivalence of $(g), (h), (i)$ and (1) follows because M_0 is Poisson distributed with parameter $u\mathbb{E}[\text{Vol}(C)]$ and therefore finite almost surely if and only if the parameter is finite. The implications $(d) \Rightarrow (f) \Rightarrow (e)$ are trivial. The implications $(f) \Rightarrow (i)$ and $(e) \Rightarrow (h)$ follow as $N_0 \geq M_0 - 1$ under the Palm distribution. Finally, to show the implication $(1) \Rightarrow (c)$ we note that $\mathbb{P}(0 \in \mathcal{C}) = \mathbb{P}(M_0 \geq 1) < 1$ because M_0 is Poisson distributed with parameter $u\mathbb{E}[\text{Vol}(C)] < \infty$. \square

2.2.2 Universal criteria for robustness

We now prove the first part of Theorem 2.2. The idea of the proof is to construct, for every $u > 0$, an infinite self-avoiding path in \mathcal{G} . The path is constructed such that the convex bodies attached to the vertices on the path are growing faster than a given increasing threshold sequence. Note that without loss of generality we can assume that $\alpha_k \geq k$, for all $k \in \{1, \dots, d\}$, since otherwise $\text{Vol}(C) \notin \mathcal{L}^1$ and by Proposition 2.1 there is nothing left to show. Again we use $c \in (0, \infty)$ as a generic constant which may change its value at every inequality, but is always finite with possibly dependence on d, k, α_k and $\varepsilon > 0$.

Remark 2.2.1. In this and the following section we bound the set of orientations which result in an intersection of two convex bodies using the fol-

lowing known geometric property. Consider two points $x, y \in \mathbb{R}^d$ at distance $a := |x - y|$. Let A be a $(d - 1)$ -dimensional set which contains y and lies in the hyperplane through y perpendicular to $x - y$. Denote further by λ_{d-1} the $(d - 1)$ -dimensional Lebesgue measure. Then, if $a > \text{diam}(A)$, the volume of the set of orientations of (infinitely long) lines that go through x and intersect A can be bounded from below by $\frac{\lambda_{d-1}(A)}{2^{d-1}a^{d-1}}$ and from above by $\frac{\lambda_{d-1}(A)}{a^{d-1}}$. Note that the upper bound is not only true for $a > \text{diam}(A)$.

Proof of Theorem 2.2, part one. As in the proof of Proposition 2.1 the point process given by the points $x + m_x, x \in \mathcal{P}$ is a homogeneous Poisson point process. As done there, we also replace the independent attachments (C, m) by $(C - m, 0)$ so that the new grains contain a ball of radius ϵ around the origin and, by the rotation invariance assumption, their distribution is invariant under rotations around the origin. Reverting to the original notation we may assume henceforth that $B_\epsilon(x) \subset C_x$ for all $x \in \mathcal{P}$.

For $1 \leq k < d$ with $\alpha_k \neq k$ we define the increasing threshold sequence $(f_n)_{n \in \mathbb{N}}$ by

$$f_n := (f_{n-1})^{\frac{\min\{d-k, k\}}{\alpha_k - k} - \epsilon}, \text{ for } n \in \mathbb{N}, \quad (2.2)$$

where $f_0 > 1$ can be chosen arbitrarily and will be set large later in the proof, and $0 < \epsilon < \frac{1}{4}$ is such that the exponent in this sequence is strictly bigger than 1 in order to guarantee that the sequence is increasing. This is possible by our assumption that $\alpha_k < \min\{2k, d\}$. Note that we can without loss of generality take this ϵ to be the same as in the requirement that $B_\epsilon(0) \subset C$, by replacing the larger of the two with the smaller if necessary. We comment on the cases $k = d$ and $\alpha_k = k$ at the end of the proof.

Let therefore $k \in \{1, \dots, d - 1\}$ and assume for now that $f_0 > 1$. Furthermore let

$$A_0 := \left\{ \exists \mathbf{x}_0 \in \mathcal{X} \cap B_{f_0}(0) : D_{\mathbf{x}_0}^{(k)} \geq 2^{2(d-1)+\epsilon} f_0 \right\}.$$

We will remark on the factor $2^{2(d-1)+\epsilon}$ later when considering a more general case of A_0 . As $D^{(k)}$ is regularly varying with index $-\alpha_k$, we have that the probability of A_0 is

$$\begin{aligned} \mathbb{P}(A_0) &= 1 - \exp\left(-u \int_{B_{f_0}(0)} \mathbb{P}(D^{(k)} \geq 2^{2(d-1)+\epsilon} f_0) d\lambda(x)\right) \\ &\geq 1 - \exp(-uc f_0^{d-\alpha_k-\epsilon}), \end{aligned} \quad (2.3)$$

where we note that $\epsilon > 0$ was chosen such that $d - \alpha_k - \epsilon > 0$. In the last

inequality we have applied the Potter bounds (see [39, Prop. 1.4.1]), which for a non-negative regularly varying random variable X with index $-\alpha < 0$ and every $\varepsilon \in (0, \alpha)$ yield a constant $c(\varepsilon) > 0$, such that

$$c(\varepsilon)^{-1} x^{-\alpha-\varepsilon} \leq \mathbb{P}(X > x) \leq c(\varepsilon) x^{-\alpha+\varepsilon}$$

holds for $x \geq \varepsilon$. For $\mathbf{x} \in \mathcal{X}$ we define the set

$$O_i(\mathbf{x}) := \left\{ \begin{array}{l} y \in \mathbb{R}^d : |x - y| \in [\frac{1}{2}f_i, f_i], \angle(x - y, v) > \varphi, \\ \text{for } v \in \text{span}\{p_x^{(j)} : 1 \leq j \leq k\} \end{array} \right\}, \quad (2.4)$$

where $\varphi = 2^{-(d+1)}(d+1)^{-1}$ and $\angle(x, y)$ denotes the angle between vectors $x, y \in \mathbb{R}^d$. For $y \in \mathbb{R}^d$ we define

$$B_{f_{i-1}}^*(\mathbf{x}, y) = P_{H_{x-y}}(C_x \cap B_{f_{i-1}}(x)), \quad (2.5)$$

where H_{x-y} is the hyperplane perpendicular to $x-y$ with $|H_{x-y} \cap \partial B_{f_{i-1}}(x)| = 1$ and $\text{Dist}(H_{x-y}, x) < \text{Dist}(H_{x-y}, y)$, i.e. the hyperplane that touches the ball of radius f_{i-1} with x as the centre, see Figure 2.2 on this page.

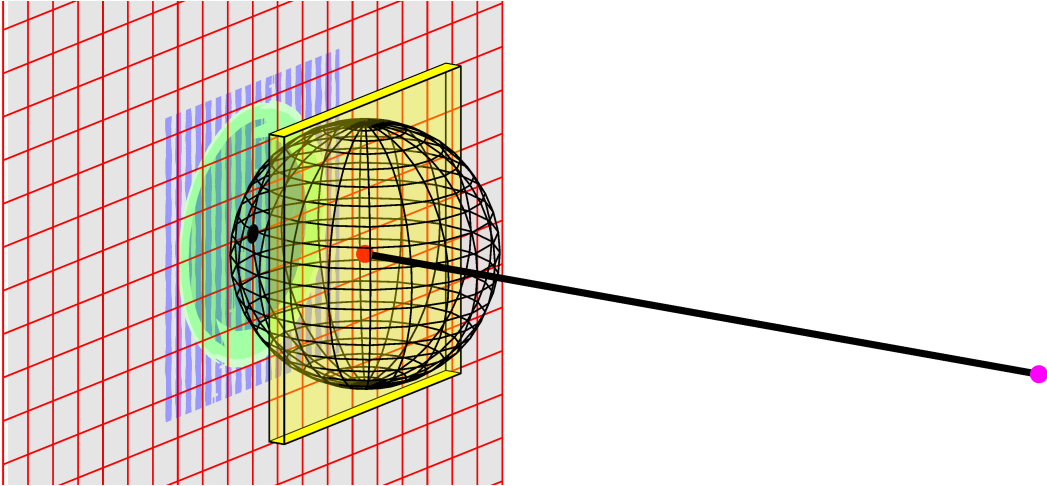


Figure 2.2: The various sets and their relationships from the proof of the first part of Theorem 2.2: The point y is in pink, x in red. The yellow area is C_x . The orthogonal projection of C_x is dark blue and H_{x-y} is the grey plane with the red grid. $B_{f_{i-1}}^*(\mathbf{x}, y)$ is lime green. Drawn in black are the line with orientation $x - y$, the point lying in $H_{x-y} \cap \partial B_{f_{i-1}}(x)$ and the ball $B_{f_{i-1}}(x)$ containing the location x of the vertex \mathbf{x} corresponding to C_x .

For $n \in \mathbb{N}$, define the events

$$A_n := \left\{ \begin{array}{l} \exists \mathbf{x}_1, \dots, \mathbf{x}_n \in \mathcal{X}: \mathbf{x}_i \neq \mathbf{x}_m \text{ for all } i \neq m, D_{x_i}^{(k)} \geq 2^{2(d-1)+\epsilon} f_i, \\ x_i \in O_i(\mathbf{x}_{i-1}) \text{ and } C_{x_i} \cap B_{f_{i-1}}^*(\mathbf{x}_{i-1}, x_i) \neq \emptyset \text{ for all } 1 \leq i \leq n \end{array} \right\}. \quad (2.6)$$

Note that A_n is implicitly dependent on \mathbf{x}_0 , but we omit this in the notation to keep it concise and we will use this sequence in Chapter 3 to prove results on the chemical distance as the construction in the proof of the robustness is crucial for it. Roughly speaking, A_n is the event that we find a path of length n with the properties that, for every $i \in \{1, \dots, n\}$,

- the first k diameters of the convex body C_{x_i} do not fall below the threshold $2^{2(d-1)+\epsilon} f_i$. For the choice of factor $2^{2(d-1)+\epsilon}$, it can easily be checked that a convex body with diameters $D^{(1)}, \dots, D^{(d)}$ contains a rectangle with side-lengths $2^{2(d-1)} D^{(1)}, \dots, 2^{2(d-1)} D^{(d)}$. This claim is stated in Lemma A.1. This Lemma and its proof can be found in Section A.1.
- x_i does not lie “too close” to the affine subspace through x_{i-1} spanned by the orientations $p_{x_{i-1}}^{(1)}, \dots, p_{x_{i-1}}^{(k)}$ of the big diameters of \mathbf{x}_{i-1} . More precisely, we require the angle between any spanning vector of this subspace through x_{i-1} and the vector $x_i - x_{i-1}$ to be larger than φ . This is in order to keep the condition on the orientation of \mathbf{x}_i from becoming too restrictive when we formulate the requirement that C_{x_i} intersects $C_{x_{i-1}}$. Finally,
- the convex body C_{x_i} intersects a part of a hyperplane “behind” the convex body $C_{x_{i-1}}$, see Figure 2.2.

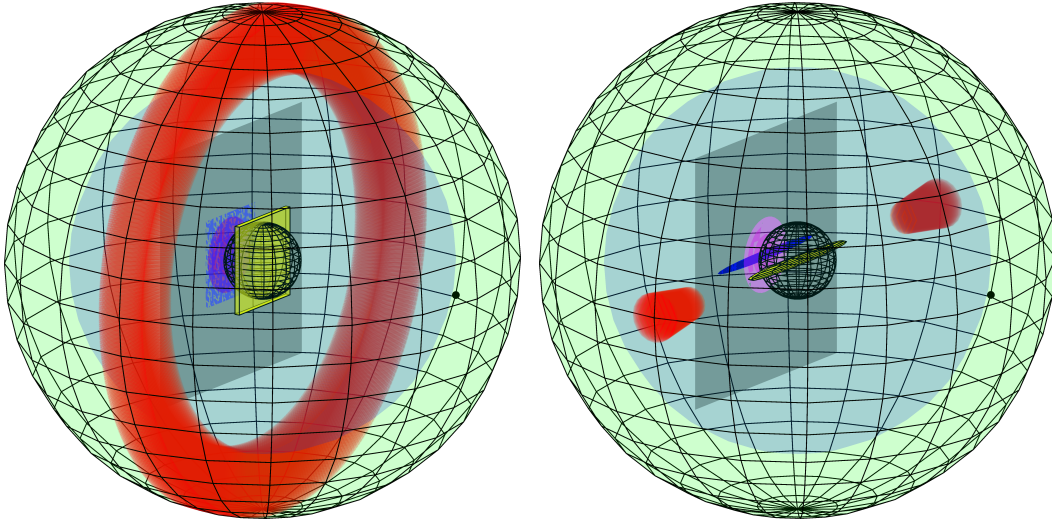
In addition to these restrictions that ensure that the points and their respective convex bodies are sufficiently close, suitably aligned and large enough to keep the chain of intersections going, A_n also gives

- The distance between points x_{i-1} and x_i is at least $\frac{1}{2}f_i$ and $x_i \in B_{2f_i}(0)$.

This last property allows us to search for each point x_i in an annulus disjoint from those of the previous points x_1, \dots, x_{i-1} .

We now construct an infinite sequence of points $\mathbf{x}_1, \mathbf{x}_2 \dots \in \mathcal{X}$ such that the first n points satisfy the event A_n with a probability bounded from below. Recall that the existence of \mathbf{x}_0 satisfying A_0 has already been taken care of

in (2.3). We let \mathfrak{F}_n be the σ -algebra generated by the restriction of the Poisson Boolean base model to the points with locations in $B_{2f_n}(0)$. Then A_n is \mathfrak{F}_n -measurable and we find \mathbf{x}_{n+1} , assuming that $\mathbf{x}_1, \dots, \mathbf{x}_n \in \mathcal{X}$ have been found satisfying A_n , such that $\mathbf{x}_1, \dots, \mathbf{x}_{n+1} \in \mathcal{X}$ satisfy A_{n+1} with a conditional probability bounded from below. Figures 2.3(a) and 2.3(b) are sketches of the $(n+1)$ st step in the construction. On the event A_n we calculate



(a) i th step of the construction in \mathbb{R}^3 with $k = 2$. (b) i th step of the construction in \mathbb{R}^3 with $k = 1$.

Figure 2.3: The recursive construction of the proof of the first part of Theorem 2.2. The convex set $C_{x_{i-1}}$ is in yellow. Mint green is used for $B_{f_i}(x_{i-1}) \setminus B_{f_i/2}(x_{i-1})$; i.e. the possible area for x_i . The part in which x_i is not permitted to be is in red. Grey is used for $H_{x_{i-1}-x_i}$, with dark blue for the orthogonal projection of $C_{x_{i-1}}$. In pink, the orthogonal projection of $B_{f_{i-1}}(x_{i-1})$. Finally, the black point is a possible position for x_i .

$$\begin{aligned} \mathbb{P}[A_{n+1}^c \mid \mathfrak{F}_n] &\leq \mathbb{P}[\text{there exists no } \mathbf{x} \in \mathcal{X} \text{ with } x \in B_{2f_{n+1}}(0) \setminus B_{2f_n}(0) \text{ such} \\ &\quad \text{that } D_x^{(k)} \geq 2^{2(d-1)+\epsilon} f_{n+1}, x \in O_{n+1}(\mathbf{x}_n) \text{ and} \\ &\quad C_x \cap B_{f_n}^*(\mathbf{x}_n, x) \neq \emptyset \mid \mathfrak{F}_n]. \end{aligned}$$

Recall that rot_ϑ is a rotation such that $\text{rot}_\vartheta(e_1) = \vartheta$. For our purpose it matters only that the shortest diameter is suitably oriented after this rotation. For $x, y \in \mathbb{R}^d$ we define $\rho_{x,y} := \frac{x-y}{|x-y|} \in \mathbb{S}^{d-1}$ as the orientation of the vector

$x - y$. With that we define

$$Q_{f_n}(x, y) := \text{rot}_{\rho_{x,y}} \left(\text{conv} \left(\left\{ -\frac{\epsilon}{2} e_i, \frac{\epsilon}{2} e_i : 1 \leq i \leq d - k \right\} \cup \left\{ -\frac{f_n}{2} e_m, \frac{f_n}{2} e_m : d - k + 1 \leq m \leq d \right\} \right) \right) + x \quad (2.7)$$

with $\text{conv}(A)$ being the convex hull of the set A and define

$$Q_{f_n}^*(x, y) := P_{H_{x-y}}(Q_{f_n}(x, y)).$$

Choosing $y = x_n$ the choice of $Q_{f_n}(x_n, x)$ allows us to obtain a lower bound for the probability that $D_x^{(k)} \geq 2^{2(d-1)+\epsilon} f_{n+1}$ and $C_x \cap B_{f_n}^*(\mathbf{x}_n, x) \neq \emptyset$, uniformly across all C_x satisfying $D_x^{(k)} \geq 2^{2(d-1)+\epsilon} f_{n+1}$, for all $x \in O_{n+1}(\mathbf{x}_n)$, by replacing $B_{f_n}^*(\mathbf{x}_n, x)$ with the set $Q_{f_n}^*(x_n, x)$. To see why, note that $Q_{f_n}^*(x_n, x)$ has smaller $(d-1)$ -dimensional Lebesgue measure than $B_{f_n}^*(\mathbf{x}_n, x)$ for all \mathbf{x}_n that satisfy $D^{(k)} \geq 2^{2(d-1)+\epsilon} f_n$.

Abbreviating $I_{n+1} := (B_{2f_{n+1}}(0) \setminus B_{2f_n}(0)) \cap O_{n+1}(\mathbf{x}_n)$ we get

$$\begin{aligned} & \mathbb{P}[A_{n+1}^c | A_n] \\ & \leq \mathbb{E} \left[\mathbb{P} \left[\text{there exists no } \mathbf{x} \in \mathcal{X} \text{ such that } x \in B_{2f_{n+1}}(0) \setminus B_{2f_n}(0) \right. \right. \\ & \quad \left. \left. D_x^{(k)} \geq 2^{2(d-1)+\epsilon} f_{n+1}, x \in O_{n+1}(\mathbf{x}_n) \text{ and } C_x \cap B_{f_n}^*(\mathbf{x}_n, x) \neq \emptyset \mid \mathfrak{F}_n \right] \right. \\ & \quad \left. \times \mathbb{1}_{A_n} \right] / \mathbb{P}(A_n) \\ & = \mathbb{E} \left[\exp \left(-u \int_{I_{n+1}} \mathbb{P}_C(D_C^{(k)} \geq 2^{2(d-1)+\epsilon} f_{n+1}, (x+C) \cap B_{f_n}^*(\mathbf{x}_n, x) \neq \emptyset) d\lambda(x) \right) \right. \\ & \quad \left. \times \mathbb{1}_{A_n} \right] / \mathbb{P}(A_n) \\ & \leq \mathbb{E} \left[\exp \left(-u \int_{I_{n+1}} \mathbb{P}_C(D_C^{(k)} \geq 2^{2(d-1)+\epsilon} f_{n+1}, (x+C) \cap Q_{f_n}^*(x_n, x) \neq \emptyset) d\lambda(x) \right) \right. \\ & \quad \left. \times \mathbb{1}_{A_n} \right] / \mathbb{P}(A_n). \end{aligned}$$

We rewrite the last term as

$$\begin{aligned} & \mathbb{E} \left[\exp \left(-u \int_{I_{n+1}} \mathbb{P}_C((x+C) \cap Q_{f_n}^*(x_n, x) \neq \emptyset \mid D_C^{(k)} \geq 2^{2(d-1)+\epsilon} f_{n+1}) \right. \right. \\ & \quad \left. \left. \times \mathbb{P}_C(D_C^{(k)} \geq 2^{2(d-1)+\epsilon} f_{n+1}) d\lambda(x) \right) \mathbb{1}_{A_n} \right] / \mathbb{P}(A_n) \end{aligned}$$

and focus on the integrand. *First*, we bound the conditional probability from below. We use rotation invariance of the law of C to bound the probability of the intersection from below by the $(d-1)$ -dimensional Lebesgue measure of a subset of S^{d-1} of rotations of C for which we can ensure a non-empty

intersection with $Q_{f_n}^*(x_n, x)$. Using that C , having k diameters of size at least $2^{2(d-1)+\epsilon}f_{n+1}$, needs to hit a target with k diameters with size of order f_n , at distance at most $2f_{n+1}$, we find using a simple inductive argument over d and Remark 2.2.1 such a set of rotations that has measure $c f_n^{\min\{d-k, k\}} f_{n+1}^{-d+k}$. Note that the proof of this lower bound is given in Section A.3.

Second, we look at the factor $\mathbb{P}_C(D_C^{(k)} \geq 2^{2(d-1)+\epsilon}f_{n+1})$ and recall that the tail of $D_C^{(k)}$ is a regularly varying function with index $-\alpha_k$. Using the Potter bounds we get

$$\begin{aligned} \mathbb{P}_C((x+C) \cap Q_{f_n}^*(x_n, x) \neq \emptyset \mid D_C^{(k)} \geq 2^{2(d-1)+\epsilon}f_{n+1}) & \mathbb{P}_C(D_C^{(k)} \geq 2^{2(d-1)+\epsilon}f_{n+1}) \\ & \geq c \frac{f_n^{\min\{d-k, k\}}}{f_{n+1}^{d-k}} f_{n+1}^{-(\alpha_k+\epsilon)}, \end{aligned} \tag{2.8}$$

where $c > 0$ depends again only on ϵ, α_k, d, k and ϵ . As there exists a further $c > 0$ such that, for f_0 big enough, points in $O_{n+1}(\mathbf{x}_n)$ have distance bigger than $c f_{n+1}$ from the origin, the volume of I_{n+1} is of order f_{n+1}^d . This yields for $\mathbb{P}[A_{n+1}^c | A_n]$ the bound

$$\begin{aligned} \mathbb{E} \left[\exp \left(-u \int_{I_{n+1}} c \frac{f_n^{\min\{d-k, k\}}}{f_{n+1}^{d-k}} f_{n+1}^{-(\alpha_k+\epsilon)} d\lambda(x) \right) \mathbb{1}_{A_n} \right] / \mathbb{P}(A_n) \\ \leq \mathbb{E} \left[\exp \left(-uc f_n^{\min\{d-k, k\}} f_{n+1}^{-(\alpha_k+\epsilon-k)} \right) \mathbb{1}_{A_n} \right] / \mathbb{P}(A_n). \end{aligned}$$

For fixed $0 < \epsilon < (\alpha_k - k)^2 \epsilon / (2 \min\{d - k, k\})$ we get the inequality

$$-\epsilon \frac{\min\{d - k, k\}}{\alpha_k - k} + \epsilon(\alpha_k + \epsilon - k) > \frac{\epsilon}{2}(\alpha_k - k) > 0,$$

and combining the above with the definition of our threshold sequence and the Potter bounds we get for $\mathbb{P}[A_{n+1}^c | A_n]$ the upper bound

$$\exp(-uc f_{n+1}^{-(\alpha_k+\epsilon-k)} f_n^{\min\{d-k, k\}}) \leq \exp(-uc f_n^{\epsilon(\alpha_k-k)/2}).$$

We can now bound the probability of A_n from below as follows.

$$\begin{aligned} \mathbb{P}(A_n) &= \mathbb{P}(A_0) \prod_{\ell=0}^{n-1} \mathbb{P}[A_{\ell+1} | A_\ell] \\ &\geq \left(1 - \exp(-uc f_0^{d-\alpha_k-\epsilon})\right) \prod_{\ell=0}^{n-1} \left(1 - \exp(-uc f_\ell^{\epsilon(\alpha_k-k)/2})\right) \end{aligned}$$

$$= \exp \left\{ \log(1 - \exp(-ucf_0^{d-\alpha_k-\varepsilon})) + \sum_{\ell=0}^{n-1} \log(1 - \exp(-ucf_\ell^{\varepsilon(\alpha_k-k)/2})) \right\}.$$

Using that for small $x < 0$ we have $\log(1+x) \geq 2x$ and $\exp(-x) \geq 1-x$ we get

$$\begin{aligned} \mathbb{P}(A_n) &\geq 1 - 2 \exp(-ucf_0^{d-\alpha_k-\varepsilon}) - 2 \sum_{\ell=0}^{\infty} \exp(-ucf_\ell^{\varepsilon(\alpha_k-k)/2}) \\ &= 1 - 2 \exp(-ucf_0^{d-\alpha_k-\varepsilon}) - 2 \sum_{\ell=0}^{\infty} \exp \left(-uc \left\{ f_0^{\varepsilon(\alpha_k-k)/2} \right\}^{\left(\frac{\min\{d-k,k\}}{\alpha_k-k} - \varepsilon \right)^\ell} \right). \end{aligned}$$

Due to our assumption that $k < \alpha_k < \min\{2k, d\}$, the last sum is finite and by choosing f_0 large enough this lower bound can be made arbitrarily close to 1.

If $\alpha_d < d$ we can look at the classic Poisson Boolean model with balls as convex grains with radius $D^{(d)}$. Then this grains distribution is dense and therefore also robust. In the case that there exists k such that $\alpha_k = k$, we can choose $f_n = f_0^n$ for $n \in \mathbb{N}$ with $f_0 > 0$ large enough. Using $(A_n)_{n \in \mathbb{N}}$ as before we get by the same arguments

$$\mathbb{P}(A_0) \geq 1 - \exp(-uf_0^{d-k-\varepsilon})$$

and

$$\begin{aligned} \mathbb{P}(A_{n+1}^c | A_n) &\leq \exp(-ucf_{n+1}^{-\varepsilon} f_n^{\min\{d-k,k\}}) \\ &= \exp(-ucf_0^{-\varepsilon(n+1)+\min\{d-k,k\}n}). \end{aligned}$$

The rest of the calculation can be done analogously to the calculation for $\alpha_k \neq k$ by choosing $\varepsilon > 0$ small enough. \square

2.2.3 Specific criteria for robustness

In this section we are dealing with the diameters that are strongly correlated as follows. Let D be regularly varying with index $-\alpha_1 < 0$. Let $D^{(1)} = D$ and, for $k \in \{2, \dots, d\}$, let $\gamma_k \in (0, 1)$ and $D^{(k)} = D^{\gamma_k}$, i.e. $D^{(k)}$ is regularly varying with parameter $\alpha_k = \frac{\alpha_1}{\gamma_k}$. To get the correct ordering of the diameters we use $\gamma_j \geq \gamma_{j+1}$.

Proof of Theorem 2.2, part two. The proof is similar to the one in the previous

section. We therefore only point out the differences here and omit the details that remain unchanged. As before let $k \in \{1, \dots, d-1\}$. Note that we still assume that $\alpha_k > k$. Furthermore, we only need to argue the case $k \leq \lfloor d/2 \rfloor$, since the case $k > \lfloor d/2 \rfloor$ follows from the previous section. We consider, as in the previous proof, a threshold sequence; let $(\tilde{f}_n)_{n \in \mathbb{N}}$ be this sequence defined as

$$\tilde{f}_n := \tilde{f}_{n-1}^{\frac{k + \frac{1}{\gamma_k} \sum_{j=k+1}^{d-k} \gamma_j}{\alpha_k - k} - \epsilon},$$

where $\tilde{f}_0 > 1$ will be set large later in the proof. Let also $0 < \epsilon < \frac{1}{4}$ be small enough to obtain that the exponent is strictly bigger than one in order to guarantee that the sequence is increasing. Note that due to our assumption this is possible.

We argue again that an infinite path exists in the Palm version of the process. For this we need again a sequence of events $(\tilde{A}_n)_{n \in \mathbb{N}}$ that describe the properties of this infinite path. The first element of the sequence remains unchanged, i.e. $\tilde{A}_0 := A_0$. For $n \in \mathbb{N}$ we need to make some further changes to the definitions of the relevant sets. For $\mathbf{x} \in \mathcal{X}$ we modify the set $O_i(\mathbf{x})$ and instead consider the set

$$\tilde{O}_i(\mathbf{x}) := \left\{ \begin{array}{l} y \in \mathbb{R}^d : |x - y| \in [\frac{1}{2}\tilde{f}_i, \tilde{f}_i], \angle(x - y, v) > \varphi, \\ \text{for } v \in \text{span}\{p_x^{(j)} : 1 \leq j \leq d-1\} \end{array} \right\},$$

with $\varphi = 2^{-(d+1)}(d+1)^{-1}$. The relevant change here is that compared to $O_i(\mathbf{x})$ we impose requirements on the orientations $p_x^{(k+1)}, \dots, p_x^{(d-1)}$. For $n \in \mathbb{N}$ we define

$$\tilde{A}_n := \left\{ \begin{array}{l} \exists \mathbf{x}_1, \dots, \mathbf{x}_n \in \mathcal{X} : \mathbf{x}_i \neq \mathbf{x}_m \text{ for all } i \neq m, D_{x_i}^{(k)} \geq 2^{2(d-1)+\epsilon} \tilde{f}_i, \\ x_i \in \tilde{O}_i(\mathbf{x}_{i-1}) \text{ and } C_{x_i} \cap B_{\tilde{f}_{i-1}}^*(\mathbf{x}_{i-1}, x_i) \neq \emptyset \text{ for all } 1 \leq i \leq n \end{array} \right\}.$$

Compared to $(A_n)_{n \in \mathbb{N}}$ we have that we additionally do not allow x_i to lie “to close” to the affine subspace through x_{i-1} spanned by the orientations $p_{x_{i-1}}^{(1)}, \dots, p_{x_{i-1}}^{(d-1)}$ of first $d-1$ diameters of \mathbf{x}_{i-1} for all $i \in \{1, \dots, n\}$. All other properties of $(A_n)_{n \in \mathbb{N}}$ still hold for $(\tilde{A}_n)_{n \in \mathbb{N}}$ by replacing $(f_n)_{n \in \mathbb{N}}$ by the new threshold sequence $(\tilde{f}_n)_{n \in \mathbb{N}}$.

To get now a suitable lower bound for $\mathbb{P}(\tilde{A}_n)$ we find similarly as before an upper bound for $\mathbb{P}[\tilde{A}_{n+1}^c | \tilde{A}_n]$. We use the same considerations as in the previous section but replace the definition for $x, y \in \mathbb{R}^d$ of $Q_{f_n}(x, y)$ by

$$\begin{aligned} \tilde{Q}_{\tilde{f}_n}(x, y) := \text{rot}_{\rho_{x,y}} \Big(& \text{conv} \left(\left\{ -\frac{\tilde{f}_n^{\gamma_{k+i}/\gamma_k}}{2} e_i, \frac{\tilde{f}_n^{\gamma_{k+i}/\gamma_k}}{2} e_i : 1 \leq i \leq d-k \right\} \right. \\ & \left. \cup \left\{ -\frac{\tilde{f}_n}{2} e_m, \frac{\tilde{f}_n}{2} e_m : d-k+1 \leq m \leq d \right\} \right) \Big) + x. \end{aligned}$$

and define

$$\tilde{Q}_{\tilde{f}_n}^*(x, y) := P_{H_{x-y}}(\tilde{Q}_{\tilde{f}_n}(x, y)).$$

Recall that the key step of the calculation in the previous section was to find a lower bound for $\mathbb{P}_C((x+C) \cap Q_{f_n}^*(x_n, x) \neq \emptyset \mid D_C^{(k)} \geq 2^{2(d-1)+\epsilon} f_{n+1}) \mathbb{P}_C(D_C^{(k)} \geq 2^{2(d-1)+\epsilon} f_{n+1})$. Using the same reasoning as there, we get

$$\begin{aligned} \mathbb{P}_C((x+C) \cap \tilde{Q}_{\tilde{f}_n}^*(x_n, x) \neq \emptyset \mid D_C^{(k)} \geq 2^{2(d-1)+\epsilon} \tilde{f}_{n+1}) & \mathbb{P}_C(D_C^{(k)} \geq 2^{2(d-1)+\epsilon} \tilde{f}_{n+1}) \\ & \geq c \frac{\tilde{f}_n^{k+\frac{1}{\gamma_k} \sum_{j=k+1}^{d-k} \gamma_j}}{\tilde{f}_{n+1}^{d-k}} \tilde{f}_{n+1}^{-(\alpha_k+\epsilon)}, \end{aligned} \quad (2.9)$$

where the extra term in the exponent of \tilde{f}_n is given due to the bigger area that is crucial for the intersection of $C_{x_{n+1}}$ and C_{x_n} . Completing the calculation with this new lower bound we get that

$$\mathbb{P}(\tilde{A}_n) \geq 1 - 2 \exp(-uc f_0^{d-\alpha_k-\epsilon}) - 2 \sum_{\ell=0}^{\infty} \exp\left(-uc \left\{ f_0^{\epsilon(\alpha_k-k)/2} \right\} \left(\frac{k+\frac{1}{\gamma_k} \sum_{j=k+1}^{d-k} \gamma_j}{\alpha_k-k} - \epsilon \right)^\ell\right).$$

The sum is finite due to our assumption $\alpha_1 < 2k\gamma_k + \sum_{j=k+1}^{d-k} \gamma_j$ as this can be translated to the inequality $\alpha_k < 2k + \frac{1}{\gamma_k} \sum_{j=k+1}^{d-k} \gamma_j$ and this lower bound is strictly positive by choosing f_0 large enough. \square

Remark 2.2.2. The model in this section is a reparametrisation of ellipsoids with strongly dependent axes which can be found in Chapter 4, obtained by setting $\gamma_k = \frac{\beta_{d-k+1}}{\beta_d}$ for $k \in \{1, \dots, d\}$. This can be seen by $D^{(k)}$ is regularly varying with parameter $-\frac{\alpha}{\gamma_k} = -\frac{1}{\beta_{d-k+1}}$ for $k \in \{1, \dots, d\}$.

2.2.4 Specific criteria for non-robustness

In this section we prove non-robustness for a generalisation of the 2-dimensional ellipses model of [53] in higher dimension. Since the second criterion of Theorem 2.3 is true by dominating the model with a Poisson Boolean model with

balls of radius $D^{(1)}$, we only have to argue the first criterion, that is, we prove that if $\text{Vol}(C) \in \mathcal{L}^2$ and $\alpha_k > 2k$ for some $k \in \{1, \dots, d-1\}$ the grain distribution is non-robust. The proof is based on the idea of Section 4 in [31]. We show that in the Palm version of the point process the expected number of vertices that are connected by a path to the origin is finite for small enough intensity u . The result follows from this. Note again that $c \in (0, \infty)$ is a generic constant just depending on the model parameters and may change in different inequalities.

Proof of Theorem 2.3. We prove our claim by induction and use throughout the proof the notation

$$\sum_{\mathbf{x}_1, \dots, \mathbf{x}_n \in \mathcal{X}}^{\neq} \prod_{i=1}^n \mathbb{1}_{\mathbf{x}_{i-1} \sim \mathbf{x}_i} := \left| \left\{ \mathbf{x}_n \in \mathcal{X} : \sum_{\mathbf{x}_1, \dots, \mathbf{x}_{n-1} \in \mathcal{X}} \prod_{i=1}^n \mathbb{1}_{\mathbf{x}_{i-1} \sim \mathbf{x}_i} > 0 \right\} \right|,$$

that is the number of vertices \mathbf{x}_n that are the final vertex of a path of length n starting in the vertex \mathbf{x}_0 .

Assuming without loss of generality that the origin is the location of a vertex of \mathcal{X} we are first interested in the expected number of vertices that are connected to the origin via a path of length two. This is given by

$$\mathbb{E}_0 \left[\sum_{\mathbf{y} \in \mathcal{X}} \mathbb{1}_{\mathbf{0} \sim \mathbf{y}} \right] = \mathbb{E}_0 \left[\sum_{\mathbf{x}, \mathbf{y} \in \mathcal{X}}^{\neq} \mathbb{1}_{\mathbf{0} \sim \mathbf{x}} \mathbb{1}_{\mathbf{x} \sim \mathbf{y}} \right].$$

After finding an upper bound for this expectation, we will bound

$$\mathbb{E}_0 \left[\sum_{\mathbf{x} \in \mathcal{X}} \mathbb{1}_{\mathbf{0} \sim \mathbf{x}}^n \right] = \mathbb{E}_0 \left[\sum_{\mathbf{x}_1, \dots, \mathbf{x}_n \in \mathcal{X}}^{\neq} \prod_{i=1}^n \mathbb{1}_{\mathbf{x}_{i-1} \sim \mathbf{x}_i} \right]$$

from above for $\mathbf{x}_0 = \mathbf{0}$, first for $n \in \mathbb{N}$ even and after that for n odd, and show that choosing u small enough ensures that

$$\sum_{n \in \mathbb{N}} \mathbb{E}_0 \left[\sum_{\mathbf{x} \in \mathcal{X}} \mathbb{1}_{\mathbf{0} \sim \mathbf{x}}^n \right] < \infty.$$

Note that the upper bound for the case $n = 1$ is already done in the proof of Proposition 2.1. To bound the expectations from above we dominate our model by replacing the convex body C with diameters $D^{(1)}, \dots, D^{(d)}$ with rectangles \bar{R} similar to Section 2.2.1. Instead of C_x we look at rectangles \bar{R}_x taken as the sum of x and the cartesian product of the intervals $[-\bar{D}_x^{(i)}, \bar{D}_x^{(i)}]$ with respect

to the orthonormal basis given by directions $p_{C_x}^{(i)}$, where we use the notation

$$\bar{L} := \min\{n \in \mathbb{N} : n > L\}, \text{ for } L \geq 0.$$

Note that the tails of $\bar{D}^{(1)}, \dots, \bar{D}^{(d)}$ can also be bounded via suitable Potter bounds since $D^{(1)}, \dots, D^{(d)}$ are regularly varying. For $\mathbf{x}, \mathbf{y} \in \mathcal{X}$ we get

$$\mathbb{1}_{C_x \cap C_y \neq \emptyset} \leq \mathbb{1}_{\bar{R}_x \cap \bar{R}_y \neq \emptyset}.$$

We therefore get, by denoting $\bar{D} := (\bar{D}^{(1)}, \dots, \bar{D}^{(d)})$,

$$\begin{aligned} \mathbb{E}_0 \left[\sum_{\mathbf{y} \in \mathcal{X}} \mathbb{1}_{\mathbf{0} \sim \mathbf{y}} \right] &\leq \mathbb{E}_0 \left[\sum_{\mathbf{y} \in \mathcal{X}} \mathbb{1}_{y \in 2\bar{R}_0} \right] + \mathbb{E}_0 \left[\sum_{\mathbf{y} \in \mathcal{X}} \mathbb{1}_{y \in (2\bar{R}_y - y)} \right] \\ &\quad + \mathbb{E}_0 \left[\sum_{j_0, j_2 \in \mathbb{N}^d} \sum_{\mathbf{x}, \mathbf{y} \in \mathcal{X}} \mathbb{1}_{\mathbf{0} \sim \mathbf{x}} \mathbb{1}_{\mathbf{x} \sim \mathbf{y}} \mathbb{1}_{\bar{D}_0 = j_0} \mathbb{1}_{\bar{D}_y = j_2} \mathbb{1}_{y \notin 2\bar{R}_0} \mathbb{1}_{0 \notin 2\bar{R}_y} \mathbb{1}_{\bar{R}_0 \cap \bar{R}_y = \emptyset} \right], \end{aligned} \tag{2.10}$$

bounding the expectation from above by counting every vertex in $2\bar{R}_0$, every vertex \mathbf{y} such that $0 \in 2\bar{R}_y$, and for every other vertex \mathbf{y} all the vertices \mathbf{x} connected by an edge to $\mathbf{0}$ and \mathbf{y} . In addition, we have rewritten the second term using distributional symmetry.

We now focus on the last term in the expression. Recall that $\rho_{v,w}$ is the orientation of the vector $v - w$. Set

$$\mathcal{W}_{w,v}^- := \text{rot}_{\rho_{v,w}}((-\infty, 0] \times \mathbb{R}^{d-1}) + w, \quad \mathcal{W}_{w,v}^+ := \text{rot}_{\rho_{v,w}}([0, \infty) \times \mathbb{R}^{d-1}) + v,$$

and $\mathcal{W}_{w,v} := \mathbb{R}^d \setminus (\mathcal{W}_{w,v}^- \cup \mathcal{W}_{w,v}^+)$. Define for $\mathbf{w}, \mathbf{v} \in \mathcal{X}$ the sets $\mathcal{T}_{\mathbf{w},\mathbf{v}} := \mathcal{T}(\mathbf{w}, \mathbf{v}) \cup \mathcal{T}(\mathbf{v}, \mathbf{w})$ where \mathcal{T} is given as

$$\begin{aligned} \mathcal{T}(\mathbf{w}, \mathbf{v}) := \left\{ \text{rot}_{\rho_{v,w}} \left(\{ \bar{D}_w^{(d)} + \lambda \} \times \bigtimes_{i=1}^{d-1} [-\bar{D}_w^{(i)} - f_i(\mathbf{w}, \mathbf{v}, \lambda), \bar{D}_w^{(i)} + f_i(\mathbf{w}, \mathbf{v}, \lambda)] \right) \right. \\ \left. + w : \lambda \in (0, \infty) \right\} \end{aligned}$$

with

$$f_i(\mathbf{w}, \mathbf{v}, \lambda) := \lambda \frac{\bar{D}_v^{(i)} - \bar{D}_w^{(i)}}{|v - w| - \bar{D}_v^{(d)} - \bar{D}_w^{(d)}} \mathbb{1}_{\bar{D}_v^{(i)} \geq \bar{D}_w^{(i)}} + (\bar{D}_v^{(i)} - \bar{D}_w^{(i)}) \mathbb{1}_{\bar{D}_v^{(i)} < \bar{D}_w^{(i)}},$$

for $1 \leq i < d$. We define a partition $(\mathcal{A}_m(\mathbf{w}, \mathbf{v}))_{m=1, \dots, 8}$ of \mathbb{R}^d which only depends on the locations w and v and the corresponding diameters of \mathbf{w} and

\mathbf{v} , as

$$\begin{aligned}\mathcal{A}_1(\mathbf{w}, \mathbf{v}) &:= \text{rot}_{\rho_{v,w}} \left([-\bar{D}_w^{(d)}, \bar{D}_w^{(d)}] \times \bigtimes_{i=1}^{d-1} [-\bar{D}_w^{(i)}, \bar{D}_w^{(i)}] \right) + w, \\ \mathcal{A}_2(\mathbf{w}, \mathbf{v}) &:= \mathcal{A}_1(\mathbf{v}, \mathbf{w})\end{aligned}\tag{2.11}$$

$$\begin{aligned}\mathcal{A}_3(\mathbf{w}, \mathbf{v}) &:= \mathcal{T}_{\mathbf{w}, \mathbf{v}} \cap \mathcal{W}_{w,v}^- \setminus (\mathcal{A}_1(\mathbf{w}, \mathbf{v}) \cup \mathcal{A}_2(\mathbf{w}, \mathbf{v})), \\ \mathcal{A}_4(\mathbf{w}, \mathbf{v}) &:= \mathcal{T}_{\mathbf{w}, \mathbf{v}} \cap \mathcal{W}_{w,v}^+ \setminus (\mathcal{A}_1(\mathbf{w}, \mathbf{v}) \cup \mathcal{A}_2(\mathbf{w}, \mathbf{v})), \\ \mathcal{A}_5(\mathbf{w}, \mathbf{v}) &:= \mathcal{T}_{\mathbf{w}, \mathbf{v}} \cap \mathcal{W}_{w,v} \setminus (\mathcal{A}_1(\mathbf{w}, \mathbf{v}) \cup \mathcal{A}_2(\mathbf{w}, \mathbf{v})), \\ \mathcal{A}_6(\mathbf{w}, \mathbf{v}) &:= \mathcal{W}_{w,v}^- \setminus (\mathcal{T}_{\mathbf{w}, \mathbf{v}} \cup \mathcal{A}_1(\mathbf{w}, \mathbf{v}) \cup \mathcal{A}_2(\mathbf{w}, \mathbf{v})), \\ \mathcal{A}_7(\mathbf{w}, \mathbf{v}) &:= \mathcal{W}_{w,v} \setminus (\mathcal{T}_{\mathbf{w}, \mathbf{v}} \cup \mathcal{A}_1(\mathbf{w}, \mathbf{v}) \cup \mathcal{A}_2(\mathbf{w}, \mathbf{v})), \\ \mathcal{A}_8(\mathbf{w}, \mathbf{v}) &:= \mathcal{W}_{w,v}^+ \setminus (\mathcal{T}_{\mathbf{w}, \mathbf{v}} \cup \mathcal{A}_1(\mathbf{w}, \mathbf{v}) \cup \mathcal{A}_2(\mathbf{w}, \mathbf{v})).\end{aligned}$$

Figure 2.4 on the current page is a visualisation of $\mathcal{T}_{\mathbf{w}, \mathbf{v}}$ as a union of $\mathcal{T}(\mathbf{w}, \mathbf{v})$

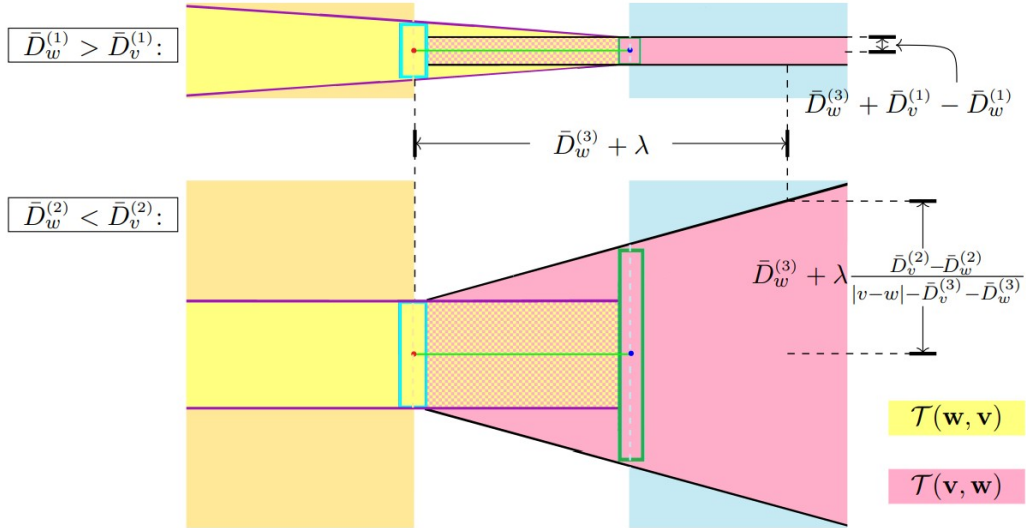


Figure 2.4: Visualisation of $\mathcal{T}_{\mathbf{w}, \mathbf{v}}$ in 3 dimensions by colouring of the different parts of $\mathcal{T}(\mathbf{w}, \mathbf{v})$ and $\mathcal{T}(\mathbf{v}, \mathbf{w})$. The perspective in the top figure is along $\text{rot}_{\rho_{v,w}}(e_2)$ and along $\text{rot}_{\rho_{v,w}}(e_3)$ in the bottom figure. The turquoise rectangle represents the set $\text{rot}_{\rho_{v,w}}([- \bar{D}_w^{(d)}, \bar{D}_w^{(d)}] \times \bigtimes_{i=1}^{d-1} [- \bar{D}_w^{(i)}, \bar{D}_w^{(i)}])$ and the dark green one represents $\text{rot}_{\rho_{v,w}}([- \bar{D}_v^{(d)}, \bar{D}_v^{(d)}] \times \bigtimes_{i=1}^{d-1} [- \bar{D}_v^{(i)}, \bar{D}_v^{(i)}])$. The light orange area and the area on the left side of the orange dashed line is $\mathcal{W}_{w,v}^-$ and the light blue area and the area on the right side of the blue dashed line $\mathcal{W}_{w,v}^+$. The green line is the connection line of w and v given as the red and blue point. The purple lines are $f_i(w, v, \lambda)$ and the black lines $f_i(v, w, \lambda)$ for $i \in \{2, 3\}$ and $\lambda > 0$.

and $\mathcal{T}(\mathbf{v}, \mathbf{w})$. To help with understanding how $\mathcal{T}_{\mathbf{w}, \mathbf{v}}$ relates to the partition $(\mathcal{A}_m(\mathbf{w}, \mathbf{v}))_{m=1, \dots, 8}$, see also Figures 2.5(a) to 2.5(c) on the facing page. In all sub-figures of Figure 2.5, $\mathcal{T}_{\mathbf{w}, \mathbf{v}}$ is the union of the black (middle), pink

(rightmost) and red (leftmost) shaped volumes. In Figure 2.5(c) the red (left) plane is the boundary of $\mathcal{W}_{w,v}^-$ and the pink (right) plane the boundary of $\mathcal{W}_{w,v}^+$. It is now possible to recognise the partition $(\mathcal{A}_m(\mathbf{w}, \mathbf{v}))_{m=1,\dots,8}$: The set $\mathcal{A}_1(\mathbf{w}, \mathbf{v})$ is the turquoise part and $\mathcal{A}_2(\mathbf{w}, \mathbf{v})$ the dark blue part. Furthermore $\mathcal{A}_3(\mathbf{w}, \mathbf{v})$, $\mathcal{A}_4(\mathbf{w}, \mathbf{v})$ and $\mathcal{A}_5(\mathbf{w}, \mathbf{v})$ are given respectively by the red, pink and black shapes in the figures. In Figure 2.5(a) and 2.5(b) we see that $\mathcal{A}_6(\mathbf{w}, \mathbf{v})$ is the white part on the left side of the first orthogonal black line including the line itself, $\mathcal{A}_7(\mathbf{w}, \mathbf{v})$ the white part between both orthogonal black lines and $\mathcal{A}_8(\mathbf{w}, \mathbf{v})$ the white part on the right side of the second orthogonal black line, again including the line itself. Looking at Figure 2.5(c), the first black line is the red plane and the second black line the pink plane, i.e. $\mathcal{A}_6(\mathbf{w}, \mathbf{v})$ is the white part on the left side of the red plane joined with the red plane, $\mathcal{A}_7(\mathbf{w}, \mathbf{v})$ the white part between the red and pink plane and $\mathcal{A}_8(\mathbf{w}, \mathbf{v})$ the white part on the right side of the pink plane joined with the pink plane.

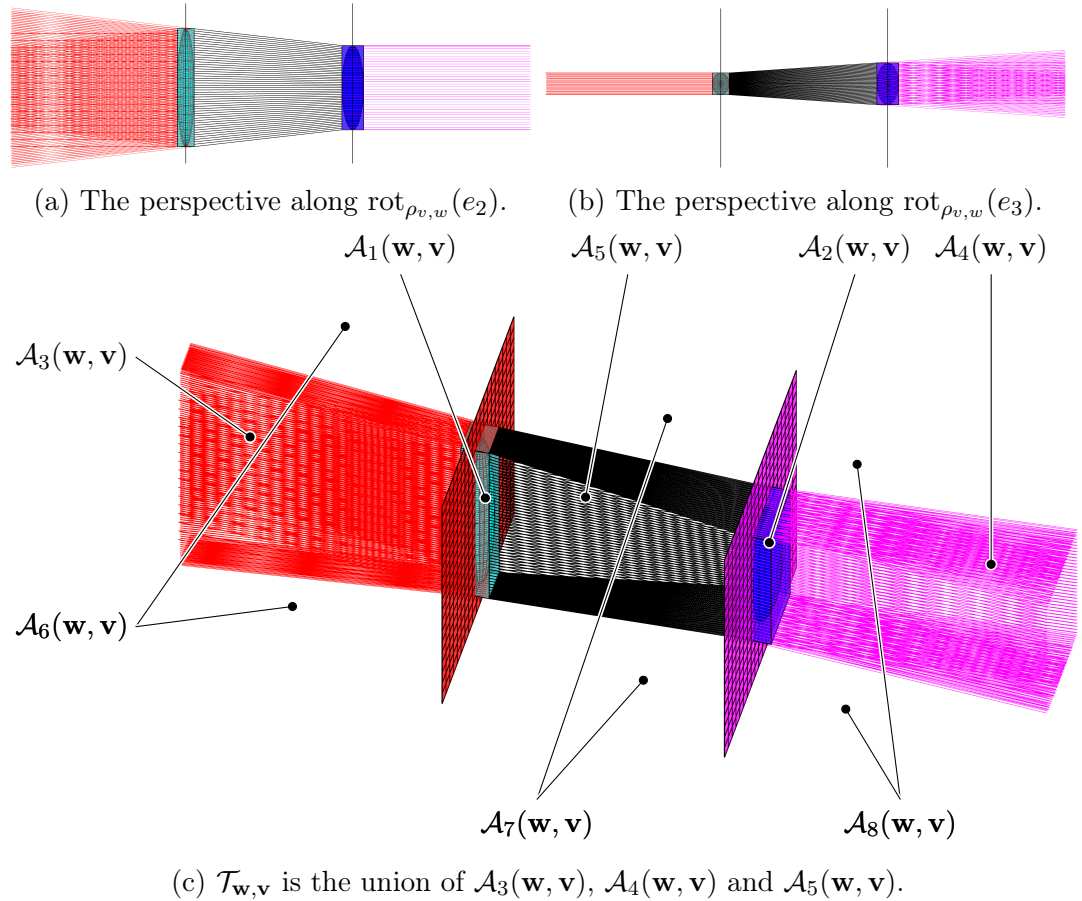


Figure 2.5: The partition $(\mathcal{A}_m(\mathbf{w}, \mathbf{v}))_{m=1,\dots,8}$ of \mathbb{R}^3 from various perspectives.

We now return to considering the full expression in (2.10). Using the above partition and setting p_q to be the probability that $(\bar{D}^{(i)})_{i \in \{1, \dots, d\}}$ is equal to $q \in \mathbb{N}^d$, we can upper bound (2.10) by

$$\begin{aligned}
 & u[M] \sum_{j_0 \in \mathbb{N}^d} p_{j_0} \prod_{i=1}^{d-1} 4j_0^{(i)} + u[M] \sum_{j_2 \in \mathbb{N}^d} p_{j_2} \prod_{i=1}^{d-1} 4j_2^{(i)} \\
 & + \sum_{m=1}^8 \mathbb{E}_0 \left[\sum_{j_0, j_2 \in \mathbb{N}^d} \sum_{\mathbf{x}, \mathbf{y} \in \mathcal{X}} \mathbb{1}_{\mathbf{0} \sim \mathbf{x}} \mathbb{1}_{\mathbf{x} \sim \mathbf{y}} \mathbb{1}_{\bar{D}_0 = j_0} \mathbb{1}_{\bar{D}_y = j_2} \mathbb{1}_{x \in \mathcal{A}_m(\mathbf{0}, \mathbf{y})} \mathbb{1}_{y \notin 2\bar{R}_0} \mathbb{1}_{0 \notin 2\bar{R}_y} \mathbb{1}_{\bar{R}_0 \cap \bar{R}_y = \emptyset} \right] \\
 & =: u4^d [M] \sum_{j_0, j_2 \in \mathbb{N}^d} p_{j_0} p_{j_2} \left(\prod_{i=1}^{d-1} j_0^{(i)} + \prod_{i=1}^{d-1} j_2^{(i)} \right) + \sum_{m=1}^8 S_m, \tag{2.12}
 \end{aligned}$$

where each individual S_m corresponds to the expectation in (2.12) within the area \mathcal{A}_m . Recall that $\bar{D}^{(d)} \leq [M]$ almost surely by definition of the generalisation of the ellipses model as we have $k \in \{1, \dots, d-1\}$; this is where the $[M]$ term in the previous bound comes from. Note that we have $p_q = 0$ for all q in

$$\{q = (q^{(1)}, \dots, q^{(d)}) : q^{(i)} \geq [\epsilon], i \leq k, q^{(j)} \leq [M], \forall j \geq k+1\}^c.$$

Since we use the structure of the proof on the example in Chapter 4 we keep the notation general with $q = (q^{(1)}, \dots, q^{(d)}) \in \mathbb{N}^d$ and do not use, for example, $(j_0^{(1)})^k [M]^{d-k}$ when looking at an upper bound for $[M] \prod_{i=1}^{d-1} j_0^{(i)}$.

We abbreviate $\gamma = 2j_0^{(d)}$ and get upper bounds for $(S_m)_{m=1, \dots, 8}$ as

$$S_m \leq u^2 \sum_{j_0, j_2 \in \mathbb{N}^d} p_{j_0} p_{j_2} \int_{\mathbb{R}^d \setminus B_\gamma(0)} \int_{\mathcal{A}_m(\mathbf{0}, \mathbf{y})} \mathbb{P}_{0, x, y}(\mathbf{0} \sim \mathbf{x}, \mathbf{x} \sim \mathbf{y}, \mathbf{0} \not\sim \mathbf{y}, 0 \notin 2\bar{R}_y) d\lambda(x) d\lambda(y).$$

Looking at $\mathbb{P}_{0, x, y}(\mathbf{0} \sim \mathbf{x}, \mathbf{x} \sim \mathbf{y}, \mathbf{0} \not\sim \mathbf{y}, 0 \notin 2\bar{R}_y)$ we use that the event $\{\mathbf{0} \sim \mathbf{x}, \mathbf{x} \sim \mathbf{y}\}$ roughly corresponds to the event that the diameters of \mathbf{x} are “big enough” and their orientations are “good enough” so that intersections of the rectangles \bar{R}_0 and \bar{R}_x , and of \bar{R}_x and \bar{R}_y are possible. In addition to that we bound the permissible area for the orientation of the diameters of \bar{R}_x from above by assuming that the largest face of \bar{R}_0 , resp. \bar{R}_y , is perpendicular to the vector $x \in \mathbb{R}^d$, resp. $y - x \in \mathbb{R}^d$. It can easily be checked that given j_0 , resp. j_2 , the set of rotations that result in an intersection under this assumption

is larger than for any other rotation of \bar{R}_0 , resp. \bar{R}_y . We have

$$\mathbb{P}_{0,x,y} \left(\mathbf{0} \sim \mathbf{x}, \mathbf{x} \sim \mathbf{y}, \begin{array}{l} \mathbf{0} \not\sim \mathbf{y}, 0 \notin 2\bar{R}_y \\ \bar{R}_0 \cap \bar{R}_x \neq \emptyset, \bar{R}_x \cap \bar{R}_y \neq \emptyset, \mathbf{0} \not\sim \mathbf{y}, 0 \notin 2\bar{R}_y \end{array} \right) \leq \mathbb{P}_{0,x,y} \left(\begin{array}{l} \bar{D}_x^{(k)} \geq \max(\text{dist}(\bar{R}_0, x), \text{dist}(\bar{R}_y, x)), \\ \bar{R}_0 \cap \bar{R}_x \neq \emptyset, \bar{R}_x \cap \bar{R}_y \neq \emptyset, \mathbf{0} \not\sim \mathbf{y}, 0 \notin 2\bar{R}_y \end{array} \right). \quad (2.13)$$

Looking now just at the first summand S_1 from (2.12) and considering a given pair $j_0, j_2 \in \mathbb{N}^d$, we can bound the integral of S_1 from above by

$$\begin{aligned} & \int_{\mathbb{R}^d \setminus B_\gamma(0)} \int_{\mathcal{A}_1(\mathbf{0}, \mathbf{y})} \mathbb{P}_{0,x,y} \left(\begin{array}{l} \bar{D}_x^{(k)} \geq \max(\text{dist}(\bar{R}_0, x), \text{dist}(\bar{R}_y, x)), \\ \bar{R}_0 \cap \bar{R}_x \neq \emptyset, \bar{R}_x \cap \bar{R}_y \neq \emptyset, \mathbf{0} \not\sim \mathbf{y} \end{array} \right) d\lambda(x) d\lambda(y) \\ & \leq \int_{\mathbb{R}^d \setminus B_\gamma(0)} \int_{\mathcal{A}_1(\mathbf{0}, \mathbf{y})} c(|x| + |y|)^{-(\alpha_k - \varepsilon)} \prod_{s=1}^{d-k} \frac{j_2^{(s)}}{|x| + |y|} d\lambda(x) d\lambda(y), \end{aligned}$$

where we used that $\max\{\text{dist}(\bar{R}_0, x), \text{dist}(\bar{R}_y, x)\} \asymp |x| + |y|$ and the above assumption on the orientation of \bar{R}_x . We also used the Potter bounds resulting in the ε term. Note that similar Potter bounds will also appear in the upper bounds of S_m for $m \in \{2, 3, \dots, 8\}$. Using that the exponent $-(\alpha_k - \varepsilon + d - k)$ is negative we bound $|x|$ from below by 0 and obtain the following upper bound for the last expression

$$\begin{aligned} & \prod_{s=1}^{d-k} j_2^{(s)} \int_{\mathbb{R}^d \setminus B_\gamma(0)} c|y|^{-(\alpha_k - \varepsilon + d - k)} \lambda(\mathcal{A}_1(\mathbf{0}, \mathbf{y})) d\lambda(y) \\ & \leq c \prod_{s=1}^{d-1} j_2^{(s)} \prod_{l=1}^{d-1} j_0^{(l)} \int_{\mathbb{R}^d \setminus B_1(0)} |y|^{-(\alpha_k - \varepsilon + d - k)} d\lambda(y) \\ & = c \prod_{s=1}^{d-1} j_2^{(s)} \prod_{l=1}^{d-1} j_0^{(l)} \int_1^\infty r^{-(\alpha_k - \varepsilon + d - k - d + 1)} dr, \end{aligned}$$

while $c \in (0, \infty)$ depends additionally here and also in the rest of the section on M . In the inequality we also use that the diameters of \bar{R}_0 are all at least 1, which has as a consequence that $|y| \geq 1$. Remember that the Potter bounds are given for every $\varepsilon > 0$ and so taking ε small enough, the last integral is finite if $\alpha_k > k$, which is the case. We consequently have

$$S_1 \leq cu^2 \sum_{j_0, j_2 \in \mathbb{N}^d} p_{j_0} p_{j_2} \prod_{s=1}^{d-1} j_2^{(s)} \prod_{l=1}^{d-1} j_0^{(l)}, \quad (2.14)$$

and can obtain an analogous upper bound for S_2 , namely

$$S_2 \leq cu^2 \sum_{j_0, j_2 \in \mathbb{N}^d} p_{j_0} p_{j_2} \prod_{s=1}^{d-1} j_0^{(s)} \prod_{l=1}^{d-1} j_2^{(l)}. \quad (2.15)$$

By using similar observations, i.e. $\max\{\text{dist}(\bar{R}_0, x), \text{dist}(\bar{R}_y, x)\} \asymp |x| + |y|$ in $\mathcal{A}_m(\mathbf{0}, \mathbf{y})$ for $m \in \{3, 4, 6, 7, 8\}$ and $\max\{\text{dist}(\bar{R}_0, x), \text{dist}(\bar{R}_y, x)\} \asymp |y|$ in $\mathcal{A}_5(\mathbf{0}, \mathbf{y})$, the calculation of the upper bounds of S_m for $m \geq 3$ can be related to the bounds for S_1 and S_2 as follows. For S_3 we, like before, focus first on the integral with fixed $j_0, j_2 \in \mathbb{N}^d$ and get, defining $j := 2(j_0^{(d)} + j_2^{(d)})$, that

$$\begin{aligned} & \int_{\mathbb{R}^d \setminus B_j(0)} \int_{\mathcal{A}_3(\mathbf{0}, \mathbf{y})} \mathbb{P}_{0, x, y}(\mathbf{0} \sim \mathbf{x}, \mathbf{x} \sim \mathbf{y}, \mathbf{0} \not\sim \mathbf{y}, 0 \notin 2\bar{R}_y) \, d\lambda(x) d\lambda(y) \\ & \leq c \int_{\mathbb{R}^d \setminus B_j(0)} \int_{\mathcal{A}_3(\mathbf{0}, \mathbf{y})} \prod_{s=1}^{d-k} \frac{\min\{j_0^{(s)}, j_2^{(s)}\}}{|x| + |y|} (|x| + |y|)^{-(\alpha_k - \varepsilon)} \, d\lambda(x) d\lambda(y) \\ & \leq c \prod_{s=1}^{d-k} \min\{j_0^{(s)}, j_2^{(s)}\} \int_{\mathbb{R}^d \setminus B_j(0)} \int_{\mathcal{A}_3(\mathbf{0}, \mathbf{y})} (|x| + |y|)^{-(\alpha_k - \varepsilon + d - k)} \, d\lambda(x) d\lambda(y). \end{aligned}$$

In the first inequality we use the Potter bound to get $(|x| + |y|)^{-(\alpha_k - \varepsilon)}$. The product in the integral appears since we consider orientations of \bar{R}_0 and \bar{R}_y such that all of the diameters have pairwise the same orientation (i.e. the first diameter of \bar{R}_0 has the same orientation as the first diameter of \bar{R}_y , and similarly for the remaining $d - 1$ diameters), which gives an upper bound for the largest set of orientations of \bar{R}_x that result in an intersection with both. The $\min\{j_0^{(s)}, j_2^{(s)}\}$ part appears as \bar{R}_x has to intersect \bar{R}_0 and \bar{R}_y so that the minimum determines the size of this largest set. Together with $|x| + |y|$ and using Remark 2.2.1 this gives the probability of an appropriate orientation of \bar{R}_x existing.

The set $\mathcal{A}_3(\mathbf{0}, \mathbf{y})$ can be split in two parts. For that we define

$$\mathcal{A}'_3(\mathbf{0}, \mathbf{y}) := \text{rot}_{\rho_{y,0}}([- \bar{D}_0^{(d)}, \bar{D}_0^{(d)}] \times \mathbb{R}^{d-1}) + 0$$

and look at $\mathcal{A}_3(\mathbf{0}, \mathbf{y}) \cap \mathcal{A}'_3(\mathbf{0}, \mathbf{y})$ and $\mathcal{A}_3(\mathbf{0}, \mathbf{y}) \setminus \mathcal{A}'_3(\mathbf{0}, \mathbf{y})$. Since $-(\alpha_k - \varepsilon + d - k)$ is negative we can bound the first part of $\mathcal{A}_3(\mathbf{0}, \mathbf{y})$ from above via

$$c \prod_{s=1}^{d-k} \min\{j_0^{(s)}, j_2^{(s)}\} \int_{\mathbb{R}^d \setminus B_j(0)} \int_{\mathcal{A}_3(\mathbf{0}, \mathbf{y}) \cap \mathcal{A}'_3(\mathbf{0}, \mathbf{y})} (|x| + |y|)^{-(\alpha_k - \varepsilon + d - k)} \, d\lambda(x) d\lambda(y)$$

$$\begin{aligned}
 &\leq c \prod_{s=1}^{d-1} \min\{j_0^{(s)}, j_2^{(s)}\} \prod_{t=1}^{d-1} \max\{j_0^{(t)}, j_2^{(t)}\} \int_{\mathbb{R}^d \setminus B_j(0)} |y|^{-(\alpha_k - \varepsilon + d - k)} d\lambda(y) \\
 &\leq c \prod_{s=1}^{d-1} \min\{j_0^{(s)}, j_2^{(s)}\} \prod_{t=1}^{d-1} \max\{j_0^{(t)}, j_2^{(t)}\} \int_j^\infty r^{-(\alpha_k - \varepsilon + d - k - d + 1)} dr,
 \end{aligned}$$

which is finite for $\alpha_k > k$. In the first inequality we use that $|x| \geq 0$ and bound the volume of the first part of $\mathcal{A}_3(\mathbf{0}, \mathbf{y})$ from above by

$$c \prod_{t=1}^{d-1} \max\{j_0^{(t)}, j_2^{(t)}\}.$$

To see how, we use that the minimal distance of \bar{R}_0 and \bar{R}_y is bigger then

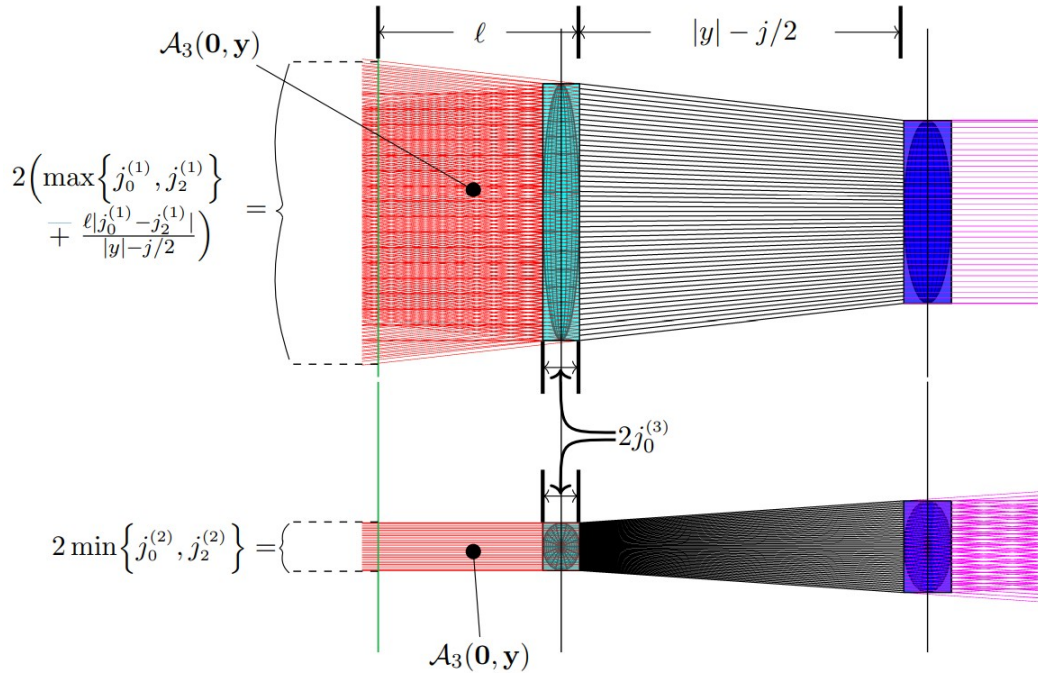


Figure 2.6: Visualisation of the role of ℓ in the calculation for S_3 , with the perspective along $\text{rot}_{\rho_{v,w}}(e_2)$ in the top and $\text{rot}_{\rho_{v,w}}(e_3)$ in the bottom figure. Note also that $\mathcal{A}'_3(\mathbf{0}, \mathbf{y})$ represents the everything “above” and “below” of the turquoise box including the box itself. Consequently, $\mathcal{A}_3(\mathbf{0}, \mathbf{y}) \cap \mathcal{A}'_3(\mathbf{0}, \mathbf{y})$ represents the two small red areas “above” and “below” the turquoise box.

$j_0^{(d)} + j_2^{(d)}$ so that the boundary of $\mathcal{A}_3(\mathbf{0}, \mathbf{y})$ has in the direction of the i th diameter of $\mathcal{A}_1(\mathbf{0}, \mathbf{y})$ distance from $\mathcal{A}_1(\mathbf{0}, \mathbf{y})$ given bounded from above by $\max\{j_0^{(i)}, j_2^{(i)}\}$ (see Figure 2.6). Looking now at $\mathcal{A}_3(\mathbf{0}, \mathbf{y}) \setminus \mathcal{A}'_3(\mathbf{0}, \mathbf{y})$ we are

interested in

$$\ell := \text{Dist}(x, \text{rot}_{\rho_{y,0}}(\{0\} \times \mathbb{R}^{d-1} + \bar{D}_0^{(d)} e_1) + 0),$$

that is, the distance from x to the hyperplane orthogonal to $y - 0$ and intersecting with $\mathcal{A}_1(\mathbf{0}, \mathbf{y})$ that is furthest away from x (see again Figure 2.6). This gives us the following upper bound for the second part of $\mathcal{A}_3(\mathbf{0}, \mathbf{y})$

$$\begin{aligned} & c \prod_{s=1}^{d-k} \min\{j_0^{(s)}, j_2^{(s)}\} \int_{\mathbb{R}^d \setminus B_j(0)} \int_{j_0^{(d)}}^{\infty} (\ell + |y|)^{-(\alpha_k - \varepsilon + d - k)} \prod_{t=1}^{d-1} 2 \left\{ \min\{j_0^{(t)}, j_2^{(t)}\} \mathbb{1}_{\min\{j_0^{(t)}, j_2^{(t)}\} = j_0^{(t)}} \right. \\ & \quad \left. + \left[\max\{j_0^{(t)}, j_2^{(t)}\} + \frac{\ell |j_0^{(t)} - j_2^{(t)}|}{|y| - j/2} \right] \mathbb{1}_{\max\{j_0^{(t)}, j_2^{(t)}\} = j_0^{(t)}} \right\} d\ell d\lambda(y) \\ & \leq c \prod_{s=1}^{d-k} \min\{j_0^{(s)}, j_2^{(s)}\} \prod_{t=1}^{d-1} \max\{j_0^{(t)}, j_2^{(t)}\} \int_{\mathbb{R}^d \setminus B_j(0)} \int_{j_0^{(d)}}^{\infty} (\ell + |y|)^{-(\alpha_k - \varepsilon + d - k)} \\ & \quad \times \left(1 + \frac{\ell}{|y| - j/2} \right)^{d-1} d\ell d\lambda(y) \\ & \leq c \prod_{s=1}^{d-1} \min\{j_0^{(s)}, j_2^{(s)}\} \prod_{t=1}^{d-1} \max\{j_0^{(t)}, j_2^{(t)}\} \int_j^{\infty} r^{d-1} (r/2)^{1-d} \int_{j_0^{(d)}}^{\infty} (\ell + r)^{-(\alpha_k - \varepsilon + 1 - k)} d\ell dr, \end{aligned}$$

where we used in the last inequality that $|y| \geq j$ to obtain the term $(r/2)^{1-d}$. This integral is finite if $\alpha_k > k + 1$, which is the case. In summary we get

$$S_3 \leq cu^2 \sum_{j_0, j_2 \in \mathbb{N}^d} p_{j_0} p_{j_2} \prod_{s=1}^{d-1} j_0^{(s)} j_2^{(s)}. \quad (2.16)$$

Using the symmetry of the partition we get the same upper bound for S_4 . For S_5 we get

$$\begin{aligned} & \int_{\mathbb{R}^d \setminus B_\gamma(0)} \int_{\mathcal{A}_5(\mathbf{0}, \mathbf{y})} \mathbb{P}_{0,x,y}(\mathbf{0} \sim \mathbf{x}, \mathbf{x} \sim \mathbf{y}, \mathbf{0} \not\sim \mathbf{y}, 0 \notin 2\bar{R}_y) d\lambda(x) d\lambda(y) \\ & \leq c \int_{\mathbb{R}^d \setminus B_\gamma(0)} \int_{\mathcal{A}_5(\mathbf{0}, \mathbf{y})} \prod_{s=1}^{d-k} \frac{\min\{j_0^{(s)}, j_2^{(s)}\}}{|y|} |y|^{-(\alpha_k - \varepsilon)} d\lambda(x) d\lambda(y). \end{aligned}$$

As before we used the Potter bound to get $|y|^{-(\alpha_k - \varepsilon)}$, and consider again that the orientations of \bar{R}_0 and \bar{R}_y are such that all of the diameters have pairwise

the same orientation. Additionally the smallest diameters are taken to have the same orientation as $|y|$. This gives us the largest possible area relative to the location of the connector \mathbf{x} , which we use to obtain an upper bound for the size of the sets of orientations that result in an intersection of \bar{R}_x with both \bar{R}_0 and \bar{R}_y , giving the stated inequality. For the orientation of \mathbf{x} we use Remark 2.2.1 as before.

Using how $\mathcal{A}_5(\mathbf{0}, \mathbf{y})$ is defined, we can bound the last expression from above as

$$\begin{aligned}
 c \int_{\mathbb{R}^d \setminus B_\gamma(0)} \prod_{s=1}^{d-k} \frac{\min\{j_0^{(s)}, j_2^{(s)}\}}{|y|} \lambda(\mathcal{A}_5(\mathbf{0}, \mathbf{y})) |y|^{-(\alpha_k - \varepsilon)} d\lambda(y) \\
 \leq c \prod_{s=1}^{d-1} \min\{j_0^{(s)}, j_2^{(s)}\} \int_{\mathbb{R}^d \setminus B_1(0)} |y| \prod_{t=1}^{d-1} (j_0^{(t)} + j_2^{(t)}) |y|^{-(\alpha_k - \varepsilon) - (d-k)} d\lambda(y) \\
 \leq c \prod_{s=1}^{d-1} \min\{j_0^{(s)}, j_2^{(s)}\} \prod_{t=1}^{d-1} (j_0^{(t)} + j_2^{(t)}) \int_1^\infty r^{-(\alpha_k - \varepsilon - k)} dr.
 \end{aligned}$$

As before, the last expression is finite, since $\alpha_k > 2k$ and therefore $\alpha_k > k + 1$ is fulfilled. For $t \in \{1, \dots, d-1\}$ we have $j_0^{(t)} + j_2^{(t)} \leq 2 \max\{j_0^{(t)}, j_2^{(t)}\}$, so we can bound S_5 from above by

$$S_5 \leq cu^2 \sum_{j_0, j_2 \in \mathbb{N}^d} p_{j_0} p_{j_2} \prod_{s=1}^{d-1} j_0^{(s)} j_2^{(s)}. \quad (2.17)$$

It remains to find bounds for S_6, S_7 and S_8 . As before it is enough to find upper bounds for S_6 and S_7 , as the upper bound for S_6 is also the upper bound for S_8 due to symmetry. For the integral of S_6 we get

$$\begin{aligned}
 \int_{\mathbb{R}^d \setminus B_\gamma(0)} \int_{\mathcal{A}_6(\mathbf{0}, \mathbf{y})} \mathbb{P}_{0,x,y}(\mathbf{0} \sim \mathbf{x}, \mathbf{x} \sim \mathbf{y}, \mathbf{0} \not\sim \mathbf{y}, 0 \notin 2\bar{R}_y) d\lambda(x) d\lambda(y) \\
 \leq c \int_{\mathbb{R}^d \setminus B_\gamma(0)} \int_{\mathcal{A}_6(\mathbf{0}, \mathbf{y})} \prod_{s=1}^{d-k} \frac{j_0^{(s)} j_2^{(s)}}{(|x| + |y|)^2} \max\{\text{dist}(\bar{R}_0, x), \text{dist}(\bar{R}_y, x)\}^{-(\alpha_k - \varepsilon)} d\lambda(x) d\lambda(y) \\
 \leq c \int_{\mathbb{R}^d \setminus B_\gamma(0)} \int_{\mathcal{A}_6(\mathbf{0}, \mathbf{y})} \prod_{s=1}^{d-k} \frac{j_0^{(s)} j_2^{(s)}}{(|x| + |y|)^2} (|x| + |y|)^{-(\alpha_k - \varepsilon)} d\lambda(x) d\lambda(y) \quad (2.18)
 \end{aligned}$$

$$= c \prod_{s=1}^{d-k} j_0^{(s)} j_2^{(s)} \int_{\mathbb{R}^d \setminus B_\gamma(0)} \int_{\mathcal{A}_6(\mathbf{0}, \mathbf{y})} (|x| + |y|)^{-(\alpha_k - \varepsilon + 2d - 2k)} d\lambda(x) d\lambda(y).$$

In the first inequality, the product is an upper bound for the probability that \bar{R}_0 and \bar{R}_y intersect with \bar{R}_x under the condition that the diameters are large enough to result in an intersection. As in the previous calculations, we used Remark 2.2.1. The second term, namely $\max\{\text{dist}(\bar{R}_0, x), \text{dist}(\bar{R}_y, x)\}^{-(\alpha_k - \varepsilon)}$ comes from the Potter bounds.

Remark 2.2.3. A careful reader might note that for S_6 , S_7 and S_8 it does not suffice that only the largest diameter of the connector is big. To ensure that \bar{R}_x intersects with \bar{R}_0 and \bar{R}_y , at least two of the diameters of \mathbf{x} have to be large enough.

Focusing now on the construction of $\mathcal{A}_6(\mathbf{0}, \mathbf{y})$, we begin by reformulating it. Using $j := 2(j_0^{(d)} + j_2^{(d)})$ as before, we define $a_i(\ell)$ for $i \in \{2, \dots, d\}$ and $\ell > 0$, as

$$a_i(\ell) := e_i \min\{j_0^{(i-1)}, j_2^{(i-1)}\} \mathbb{1}_{\min\{j_0^{(i-1)}, j_2^{(i-1)}\} = j_0^{(i-1)}} \\ + e_i \left(\max\{j_0^{(i-1)}, j_2^{(i-1)}\} + \frac{(\ell + j_0^{(d)})|j_0^{(i-1)} - j_2^{(i-1)}|}{|y| - j/2} \right) \mathbb{1}_{\max\{j_0^{(i-1)}, j_2^{(i-1)}\} = j_0^{(i-1)}}$$

(see Figure 2.7; $a_i(\ell)$ is one of the two vertical values, depending on which of the two i th diameters considered is the larger one). With this, we define

$$\mathcal{A}'_6(j_0, j_2) := \left\{ x \in \mathbb{R}^d : x^{(1)} \in (-\infty, 0], x^{(i)} \in (-\infty, -|a_i(x^{(1)})|] \cup [|a_i(x^{(1)})|, \infty), \right. \\ \left. i \in \{2, \dots, d\} \right\}.$$

Using this we can rewrite $\mathcal{A}_6(\mathbf{0}, \mathbf{y})$ and bound (2.18) from above by

$$c \prod_{s=1}^{d-k} j_0^{(s)} j_2^{(s)} \int_{\mathbb{R}^d \setminus B_\gamma(0)} \int_{\text{rot}_{\rho_y, 0}(\mathcal{A}'_6(j_0, j_2)) + 0} (|x|_1 + |y|)^{-(\alpha_k - \varepsilon + 2d - 2k)} d\lambda(x) d\lambda(y) \\ \leq c \prod_{s=1}^{d-k} j_0^{(s)} j_2^{(s)} \int_{\mathbb{R}^d \setminus B_1(0)} \left(\sum_{i=2}^d \min\{j_0^{(i)}, j_2^{(i)}\} + |y| \right)^{-(\alpha_k - \varepsilon + d - 2k)} d\lambda(y) \\ \leq c \prod_{s=1}^{d-k} j_0^{(s)} j_2^{(s)} \int_1^\infty r^{d-1} r^{-(\alpha_k - \varepsilon + d - 2k)} dr,$$

with $|\cdot|_1$ denoting the 1-norm. In the first inequality we bound the integral from above by integrating over x coordinate by coordinate, using the additivity of the 1-norm and by increasing the integration area of y . Using polar coordinates yields the second inequality. The last expression is finite since $\alpha_k > 2k$. Therefore the upper bound for S_6 is given by

$$S_6 \leq cu^2 \sum_{j_0, j_2 \in \mathbb{N}^d} p_{j_0} p_{j_2} \prod_{s=1}^{d-1} j_0^{(s)} j_2^{(s)}. \quad (2.19)$$

For S_7 we similarly define

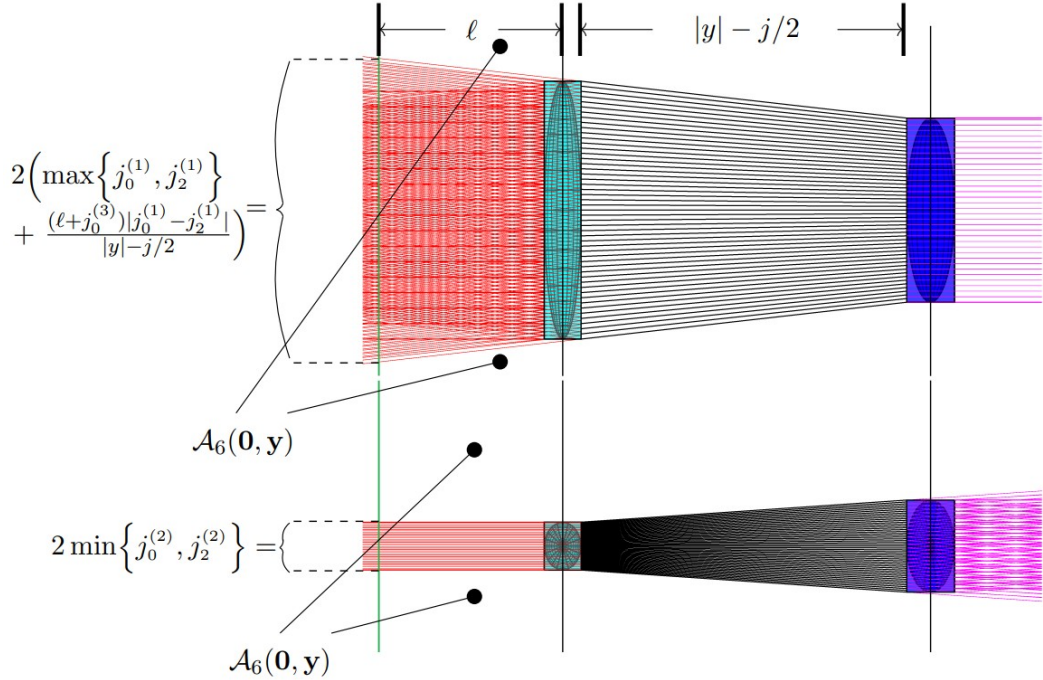


Figure 2.7: Visualisation of the role of ℓ in the calculation for S_6 , with the perspective along $\text{rot}_{\rho_{v,w}}(e_2)$ in the top and $\text{rot}_{\rho_{v,w}}(e_3)$ in the bottom figure. Note that ℓ is different from ℓ in the calculation of S_3 .

$$\mathcal{A}'_7(j_0, j_2) := (0, |y|) \times \left(\bigtimes_{i=2}^d (-\infty, -\min\{j_0^{(i-1)}, j_2^{(i-1)}\}] \cup [\min\{j_0^{(i-1)}, j_2^{(i-1)}\}, \infty) \right).$$

Using the definition of $\mathcal{A}_7(\mathbf{0}, \mathbf{y})$ we bound the integral S_7 for fixed j_0, j_2 from above by replacing $\mathcal{A}_7(\mathbf{0}, \mathbf{y})$ in the bound of the integral with the larger $\mathcal{A}'_7(\mathbf{0}, \mathbf{y})$. Moreover we use the 1-norm as before and get the following upper bound, by using the same considerations about the orientation of \bar{R}_x that

result in an intersection with \bar{R}_0 and \bar{R}_y , as well as the Potter bounds to obtain

$$\begin{aligned}
 & c \prod_{s=1}^{d-k} j_0^{(s)} j_2^{(s)} \int_{\mathbb{R}^d \setminus B_\gamma(0)} \int_{\text{rot}_{\rho_y, 0} \left(\mathcal{A}'_7(j_0, j_2) \right) + 0} (|x|_1 + |y|)^{-(\alpha_k - \varepsilon + 2d - 2k)} d\lambda(x) d\lambda(y) \\
 & \leq c \prod_{s=1}^{d-k} j_0^{(s)} j_2^{(s)} \int_{\mathbb{R}^d \setminus B_1(0)} \left(\sum_{i=2}^d \min\{j_0^{(i)}, j_2^{(i)}\} + |y| \right)^{-(\alpha_k - \varepsilon + d - 2k)} d\lambda(y) \\
 & \leq c \prod_{s=1}^{d-k} j_0^{(s)} j_2^{(s)} \int_1^\infty r^{d-1} r^{-(\alpha_k - \varepsilon + d - 2k)} dr.
 \end{aligned}$$

In the first inequality we integrated over x , bounded the integrand from above and increased the integration area of y . We see that the last integral is finite since $\alpha_k > 2k$. This yields the following upper bound for S_7

$$S_7 \leq cu^2 \sum_{j_0, j_2 \in \mathbb{N}^d} p_{j_0} p_{j_2} \prod_{s=1}^{d-1} j_0^{(s)} j_2^{(s)}. \quad (2.20)$$

Putting equations (2.14), (2.15), (2.16), (2.17), (2.19), and (2.20) together, we get for $u \in (0, 1)$ the bound

$$\mathbb{E}_0 \left[\sum_{\mathbf{y} \in \mathcal{X}} \mathbb{1}_{\mathbf{0} \sim \mathbf{y}} \right] \leq cu \sum_{j_0, j_2 \in \mathbb{N}^d} p_{j_0} p_{j_2} \left(\prod_{i=1}^{d-1} j_0^{(i)} + \prod_{i=1}^{d-1} j_2^{(i)} + 8 \prod_{i=1}^{d-1} j_0^{(i)} j_2^{(i)} \right). \quad (2.21)$$

Since $\bar{D}^{(k)} \geq 1$ for all $k \in \{1, \dots, d\}$ we have

$$V^2 \geq V := \prod_{k=1}^d \bar{D}^{(k)} \geq \prod_{k=1}^{d-1} \bar{D}^{(k)}.$$

With this we show now that the key bound of this proof is

$$\begin{aligned}
 \mathbb{E}_0 \left[\sum_{\mathbf{x} \in \mathcal{X}} \mathbb{1}_{\mathbf{0} \sim \mathbf{x}} \right] & \stackrel{(IH)}{\leq} u^n c^n \sum_{j_0, j_2, \dots, j_{2n} \in \mathbb{N}^d} p_{j_{2n}} \prod_{k=0}^{n-1} p_{j_{2k}} \left(\prod_{i=1}^{d-1} j_{2k}^{(i)} + \prod_{i=1}^{d-1} j_{2k+2}^{(i)} + 8 \prod_{i=1}^{d-1} j_{2k}^{(i)} j_{2k+2}^{(i)} \right) \\
 & \leq u^n c^n 10^n \mathbb{E}[V^2]^{n+1}.
 \end{aligned}$$

Note that the second inequality can easily be checked by using that the diameters of different vertices are i.i.d. For $n = 1$, we have just proved the claim in (2.21). We now proceed to show it for $n \geq 2$.

Proof of (IH): We split the expected number of vertices connected to $\mathbf{0}$ via the partition (2.11) as we have done for $n = 1$ and use induction over n . For that let $n \geq 2$. Recall that in the path of length $2n$ we are interested in vertices such that the last vertex satisfy $2\bar{R}_{x_{2n-1}} \cap 2\bar{R}_{x_{2n}} = \emptyset$ and count vertices that does not satisfy this as vertices that are the last vertex in a path of length $2n - 1$. We obtain

$$\begin{aligned} \mathbb{E}_0 \left[\sum_{\mathbf{x} \in \mathcal{X}} \mathbb{1}_{\mathbf{0} \stackrel{2n}{\sim} \mathbf{x}} \right] &= \mathbb{E}_0 \left[\sum_{\substack{\mathbf{x}_2, \mathbf{x}_4, \dots, \mathbf{x}_{2n} \in \mathcal{X} \\ \neq}} \prod_{i=1}^n \mathbb{1}_{\mathbf{x}_{2i-2} \stackrel{2}{\sim} \mathbf{x}_{2i}} \right] \\ &\leq \sum_{m=1}^8 \mathbb{E}_0 \left[\sum_{\substack{\mathbf{x}_2, \mathbf{x}_4, \dots, \mathbf{x}_{2n-2} \in \mathcal{X} \\ j_0, j_2, \dots, j_{2n} \in \mathbb{N}^d}} \prod_{i=0}^n \mathbb{1}_{\bar{D}_{x_{2i}}=j_{2i}} \mathbb{1}_{\mathbf{x}_{2i-2} \stackrel{2}{\sim} \mathbf{x}_{2i}} \mathbb{1}_{x_{2n} \notin 2\bar{R}_{x_{2n-2}}} \mathbb{1}_{x_{2n-2} \notin 2\bar{R}_{x_{2n}}} \right. \\ &\quad \left. \times \mathbb{1}_{x_{2n-1} \in \mathcal{A}_m(\mathbf{x}_{2n-2}, \mathbf{x}_{2n})} \mathbb{1}_{\bar{R}_{x_{2n-2}} \cap \bar{R}_{x_{2n}} = \emptyset} \right] \\ &\quad + \mathbb{E}_0 \left[\sum_{\substack{\mathbf{x}_2, \mathbf{x}_4, \dots, \mathbf{x}_{2n-2} \in \mathcal{X} \\ j_0, j_2, \dots, j_{2n} \in \mathbb{N}^d}} \prod_{i=0}^n \mathbb{1}_{\bar{D}_{x_{2i}}=j_{2i}} \mathbb{1}_{\mathbf{x}_{2i-2} \stackrel{2}{\sim} \mathbf{x}_{2i}} \mathbb{1}_{x_{2n} \in 2\bar{R}_{x_{2n-2}}} \right] \\ &\quad + \mathbb{E}_0 \left[\sum_{\substack{\mathbf{x}_2, \mathbf{x}_4, \dots, \mathbf{x}_{2n-2} \in \mathcal{X} \\ j_0, j_2, \dots, j_{2n} \in \mathbb{N}^d}} \prod_{i=0}^n \mathbb{1}_{\bar{D}_{x_{2i}}=j_{2i}} \mathbb{1}_{\mathbf{x}_{2i-2} \stackrel{2}{\sim} \mathbf{x}_{2i}} \mathbb{1}_{x_{2n-2} \in 2\bar{R}_{x_{2n}}} \right] =: \sum_{m=1}^{10} S_m^{(n)} \end{aligned}$$

Using \mathbb{P}_r as shorthand for $\mathbb{P}_{\mathbf{0}, \mathbf{x}_1, \dots, \mathbf{x}_r}$, we can write $S_m^{(n)}$, for $m \in \{1, \dots, 8\}$, as

$$\begin{aligned} S_m^{(n)} &= u^{2n} \sum_{j_0, j_2, \dots, j_{2n} \in \mathbb{N}^d} \prod_{i=0}^n p_{j_{2i}} \int \dots \int_{\mathbb{R}^d} \mathbb{P}_{2n} \left(\bigcap_{i=1}^{2n} \{ \mathbf{x}_{i-1} \sim \mathbf{x}_i \} \cap \{ \mathbf{x}_{2n-2} \not\sim \mathbf{x}_{2n} \} \right) \\ &\quad \times \mathbb{1}_{x_{2n-1} \in \mathcal{A}_m(\mathbf{x}_{2n-2}, \mathbf{x}_{2n})} d\lambda(x_1) \dots d\lambda(x_{2n}), \end{aligned}$$

while for $m \in \{9, 10\}$ we have

$$\begin{aligned} S_9^{(n)} &= u^{2n} \sum_{j_0, j_2, \dots, j_{2n} \in \mathbb{N}^d} \prod_{i=0}^n p_{j_{2i}} \int \dots \int_{\mathbb{R}^d} \mathbb{P}_{2n} \left(\bigcap_{i=1}^{2n-2} \{ \mathbf{x}_{i-1} \sim \mathbf{x}_i \} \cap \{ x_{2n} \in 2\bar{R}_{x_{2n-2}} \} \right) \\ &\quad d\lambda(x_1) \dots d\lambda(x_{2n}) \end{aligned}$$

and

$$\begin{aligned} S_{10}^{(n)} &= u^{2n} \sum_{j_0, j_2, \dots, j_{2n} \in \mathbb{N}^d} \prod_{i=0}^n p_{j_{2i}} \int \dots \int_{\mathbb{R}^d} \mathbb{P}_{2n} \left(\bigcap_{i=1}^{2n-2} \{ \mathbf{x}_{i-1} \sim \mathbf{x}_i \} \cap \{ x_{2n-2} \in 2\bar{R}_{x_{2n}} \} \right) \\ &\quad d\lambda(x_1) \dots d\lambda(x_{2n}). \end{aligned}$$

2.2. Proofs on the behaviour of the model

Defining now $(F_m^{(n)})_{m \in \{1, \dots, 10\}}$ for $n \in \mathbb{N}$ as

$$F_m^{(n)} = \prod_{s=1}^{d-1} j_{2n-2}^{(s)} j_{2n}^{(s)}, \quad \text{with } 1 \leq m \leq 8, \quad F_9^{(n)} = \prod_{s=1}^{d-1} j_{2n-2}^{(s)}, \quad F_{10}^{(n)} = \prod_{s=1}^{d-1} j_{2n}^{(s)},$$

we claim that $S_m^{(n)}$ can be bounded from above for $m \in \{1, \dots, 10\}$ and $n \in \mathbb{N}$ by

$$S_m^{(n)} \leq u^n c^n \sum_{j_0, j_2, \dots, j_{2n} \in \mathbb{N}^d} p_{j_{2n}} p_{j_{2n-2}} \prod_{k=0}^{n-2} p_{j_{2k}} \left(\prod_{i=1}^{d-1} j_{2k}^{(i)} + \prod_{i=1}^{d-1} j_{2k+2}^{(i)} + 8 \prod_{i=1}^{d-1} j_{2k}^{(i)} j_{2k+2}^{(i)} \right) F_m^{(n)}.$$

Observe that the case $n = 1$ was shown in (2.21), so it remains to consider $n > 1$ and focus on the induction step. We show the claim for $m \in \{1, 9, 10\}$ and note that the inequalities for $m \in \{2, 3, \dots, 8\}$ can be proved similarly to $m = 1$. We first focus on the integral terms of $S_m^{(n)}$ before looking at the rest. Moreover, we roughly do the following. First, we look in every integral at the last three vertices in the path of length $2n$. We count how many vertices can connect $\bar{R}_{x_{2n-2}}$ with $\bar{R}_{x_{2n}}$ and ignore the rest of the path. After that we integrate over x_{2n} before we move on to the rest by using the induction hypothesis. Note that in the following calculations we use the same consideration for \mathbf{x}_{2n} , \mathbf{x}_{2n-1} and \mathbf{x}_{2n-2} as we do for \mathbf{y} , \mathbf{x} , and $\mathbf{0}$ in the case $n = 1$. In addition to that we define similarly to the calculation for $n = 1$ the value $\tilde{\gamma} := 2j_{2n-2}^{(d)}$.

$m = 1$: We rewrite the integral of $S_1^{(n)}$ and bound it from above so we get

$$\begin{aligned} & \int_{\mathbb{R}^d} \dots \int_{\mathbb{R}^d \setminus B_{\tilde{\gamma}}(x_{2n-2})} \int_{\mathcal{A}_1(\mathbf{x}_{2n-2}, \mathbf{x}_{2n})} \mathbb{P}_{2n} \left(\bigcap_{i=1}^{2n} \{ \mathbf{x}_{i-1} \sim \mathbf{x}_i \} \cap \{ \mathbf{x}_{2n-2} \not\sim \mathbf{x}_{2n} \} \right) d\lambda(x_1) \dots d\lambda(x_{2n-2}) \\ & \quad d\lambda(x_{2n}) d\lambda(x_{2n-1}) \\ & \leq c \int_{\mathbb{R}^d} \dots \int_{\mathbb{R}^d \setminus B_{\tilde{\gamma}}(x_{2n-2})} \int_{\mathcal{A}_1(\mathbf{x}_{2n-2}, \mathbf{x}_{2n})} \mathbb{P}_{2n} \left(\bigcap_{i=1}^{2n-2} \{ \mathbf{x}_{i-1} \sim \mathbf{x}_i \} \cap \{ \mathbf{x}_{2n-2} \not\sim \mathbf{x}_{2n} \} \right) \\ & \quad \times (|x_{2n-1} - x_{2n-2}| + |x_{2n} - x_{2n-1}|)^{-(\alpha_k - \varepsilon + d - k)} \prod_{s=1}^{d-k} j_{2n}^{(s)} d\lambda(x_1) \dots \\ & \quad d\lambda(x_{2n-2}) d\lambda(x_{2n}) d\lambda(x_{2n-1}). \end{aligned}$$

The inequality is derived as in the case $n = 1$ by using that the connections between \mathbf{x}_{2n} , \mathbf{x}_{2n-1} and \mathbf{x}_{2n-2} are conditionally independent of the preceding $2n - 3$ vertices. We are now covering the cases where the k th diameter of

$\bar{R}_{x_{2n-1}}$ is big enough, i.e.

$$\max\{\text{dist}(\bar{R}_{x_{2n}}, x_{2n-1}), \text{dist}(\bar{R}_{x_{2n-2}}, x_{2n-1})\} \asymp |x_{2n-1} - x_{2n-2}| + |x_{2n} - x_{2n-1}|.$$

Using this and the Potter bounds yields the sum over k and $\alpha_k - \varepsilon$ in the exponent of $|x_{2n-1} - x_{2n-2}| + |x_{2n} - x_{2n-1}|$. We assume also that the orientation of $\bar{R}_{x_{2n}}$ is such that the largest face of this rectangle is perpendicular to the vector $x_{2n} - x_{2n-1}$ to get an upper bound for the set of orientations that result in an intersection of $\bar{R}_{x_{2n-1}}$ with $\bar{R}_{x_{2n}}$. Note that here we again use Remark 2.2.1. In the next step we use substitution and $\lambda(\mathcal{A}_1(\mathbf{x}_{2n-2}, \mathbf{x}_{2n})) = c \prod_{s=1}^{d-1} j_{2n-2}^{(s)}$ which leads to the following upper bound

$$\begin{aligned} & c \int_{\mathbb{R}^d} \dots \int_{\mathbb{R}^d \setminus B_{\tilde{\gamma}}(x_{2n-2})} \int_{\left(\mathcal{A}_1(\mathbf{x}_{2n-2}, \mathbf{x}_{2n}) - x_{2n-2}\right)_{d-k}} \mathbb{P}_{2n-2} \left(\bigcap_{i=1}^{2n-2} \{\mathbf{x}_{i-1} \sim \mathbf{x}_i\} \right) \\ & \quad \times (|\tilde{x}_{2n-1}| + |\tilde{x}_{2n}|)^{-(\alpha_k - \varepsilon) - d + k} \prod_{s=1}^{d-k} j_{2n}^{(s)} d\lambda(x_1) \dots d\lambda(x_{2n-2}) d\lambda(\tilde{x}_{2n}) d\lambda(\tilde{x}_{2n-1}) \\ & \leq c \prod_{s=1}^{d-1} j_{2n}^{(s)} \prod_{s=1}^{d-1} j_{2n-2}^{(s)} \int_{\mathbb{R}^d} \dots \int_{\mathbb{R}^d} \mathbb{P}_{2n} \left(\bigcap_{i=1}^{2n-2} \{\mathbf{x}_{i-1} \sim \mathbf{x}_i\} \right) d\lambda(x_1) \dots d\lambda(x_{2n-2}). \end{aligned}$$

Together with the induction hypothesis this leads to the claimed upper bound for $S_1^{(n)}$.

$m=9$: To bound the integral of $S_9^{(n)}$ from above we count every vertex inside $2\bar{R}_{x_{2n-2}}$, i.e. we assume that every vertex in this set is connected to \mathbf{x}_{2n-2} via a path of length 2. Therefore the integral of $S_9^{(n)}$ can be bounded from above via

$$\begin{aligned} & \int_{\mathbb{R}^d} \dots \int_{\mathbb{R}^d} \mathbb{P}_{2n-2} \left(\bigcap_{i=1}^{2n-2} \{\mathbf{x}_{i-1} \sim \mathbf{x}_i\} \cap \{x_{2n} \in 2\bar{R}_{x_{2n-2}}\} \right) d\lambda(x_1) \dots d\lambda(x_{2n-2}) d\lambda(x_{2n}) \\ & \leq c \prod_{s=1}^{d-1} j_{2n-2}^{(s)} \int_{\mathbb{R}^d} \dots \int_{\mathbb{R}^d} \mathbb{P}_{2n-2} \left(\bigcap_{i=1}^{2n-2} \{\mathbf{x}_{i-1} \sim \mathbf{x}_i\} \right) d\lambda(x_1) \dots d\lambda(x_{2n-2}). \end{aligned}$$

Using now the induction hypothesis leads the required upper bound

$$S_9^{(n)} \leq u^n c^n \sum_{j_0, j_2, \dots, j_{2n} \in \mathbb{N}^d} p_{j_{2n}} p_{j_{2n-2}} \prod_{k=0}^{n-2} p_{j_{2k}} \left(\prod_{i=0}^{d-1} j_{2k}^{(i)} + \prod_{i=1}^{d-1} j_{2k+2}^{(i)} + 8 \prod_{i=1}^{d-1} j_{2k}^{(i)} j_{2k+2}^{(i)} \right) \prod_{s=1}^{d-1} j_{2n-2}^{(s)}.$$

$m = 10$: Except for a single step the calculation is similar to the case $m = 9$. Looking at the integral of $S_{10}^{(n)}$ we want to count every vertex \mathbf{x}_{2n} such that $x_{2n-2} \in 2\bar{R}_{x_{2n}}$. We therefore assume that each such vertex is connected to \mathbf{x}_{2n-2} via a path of length 2. In the first step we rewrite the integral by using the distributional symmetry of \bar{R} . So we get for the integral of $S_{10}^{(n)}$ the following

$$\begin{aligned} & \int_{\mathbb{R}^d} \cdots \int_{\mathbb{R}^d} \mathbb{P}_{2n} \left(\bigcap_{i=1}^{2n-2} \{\mathbf{x}_{i-1} \sim \mathbf{x}_i\} \cap \{x_{2n-2} \in 2\bar{R}_{x_{2n}}\} \right) d\lambda(x_1) \dots d\lambda(x_{2n}) \\ & \leq c \prod_{s=1}^{d-1} j_{2n}^{(s)} \int_{\mathbb{R}^d} \cdots \int_{\mathbb{R}^d} \mathbb{P}_{2n-2} \left(\bigcap_{i=1}^{2n-2} \{\mathbf{x}_{i-1} \sim \mathbf{x}_i\} \right) d\lambda(x_1) \dots d\lambda(x_{2n-2}). \end{aligned}$$

The inequality follows from the distributional symmetry of \bar{R} . Using now the induction hypothesis leads to the claimed upper bound

$$S_{10}^{(n)} \leq u^n c^n \sum_{j_0, j_2, \dots, j_{2n} \in \mathbb{N}^d} p_{j_{2n}} p_{j_{2n-2}} \prod_{k=0}^{n-2} p_{j_{2k}} \left(\prod_{i=1}^{d-1} j_{2k}^{(i)} + \prod_{i=1}^{d-1} j_{2k+2}^{(i)} + 8 \prod_{i=1}^{d-1} j_{2k}^{(i)} j_{2k+2}^{(i)} \right) \prod_{s=1}^{d-1} j_{2n}^{(s)}.$$

Putting everything together, this gives us an upper bound for the expected number of vertices that are connected via a path of length $2n$ to the origin, for $n \in \mathbb{N}$, that is

$$\mathbb{E}_0 \left[\sum_{\mathbf{x} \in \mathcal{X}} \mathbb{1}_{\mathbf{0} \stackrel{2n}{\sim} \mathbf{x}} \right] \leq u^n c^n \sum_{j_0, j_2, \dots, j_{2n} \in \mathbb{N}^d} p_{j_{2n}} \prod_{k=0}^{n-1} p_{j_{2k}} \left(\prod_{i=1}^{d-1} j_{2k}^{(i)} + \prod_{i=1}^{d-1} j_{2k+2}^{(i)} + 8 \prod_{i=1}^{d-1} j_{2k}^{(i)} j_{2k+2}^{(i)} \right).$$

It remains to show that there exists a suitable upper bound also for the expected number of vertices with distance $2n + 1$ to the origin, for $n \in \mathbb{N}$. We have

$$\begin{aligned} \mathbb{E}_0 \left[\sum_{\mathbf{x} \in \mathcal{X}} \mathbb{1}_{\mathbf{0} \stackrel{2n+1}{\sim} \mathbf{x}} \right] &= \mathbb{E}_0 \left[\sum_{\substack{\mathbf{x}_2, \mathbf{x}_4, \dots, \\ \mathbf{x}_{2n}, \mathbf{x}_{2n+1} \in \mathcal{X}}}^{\neq} \prod_{i=1}^n \mathbb{1}_{\mathbf{x}_{2i-2} \stackrel{2}{\sim} \mathbf{x}_{2i}} \mathbb{1}_{x_{2n+1} \in 2\bar{R}_{x_{2n}}} \right] \\ &+ \mathbb{E}_0 \left[\sum_{\substack{\mathbf{x}_2, \mathbf{x}_4, \dots, \\ \mathbf{x}_{2n}, \mathbf{x}_{2n+1} \in \mathcal{X}}}^{\neq} \prod_{i=1}^n \mathbb{1}_{\mathbf{x}_{2i-2} \stackrel{2}{\sim} \mathbf{x}_{2i}} \mathbb{1}_{x_{2n} \in 2\bar{R}_{x_{2n+1}}} \right] \\ &+ \mathbb{E}_0 \left[\sum_{\substack{\mathbf{x}_2, \mathbf{x}_4, \dots, \\ \mathbf{x}_{2n}, \mathbf{x}_{2n+1} \in \mathcal{X}}}^{\neq} \prod_{i=1}^n \mathbb{1}_{\mathbf{x}_{2i-2} \stackrel{2}{\sim} \mathbf{x}_{2i}} \mathbb{1}_{x_{2n} \notin 2\bar{R}_{x_{2n+1}}} \mathbb{1}_{x_{2n+1} \notin 2\bar{R}_{x_{2n}}} \right]. \end{aligned}$$

To find an upper bound for this expression we are again looking at the individual summands. The first summand can be rewritten as

$$\begin{aligned}
 & u^{2n+1} \sum_{\substack{j_0, j_2, \dots, \\ j_{2n}, j_{2n+1} \in \mathbb{N}^d}} \prod_{i=0}^{n+1} p_{j_{2i}} \int \cdots \int_{\mathbb{R}^d} \int_{\mathbb{R}^d} \int_{\bar{R}_{x_{2n}}} \mathbb{P}_{2n} \left(\bigcap_{k=1}^n \{ \mathbf{x}_{2(k-1)} \overset{2}{\sim} \mathbf{x}_{2k} \} \right) d\lambda(x_1) \cdots d\lambda(x_{2n+1}) \\
 & \leq c^{n+1} u^{n+1} \sum_{\substack{j_0, j_2, \dots, \\ j_{2n}, j_{2n+1} \in \mathbb{N}^d}} \prod_{s=1}^{d-1} j_{2n}^{(s)} p_{j_{2n+1}} p_{j_{2n}} \prod_{k=0}^{n-1} p_{j_{2k}} \left(\prod_{i=1}^{d-1} j_{2k}^{(i)} + \prod_{i=1}^{d-1} j_{2k+2}^{(i)} \right. \\
 & \quad \left. + 8 \prod_{i=1}^{d-1} j_{2k}^{(i)} j_{2k+2}^{(i)} \right).
 \end{aligned}$$

We obtain the inequality by first using that $\lambda(\bar{R}_{x_{2n}}) = c \prod_{s=1}^{d-1} j_{2n}^{(s)}$ and then the previously shown result for the expected number of vertices that are connected via a path of length $2n$ from the origin. Similar to the previous calculations we get by using the distributional symmetry of \bar{R} for the second summand

$$\begin{aligned}
 & \mathbb{E}_0 \left[\sum_{\substack{\mathbf{x}_2, \mathbf{x}_4, \dots, \\ \mathbf{x}_{2n}, \mathbf{x}_{2n+1} \in \mathcal{X}}} \prod_{i=1}^n \mathbb{1}_{\mathbf{x}_{2i-2} \overset{2}{\sim} \mathbf{x}_{2i}} \mathbb{1}_{x_{2n} \in 2\bar{R}_{x_{2n+1}}} \right] \\
 & = \mathbb{E}_0 \left[\sum_{\substack{\mathbf{x}_2, \mathbf{x}_4, \dots, \\ \mathbf{x}_{2n}, \mathbf{x}_{2n+1} \in \mathcal{X}}} \prod_{i=1}^n \mathbb{1}_{\mathbf{x}_{2i-2} \overset{2}{\sim} \mathbf{x}_{2i}} \mathbb{1}_{x_{2n+1} \in (2\bar{R}_{x_{2n+1}} - x_{2n+1} + x_{2n})} \right] \\
 & \leq c^{n+1} u^{n+1} \sum_{\substack{j_0, j_2, \dots, \\ j_{2n}, j_{2n+1} \in \mathbb{N}^d}} \prod_{s=1}^{d-1} j_{2n+1}^{(s)} p_{j_{2n+1}} p_{j_{2n}} \prod_{k=0}^{n-1} p_{j_{2k}} \left(\prod_{i=1}^{d-1} j_{2k}^{(i)} + \prod_{i=1}^{d-1} j_{2k+2}^{(i)} \right. \\
 & \quad \left. + 8 \prod_{i=1}^{d-1} j_{2k}^{(i)} j_{2k+2}^{(i)} \right).
 \end{aligned}$$

Looking now at the last summand we get

$$\begin{aligned}
 & \mathbb{E}_0 \left[\sum_{\substack{\mathbf{x}_2, \mathbf{x}_4, \dots, \mathbf{x}_{2n} \in \mathcal{X}}} \prod_{i=1}^n \mathbb{1}_{\mathbf{x}_{2i-2} \overset{2}{\sim} \mathbf{x}_{2i}} \mathbb{1}_{x_{2n} \notin 2\bar{R}_{x_{2n+1}}} \mathbb{1}_{x_{2n+1} \notin 2\bar{R}_{x_{2n}}} \right] \\
 & = u^{2n+1} \sum_{j_0, j_2, \dots, j_{2n} \in \mathbb{N}^d} p_{j_{2n+1}} \prod_{m=0}^n p_{j_{2m}} \int \cdots \int_{\mathbb{R}^d} \mathbb{P}_{2n+1} \left(\bigcap_{i=1}^{2n+1} \{ \mathbf{x}_{i-1} \sim \mathbf{x}_i \} \right) \mathbb{1}_{x_{2n} \notin 2\bar{R}_{x_{2n+1}}} \\
 & \quad \times \mathbb{1}_{x_{2n+1} \notin 2\bar{R}_{x_{2n}}} d\lambda(x_1) \cdots d\lambda(x_{2n+1}) \\
 & \leq cu^{2n+1} \sum_{j_0, j_2, \dots, j_{2n} \in \mathbb{N}^d} p_{j_{2n+1}} \prod_{m=0}^n p_{j_{2m}} \int \cdots \int_{\mathbb{R}^d} \int_{B_1(x_{2n})} \mathbb{P}_{2n} \left(\bigcap_{i=1}^{2n} \{ \mathbf{x}_{i-1} \sim \mathbf{x}_i \} \right) \\
 & \quad \times (|x_{2n} - x_{2n+1}|)^{-(\alpha_k - \varepsilon)} \prod_{s=1}^{d-k} \frac{j_{2n}^{(s)}}{|x_{2n} - x_{2n+1}|} d\lambda(x_1) \cdots d\lambda(x_{2n+1}).
 \end{aligned}$$

We get the inequality since we first start again by looking at the last connection of the path. We therefore first count how many vertices are connected to \mathbf{x}_{2n} by an edge. As before we look at the k th diameter of $\bar{R}_{x_{2n+1}}$ is big enough so that an intersection of $\bar{R}_{x_{2n+1}}$ and $\bar{R}_{x_{2n}}$ is possible. For that we use similar considerations as before, namely

$$\text{Dist}(\bar{R}_{x_{2n}}, x_{2n+1}) \asymp |x_{2n} - x_{2n+1}|.$$

This leads to the term with the exponent $-(\alpha_k - \varepsilon)$. Moreover we bound the $(d-1)$ -dimensional Lebesgue measure of the set of orientations that results in an intersection from above by assuming again that the $\bar{R}_{x_{2n}}$ is oriented in such a way that the largest face of it is perpendicular to the orientation of $x_{2n+1} - x_{2n}$. This and the use of Remark 2.2.1 leads to the product term. Using now substitution we rewrite the last expression to

$$\begin{aligned} & cu^{2n+1} \sum_{j_0, j_2, \dots, j_{2n} \in \mathbb{N}^d} p_{j_{2n+1}} \prod_{m=0}^n p_{j_{2m}} \prod_{s=1}^{d-1} j_{2n}^{(s)} \int_{\mathbb{R}^d} \cdots \int_{B_1(0)} \mathbb{P}_{2n} \left(\bigcap_{i=1}^{2n} \{\mathbf{x}_{i-1} \sim \mathbf{x}_i\} \right) \\ & \quad \times (|\tilde{x}_{2n+1}|)^{-(\alpha_k - \varepsilon + d - k)} d\lambda(x_1) \dots d\lambda(\tilde{x}_{2n+1}) \\ & \leq cu^{2n+1} p_{j_{2n+1}} \prod_{m=0}^n p_{j_{2m}} \prod_{s=1}^{d-1} j_{2n}^{(s)} \int_{\mathbb{R}^d} \cdots \int_{\mathbb{R}^d} \int_1^\infty \mathbb{P}_{2n} \left(\bigcap_{i=1}^{2n} \{\mathbf{x}_{i-1} \sim \mathbf{x}_i\} \right) \\ & \quad \times r^{-(\alpha_k - \varepsilon + d - k) + d - 1} d\lambda(x_1) \dots d\lambda(x_{2n}) dr \\ & \leq cu^{2n+1} p_{j_{2n+1}} \prod_{m=0}^n p_{j_{2m}} \prod_{s=1}^{d-1} j_{2n}^{(s)} \int_{\mathbb{R}^d} \cdots \int_{\mathbb{R}^d} \mathbb{P}_{2n} \left(\bigcap_{i=1}^{2n} \{\mathbf{x}_{i-1} \sim \mathbf{x}_i\} \right) \\ & \quad d\lambda(x_1) \dots d\lambda(x_{2n}). \end{aligned}$$

In the first inequality we use polar coordinates and in the second inequality we integrate over r , which leads to a finite term since $\alpha_k > 2k$. Using now (IH) leads to the following upper bound

$$u^{n+1} c^{n+1} \sum_{j_0, j_2, \dots, j_{2n} \in \mathbb{N}^d} p_{j_{2n}} \prod_{s=1}^{d-1} j_{2n}^{(s)} \prod_{k=0}^{n-1} p_{j_{2k}} \left(\prod_{i=1}^{d-1} j_{2k}^{(i)} + \prod_{i=1}^{d-1} j_{2k+2}^{(i)} + 8 \prod_{i=1}^{d-1} j_{2k}^{(i)} j_{2k+2}^{(i)} \right).$$

All together this yields the upper bound for the expected number of vertices that are connected to the origin via a path of length $2n+1$

$$\mathbb{E}_0 \left[\sum_{\mathbf{x} \in \mathcal{X}} \mathbb{1}_{\mathbf{0} \stackrel{2n+1}{\sim} \mathbf{x}} \right] \leq u^{n+1} c^{n+1} 10^{n+1} \mathbb{E}[V^2]^{n+2}.$$

Choosing now $u < (10c\mathbb{E}[V^2])^{-2}$ gives us $\sum_{n \in \mathbb{N}} \mathbb{E}_0[\sum_{\mathbf{x} \in \mathcal{X}} \mathbb{1}_{\mathbf{0} \sim \mathbf{x}}] < \infty$, as desired. We therefore have non-robustness if the second moment of $\text{Vol}(C)$ is finite and $\alpha_k > 2k$. \square

Chapter 3

Chemical distance

As we have now universal criteria on the grain distribution being robust, we study in this chapter the chemical distance in the Poisson Boolean model with convex grains and establish a universal limit theorem for typical distances in such graphs. Note that, except for a few changes, the following chapter is taken from [26].

3.1 Main results on the chemical distance

For this model we have established that the grain distribution is robust if there exists $k \in \{1, \dots, d\}$ such that $\alpha_k < \min\{2k, d\}$ (see Theorem 2.2). The main result of this chapter gives us the behaviour of the chemical distance in the robust (but not dense) regime. For all other cases, i.e. having density or the universal criteria of robustness does not hold, we remark in Theorem 3.1 that the chemical distance have some different behaviour than in the robust but not dense case. For that let

$$\mathcal{M} := \{k \in \{1, \dots, d-1\} : \alpha_k \in (k, \min\{2k, d\})\},$$

which can intuitively be thought of as the index set of tail exponents that are sufficiently small for their corresponding diameters to be able to affect the chemical distances in the graph no matter which correlation is given for the diameters. We define \mathbb{P}_A for $A = \{x_1, \dots, x_n\} \subset \mathbb{R}^d$ for $n \in \mathbb{N}$ to be the probability measure of the Poisson point process under the condition that $x_1, \dots, x_n \in \mathcal{P}$, i.e. the Palm version of the process and $\text{dist}(\mathbf{x}, \mathbf{y})$ to be the chemical distance. Recall that this is the length of the shortest path between $\mathbf{x}, \mathbf{y} \in \mathcal{X}$. Then, the following holds.

Theorem 3.1. *In the Poisson-Boolean base model with regularly varying diameters with $u > 0$ and $\kappa := \operatorname{argmax}_{s \in \mathcal{M}} \frac{\min\{d-s, s\}}{\alpha_s - s}$ we have for $x, y \in \mathcal{P}$ and $\delta > 0$ in the case $\mathcal{M} \neq \emptyset$ and $\alpha_k > k$ for all $k \in \{1, \dots, d\}$ that*

$$\lim_{|x-y| \rightarrow \infty} \mathbb{P}_{x,y} \left(\frac{(2-\delta) \log \log |x-y|}{\log \left(\frac{\min\{d-\kappa, \kappa\}}{\alpha_\kappa - \kappa} \right)} \leq \operatorname{dist}(\mathbf{x}, \mathbf{y}) \leq \frac{(2+\delta) \log \log |x-y|}{\log \left(\frac{\min\{d-\kappa, \kappa\}}{\alpha_\kappa - \kappa} \right)} \mid x \leftrightarrow y \right) = 1.$$

Furthermore if there exists $k \in \{1, \dots, d\}$ such that $\alpha_k \leq k$ we have that $\operatorname{dist}(\mathbf{x}, \mathbf{y})$ is smaller than $c \log \log |x - y|$ for all $c > 0$ with high probability. In all other cases, namely $\alpha_k \geq \min\{2k, d\}$ for all $k \in \{1, \dots, d\}$, we have that $\operatorname{dist}(\mathbf{x}, \mathbf{y})$ is bigger than $c \log \log |x - y|$ for all $c > 0$.

Recall that in this theorem, $x \leftrightarrow y$ denotes the event that there exists a path in \mathcal{G} between x and y , or equivalently that x and y belong to the same connected component of \mathcal{C} .

Discussion of result. Before proceeding with the proof of this theorem, we quickly discuss the unusual nature of the scaling of chemical distances. More precisely, we comment on the scaling factor $\log \left(\frac{\min\{d-\kappa, \kappa\}}{\alpha_\kappa - \kappa} \right) / 2$ that relates the chemical to the Euclidean distance. The most illustrative comparison comes from so-called *scale-free networks*. These networks tend not to be modelled as spatial graphs, so chemical distances must be given in terms of the number of vertices in the graph rather than the Euclidean distance, with the number of vertices N roughly corresponding to $|x - y|^d$. Then, the mean-field analogue of the classical Boolean model with $\operatorname{Pareto}(-\gamma/d)$ radius distribution exhibits ultrasmallness with the scaling factor $\log \left(\frac{\gamma}{1-\gamma} \right) / 4$, whenever $\gamma \in (1/2, 1)$ - see for example [12]. Since this condition on γ also corresponds to the model being robust, one would naturally expect a similar correspondence between the parameter that leads to robustness and the scaling factor to exist in our model. Surprisingly, this is not the case.

As mentioned above Theorem 3.1, robustness in our model emerges if there exists at least one index $-\alpha_k$ such that the associated diameter is sufficiently heavy tailed relative to both the spatial dimension d and the relative ordering of the diameter k (times two), no matter which correlation is given for the diameters. The natural assumption would therefore be that the scaling of the chemical distance depends on the largest or possibly smallest diameter that satisfies this requirement. Instead, the scaling is determined by the diameter

that is, in relative terms (i.e. how $\alpha_k - k$ compares to $\min\{d - k, k\}$), the most heavy-tailed; see the definition of κ in Theorem 3.1. To understand how this comes to be, one has to remember that each “step” in a path requires two convex bodies to intersect. Consider for the sake of argument that $\mathcal{M} = \{1, \dots, d - 1\}$ and $\alpha_k - k = c \min\{d - k, k\}$ for some constant $c > 0$ and all $k \in \mathcal{M}$, that is, all $k \in \mathcal{M}$ equal κ . Consider also two vertices whose locations are at a fixed large distance. Then, using basic trigonometry one can calculate the probabilities (in terms of random rotations) that two chosen diameters (one for each body) are roughly co-linear. When combined with the distributions of said two diameters and accounting for the combinatorics of different diameter pairings, one obtains (up to constants) that each diameter contributes equally to the probability of an intersection. If, however, one of the $d - 1$ diameters (say k) is made even slightly more heavy-tailed, and consequently $\kappa \triangleq k$, as the distance between the two vertices tends to infinity, this diameter’s contribution to the probability of an intersection asymptotically dominates all others.

We find that this unexpected behaviour, as well as the decoupling of the dense and robust regimes shown in Section 2.2.2, makes the Poisson-Boolean model with regularly varying diameters uniquely interesting among its Boolean model cousins, in particular since it exhibits these features without requiring the introduction of “long edges” (in the sense of long-range percolation, see for example [27]).

3.2 Proof of the lower bound

In this section we will prove the lower bound for the chemical distance. For this and also for the upper bound we will use a construction of infinite paths similar to the one introduced in Chapter 2 and define sequences of events.

We first consider the case $\mathcal{M} \neq \emptyset$ with $\alpha_k > k$ for all $k \in \{1, \dots, d\}$ and recall the definition of the increasing threshold sequence $(f_n)_{n \in \mathbb{N}}$ from (2.2) and make a slight change, that is,

$$f_n = (f_{n-1})^{\frac{\min\{d-\kappa, \kappa\}}{\alpha_\kappa - \kappa} - \epsilon}, \text{ for } n \in \mathbb{N}.$$

Here, $f_0 > 1$ is again chosen arbitrarily big and κ is defined as in Theorem 3.1. So we change k into κ . Note that the ϵ in the definition of f_n is again the same as previously defined in Chapter 2 and without loss of generality we assume also that $0 < \epsilon < \frac{1}{4}$; this ensures again that the exponent in the above sequence is strictly bigger than 1 and makes the sequence increasing. As $\kappa \in \mathcal{M}$ this is

3.2. Proof of the lower bound

possible since $\alpha_\kappa < \min\{2\kappa, d\}$.

For $x \in \mathcal{P}$ the two afore mentioned sequences of events $(\underline{A}_n^x)_{n \in \mathbb{N}}$ and $(\bar{A}_n^x)_{n \in \mathbb{N}}$ are defined as

$$\underline{A}_n^x := \left\{ \begin{array}{l} \exists \mathbf{x}_1, \dots, \mathbf{x}_n \in \mathcal{X}: \mathbf{x}_i \neq \mathbf{x}_m \text{ for all } i \neq m, D_{x_i}^{(\kappa)} \geq 2^{2(d-1)+\epsilon} f_i, \\ D_{x_i}^{(1)} \leq 2^{2(d-1)+\epsilon} f_i^{\frac{2\alpha_\kappa}{\alpha_1}}, x_i \in O_i(\mathbf{x}_{i-1}) \text{ and } C_{x_i} \cap B_{f_{i-1}}^*(\mathbf{x}_{i-1}, x_i) \neq \emptyset \\ \text{for all } 1 \leq i \leq n, \text{ with } x_0 = x. \end{array} \right\} \quad (3.1)$$

and

$$\bar{A}_n^x := \left\{ \begin{array}{l} \exists \mathbf{x}_1, \dots, \mathbf{x}_n \in \mathcal{X}: \mathbf{x}_i \neq \mathbf{x}_m \text{ for all } i \neq m, D_{x_i}^{(\kappa)} \geq 2^{2(d-1)+\epsilon} f_i, \\ x_i \in O_i(\mathbf{x}_{i-1}) \text{ and } C_{x_i} \cap B_{f_{i-1}}^*(\mathbf{x}_{i-1}, x_i) \neq \emptyset \\ \text{for all } 1 \leq i \leq n, \text{ with } x_0 = x. \end{array} \right\}. \quad (3.2)$$

Note that in both sequences we highlight $x \in \mathcal{P}$ as the starting vertex in the event, as we are interested in the chemical distance of $\mathbf{x}, \mathbf{y} \in \mathcal{X}$.

The sequence $(\underline{A}_n^x)_{n \in \mathbb{N}}$ will be used to construct the paths in the current proof for the lower bound of the chemical distance, while $(\bar{A}_n^x)_{n \in \mathbb{N}}$, which is the same as in (2.6) but here we highlight the dependence on the starting vertex, will play a similar role for the upper bound.

Remark 3.2. Note that the definitions of \underline{A}_n^x and \bar{A}_n^x should now depend κ so that we replace k in this section in (2.6) by κ . Later on, in Section 3.3, when we will be working with \bar{A}_n^x , we will replace κ with some fixed $k \in \mathcal{M}$. This change does not affect any of the calculations that relate to \bar{A}_n^x we do in this section. However, in order to avoid writing all calculations twice, or repeatedly pointing out that κ should be replaced by k when working with \bar{A}_n^x , we allow ourselves this small abuse of notation and simply write κ overall. We will remind the reader when κ is to be replaced with k at the appropriate step in Section 3.3.

Recall the intuition of the sequence $(\bar{A}_n^x)_{n \in \mathbb{N}}$. The same intuition also holds for $(\underline{A}_n^x)_{n \in \mathbb{N}}$ but we have one additional property that has to be fulfilled. In the event \underline{A}_n^x we have additionally that for $\mathbf{x} \in \mathcal{X}$ and for every $i \in \{1, \dots, n\}$ we have that the first diameter of \mathbf{x}_i is bounded from above by $2^{2(d-1)+\epsilon} f_n^{\frac{2\alpha_\kappa}{\alpha_1}}$. This property is necessary for the proof in the lower bound to get an upper bound for the distance that can be covered by the first n vertices of a path, and is also the only difference from the other sequence.

Using $(\underline{A}_n^x)_{n \in \mathbb{N}}$ combined with the *truncated first moment method* of [24] will give us the lower bound for the chemical distance. The idea of the truncated first moment method is to choose $\Delta \in \mathbb{N}$ big enough such that $\mathbb{P}_{x,y}(\text{dist}(\mathbf{x}, \mathbf{y}) \leq 2\Delta)$ is arbitrarily small. Defining $G_n^{(x,y)}$ as the event that a *good* (in some yet to be determined sense) path of length n connecting \mathbf{x}, \mathbf{y} exists, and $B_n^{(x)}$ as the event that a *bad* (i.e. not good) path starting in \mathbf{x} of length n exists, we have by counting the numbers of bad and good paths of length Δ , respectively 2Δ , the following inequality:

$$\mathbb{P}_{x,y}(\text{dist}(\mathbf{x}, \mathbf{y}) \leq 2\Delta) \leq \sum_{n=1}^{\Delta} \mathbb{P}_x(B_n^{(x)}) + \sum_{n=1}^{\Delta} \mathbb{P}_y(B_n^{(y)}) + \sum_{n=1}^{2\Delta} \mathbb{P}_{x,y}(G_n^{(x,y)}).$$

We now formalise what a good path is. We say that a path of length n connecting \mathbf{x} and \mathbf{y} via vertices $\mathbf{x}_1, \dots, \mathbf{x}_{n-1} \in \mathcal{X}$ such that with $\mathbf{x}_0 = \mathbf{x}$ and $\mathbf{x}_n = \mathbf{y}$ is good, if the vertices $\mathbf{x}_0, \dots, \mathbf{x}_{\lceil n/2 \rceil}$ imply that $\underline{A}_{\lceil n/2 \rceil}^x$ holds and $\mathbf{x}_n, \dots, \mathbf{x}_{\lceil n/2 \rceil}$ imply that $\underline{A}_{\lceil n/2 \rceil}^y$ holds. For $n \in \mathbb{N}$ and $\mathbf{x} \in \mathcal{X}$ we say that a path consisting of vertices $\mathbf{x}_0, \dots, \mathbf{x}_n$ is bad, if the vertices $\mathbf{x}_0, \dots, \mathbf{x}_{n-1}$ imply that \underline{A}_{n-1}^x holds, but $\mathbf{x}_0, \dots, \mathbf{x}_n$ do not imply that \underline{A}_n^x holds.

Consider now a good path of length n and note that the property of being good imposes a maximum Euclidean distance such a path can reach starting from a location $x \in \mathcal{P}$. Setting Δ small enough so that the sum over the maximum lengths of the first diameters of the n convex bodies in this path is smaller than $|x - y|$, we get that $\sum_{n=1}^{2\Delta} \mathbb{P}_{x,y}(G_n^{(x,y)}) = 0$. By definition, a good path of length n satisfies $D_{x_i}^{(1)} < 2^{2(d-1)+\epsilon} f_i^{\frac{2\alpha_K}{\alpha_1}}$ for $i \in \{0, \dots, \lceil n/2 \rceil\}$ and $D_{x_{n-i+1}}^{(1)} < 2^{2(d-1)+\epsilon} f_i^{\frac{2\alpha_K}{\alpha_1}}$ for $i \in \{1, \dots, \lceil n/2 \rceil\}$. We therefore have to find the maximal even $m \in \mathbb{N}$ such that

$$2 \sum_{n=1}^{m/2} 2^{2(d-1)+\epsilon} f_n^{\frac{2\alpha_K}{\alpha_1}} < |x - y|,$$

which will give us the largest possible value for Δ . Using the definition of the threshold sequence leads to the following inequality

$$2 \sum_{n=1}^{m/2} 2^{2(d-1)+\epsilon} f_0^{\frac{2\alpha_K}{\alpha_1} \left(\frac{\min\{d-\kappa, \kappa\}}{\alpha_K - \kappa} - \epsilon \right)^n} < |x - y|. \quad (3.3)$$

3.2. Proof of the lower bound

Choosing f_0 big enough it follows that

$$2 \sum_{n=1}^{m/2} 2^{2(d-1)+\epsilon} f_0^{\frac{2\alpha_\kappa}{\alpha_1} \left(\frac{\min\{d-\kappa, \kappa\}}{\alpha_\kappa - \kappa} - \epsilon \right)^n} \leq 3 \cdot 2^{2(d-1)+\epsilon} f_0^{\frac{2\alpha_\kappa}{\alpha_1} \left(\frac{\min\{d-\kappa, \kappa\}}{\alpha_\kappa - \kappa} - \epsilon \right)^{m/2}}.$$

With that we have that (3.3) is true if

$$3 \cdot 2^{2(d-1)+\epsilon} f_0^{\frac{2\alpha_\kappa}{\alpha_1} \left(\frac{\min\{d-\kappa, \kappa\}}{\alpha_\kappa - \kappa} - \epsilon \right)^{m/2}} < |x - y|.$$

Applying a double logarithm on both sides of the inequality we see that this is equivalent to

$$\begin{aligned} \frac{m}{2} \log \left(\frac{\min\{d - \kappa, \kappa\}}{\alpha_\kappa - \kappa} - \epsilon \right) + \log \left(\frac{2\alpha_\kappa}{\alpha_1} \log(f_0) + \log(3) + \log(2^{2(d-1)+\epsilon}) \right) \\ < \log \log |x - y|. \end{aligned}$$

This leads to the following upper bound for m :

$$m < 2 \frac{\log \log |x - y| - \log \left(\frac{2\alpha_\kappa}{\alpha_1} \log(f_0) + \log(3) + \log(2^{2(d-1)+\epsilon}) \right)}{\log \left(\frac{\min\{d-\kappa, \kappa\}}{\alpha_\kappa - \kappa} - \epsilon \right)}. \quad (3.4)$$

Let $\delta > 0$. If we choose m small enough to satisfy

$$m \leq \frac{(2 - \delta) \log \log |x - y|}{\log \left(\frac{\min\{d-\kappa, \kappa\}}{\alpha_\kappa - \kappa} - \epsilon \right)},$$

we get that as $|x - y| \rightarrow \infty$, such an m also satisfies inequality (3.4) and therefore also (3.3). Choosing now

$$2\Delta = \frac{(2 - \delta) \log \log |x - y|}{\log \left(\frac{\min\{d-\kappa, \kappa\}}{\alpha_\kappa - \kappa} - \epsilon \right)}$$

therefore yields $\sum_{n=1}^{2\Delta} \mathbb{P}_{x,y}(G_n^{(x,y)}) = 0$ for $|x - y|$ large enough, as desired.

Looking now at the bad paths we will show that

$$\sum_{n=1}^{\infty} \mathbb{P}_x(B_n^{(x)}) < \delta(f_0),$$

where δ is a function satisfying $\lim_{t \rightarrow \infty} \delta(t) = 0$. We have by definition that

$$\mathbb{P}_x(B_n^{(x)}) = \mathbb{P}_x((\underline{A}_n^x)^c \cap \underline{A}_{n-1}^x) \leq \mathbb{P}_x((\underline{A}_n^x)^c \mid \underline{A}_{n-1}^x).$$

3.2. Proof of the lower bound

Finding a suitable summable upper bound for $\mathbb{P}_x((\underline{A}_n^x)^c | \underline{A}_{n-1}^x)$ for all $n \in \mathbb{N}$ will complete the proof. For this we adapt a calculation from Section 2.2.2 and highlight here only the relevant changes. Note that these changes are not necessary to prove the same statements for the events \bar{A}_n^x which we will use in the proof of the upper bound. To continue, recall the definitions $Q_{f_n}(x, y)$ from (2.7) and $Q_{f_n}^*(x, y)$ from (2.2.2).

The key step in the proof of the universal criteria of robustness was to get a suitable lower bound for

$$\mathbb{P}_C((x + C) \cap Q_{f_n}^*(x_n, x) \neq \emptyset | D_C^{(\kappa)} \geq 2^{2(d-1)+\epsilon} f_{n+1}) \mathbb{P}_C(D_C^{(\kappa)} \geq 2^{2(d-1)+\epsilon} f_{n+1}).$$

Following the same arguments as in Section 2.2.2, this is equivalent to finding a lower bound for

$$\mathbb{P}_C\left((x+C) \cap Q_{f_n}^*(x_n, x) \neq \emptyset \left| \begin{array}{l} D_C^{(\kappa)} \geq 2^{2(d-1)+\epsilon} f_{n+1}, \\ D_C^{(1)} \leq 2^{2(d-1)+\epsilon} f_{n+1}^{\frac{2\alpha_\kappa}{\alpha_1}} \end{array} \right. \right) \mathbb{P}_C\left(\begin{array}{l} D_C^{(\kappa)} \geq 2^{2(d-1)+\epsilon} f_{n+1}, \\ D_C^{(1)} \leq 2^{2(d-1)+\epsilon} f_{n+1}^{\frac{2\alpha_\kappa}{\alpha_1}} \end{array} \right). \quad (3.5)$$

The conditional probability depends only on the volume of the set of suitable orientations for C that result in an intersection of $(x + C)$ with $Q_{f_n}^*(x_n, x)$. As in Section 2.2.2 we get

$$\mathbb{P}_C\left((x + C) \cap Q_{f_n}^*(x_n, x) \neq \emptyset \left| \begin{array}{l} D_C^{(\kappa)} \geq 2^{2(d-1)+\epsilon} f_{n+1}, \\ D_C^{(1)} \leq 2^{2(d-1)+\epsilon} f_{n+1}^{\frac{2\alpha_\kappa}{\alpha_1}} \end{array} \right. \right) \geq c \frac{f_n^{\min\{d-\kappa, \kappa\}}}{f_{n+1}^{d-\kappa}}.$$

For the second probability term in (3.5) we have to use again the Potter bounds for regularly varying random variables. We therefore have for $s > \varepsilon$

$$\begin{aligned} \mathbb{P}_C(D_C^{(\kappa)} \geq s, D_C^{(1)} \leq s^{\frac{2\alpha_\kappa}{\alpha_1}}) &= \mathbb{P}_C(D_C^{(\kappa)} \geq s) - \mathbb{P}_C(D_C^{(\kappa)} \geq s, D_C^{(1)} > s^{\frac{2\alpha_\kappa}{\alpha_1}}) \\ &\geq c^{-1}(s^{-(\alpha_\kappa+\varepsilon)} - s^{-2\alpha_\kappa+\varepsilon}). \end{aligned}$$

For s big enough we then have

$$c^{-1}(s^{-(\alpha_\kappa+\varepsilon)} - s^{-2\alpha_\kappa+\varepsilon}) \geq \frac{1}{2}c^{-1}s^{-(\alpha_\kappa+\varepsilon)},$$

since for $\varepsilon > 0$ small enough we have $-(\alpha_\kappa + \varepsilon) > -2\alpha_\kappa + \varepsilon$. This gives us the following lower bound for the second probability factor of (3.5)

$$\mathbb{P}_C\left(\begin{array}{l} D_C^{(\kappa)} \geq 2^{2(d-1)+\epsilon} f_{n+1}, \\ D_C^{(1)} \leq 2^{2(d-1)+\epsilon} f_{n+1}^{\frac{2\alpha_\kappa}{\alpha_1}} \end{array} \right) \geq c f_{n+1}^{-(\alpha_\kappa+\varepsilon)}.$$

3.2. Proof of the lower bound

Following now the rest of the calculation as in Section 2.2.2 we get

$$\mathbb{P}_x((A_n^x)^c \mid A_{n-1}^x) \leq \exp(-uc f_n^{\epsilon(\alpha_\kappa - \kappa)/2}).$$

which finally gives us

$$\begin{aligned} \sum_{n=1}^{\infty} \mathbb{P}_x(B_n^{(x)}) &\leq \sum_{n=1}^{\infty} \exp\left(-uc f_n^{\epsilon \frac{\alpha_\kappa - \kappa}{2}}\right) \\ &= \sum_{\ell=0}^{\infty} \exp\left(-uc \left\{f_0^{\epsilon(\alpha_\kappa - \kappa)/2}\right\}^{\left(\frac{\min\{d-\kappa, \kappa\}}{\alpha_\kappa - \kappa} - \epsilon\right)^\ell}\right) =: \delta(f_0). \end{aligned}$$

This can be made arbitrary small by choosing f_0 big enough. Putting all of the bounds together, we obtain

$$\begin{aligned} \mathbb{P}_{x,y}(\text{dist}(\mathbf{x}, \mathbf{y}) \leq 2\Delta) &\leq \sum_{n=1}^{\Delta} \mathbb{P}_x(B_n^{(x)}) + \sum_{n=1}^{\Delta} \mathbb{P}_y(B_n^{(y)}) + \sum_{n=1}^{2\Delta} \mathbb{P}_{x,y}(G_n^{(x,y)}) \\ &< 2\delta(f_0) \xrightarrow{f_0 \rightarrow \infty} 0. \end{aligned}$$

□

Remark 3.3. If $\alpha_k \geq \min\{2k, d\}$ for all $k \in \{1, \dots, d\}$ and therefore $\mathcal{M} = \emptyset$, we use a standard almost sure coupling argument as follows. For an arbitrary realisation of the model we extend for all $\mathbf{x} \in \mathcal{X}$ their first diameters $D_x^{(1)}$ using the following deterministic transformation. Let F be the cumulative distribution function of the first diameter in the model, and G the cumulative distribution function of an arbitrary regularly varying random variable with index $-(2-\rho)$ for small $\rho > 0$. We replace a given first diameter ℓ by $G^{-1}(F(\ell))$ when this value is larger than ℓ and keep it as before otherwise. One can quickly check that the resulting model dominates the original one in the sense that all extended convex bodies contain their original versions; all of the bodies also remain convex and their further diameters remain unchanged. Crucially, the tail index of the first diameter in this updated model is $-(2-\rho)$ and therefore the updated model has $\mathcal{M} = \{1\}$ and $\alpha_k > k$ for all $k \in \{1, \dots, d\}$, so the main statement of Theorem 3.1 applies. Since this model dominates the original model for each realisation, the lower bound for its chemical distance is a lower bound for the original model as well.

As proven in this section, the lower bound is then with high probability equal to $\frac{2-\delta}{\log(2/(1-\rho))} \log \log |x - y|$ for all $\delta > 0$. The factor in front of the $\log \log$ term is strictly increasing and converges to infinity as $\rho \downarrow 0$. Consequently, we get

that for models with $\mathcal{M} = \emptyset$ such that $\alpha_k \geq \min\{2k, d\}$ for all $k \in \{1, \dots, d\}$ the chemical distance is bigger than $c \log \log |x - y|$ with high probability for any $c > 0$.

3.3 Proof of the upper bound

In this section we first focus on the case that $\mathcal{M} \neq \emptyset$ and $\alpha_k > k$ for all $k \in \{1, \dots, d\}$. The proof of the upper bound will be shown for a fixed $k \in \{1, \dots, d-1\}$ which satisfies $\alpha_k \in (k, \min\{2k, d\})$, i.e. $k \in \mathcal{M}$. Since the result will hold uniformly in k , it will in particular also hold for κ as defined in Theorem 3.1. We consider the “smallest” Boolean model satisfying the condition $\alpha_k \in (k, \min\{2k, d\})$, which has the first k diameters almost surely of the same size and regularly varying with index $-\alpha_k$. The other diameters are set to be deterministic of size $\epsilon > 0$. Since we are interested in smallest convex bodies, note that the smallest convex bodies that have diameters of size $D^{(1)}, \dots, D^{(d)}$ are the convex hulls of the endpoints of all of the diameters, i.e. the d -dimensional convex polytopes with $2d$ vertices. Each such convex polytope with diameters $D^{(1)}, \dots, D^{(d)}$ contains a box with side-lengths $2^{-2(d-1)}D^{(1)}, \dots, 2^{-2(d-1)}D^{(d)}$, which is stated in Lemma A.1 in Section A.1. So we work from here on out with these boxes instead of the larger polytopes that they are contained in. We can do this without affecting our final result, as we explain next.

For $u > 0$ we define ${}^u\mathbb{P}$ as the probability measure of the Poisson-Boolean base model where the underlying Poisson point process for the locations of the vertices has intensity $u > 0$. Let C_∞ be an unbounded connected component of this model. Recall that by [9], if C_∞ exists, it is almost surely unique. We define the percolation probability

$$\theta(u) := {}^u\mathbb{P}(0 \in C_\infty).$$

As we work here with a fixed vertex intensity $u > 0$ we can therefore write \mathbb{P} and θ instead of ${}^u\mathbb{P}$ and $\theta(u)$. Furthermore, we omit the scaling factor $2^{-2(d-1)}$ and assume that the boxes have side-lengths $D^{(1)}, \dots, D^{(d)}$. We can do this without loss of generality, since constant factors do not affect the regularly varying distribution of the diameters (and by extension side-lengths of our boxes), and the Poisson point process of intensity u rescaled by a factor $2^{-2(d-1)}$ remains a Poisson point process (with intensity $2^{-2(d-1)}u$). Consequently, using that we are in the robust regime of the model, we can start

3.3. Proof of the upper bound

with intensity $2^{-2(d-1)}u$ instead of u for the original model and proceed with our assumption. Furthermore, using the same property of regularly varying distributions as above, we will treat the side-lengths of the boxes as if they were the *de facto* diameters in order to keep geometric arguments easier to follow and the notation more concise (if we were being precise the calculations would, up to constant multiplicative factors, remain the same). We will use for the remainder of this section the terms *convex body* and *box* interchangeably, depending on which helps understand the current argument better.

With this we can proceed to the proof of the upper bound. We use a similar argument as in [35] and [24], which relies on a classical sprinkling argument to connect various parts of the graph with each other.

Recall the definition of a ball $B_r(y)$ for $r > 0$, $y \in \mathbb{R}^d$. We focus first on the regions around of 0 and x , namely $B_{\frac{3}{8}|x|}(0)$ (resp. $B_{\frac{3}{8}|x|}(x)$) and show that $\mathbf{0}$ (resp. \mathbf{x}) is connected via a path to a vertex \mathbf{z}_0 (resp. \mathbf{z}_x), with $D_{z_0}^{(k)} > f_0$ (resp. $D_{z_x}^{(k)} > f_0$) in this region, where f_0 will be chosen later and the entire path is contained inside $B_{\frac{3}{8}|x|}(0)$ (resp. $B_{\frac{3}{8}|x|}(x)$). Note that f_0 above is the first element of the threshold sequence that was introduced in Section 3.2.

Recall from Section 3.2 the definition $(\bar{A}_n^z)_{n \in \mathbb{N}}$ for a given vertex $\mathbf{z} \in \mathcal{X}$. As promised in Remark 3.2, we remind the reader now that from here on out, when referring to the arguments that we used in Section 3.2 they are to be read with $k \in \mathcal{M}$ instead of with κ . Due to Section 2.2.2 we know that starting with a convex body with $D_z^{(k)} > f_0$, for some $\mathbf{z} \in \mathcal{X}$, the probability that we cannot find a path consisting of convex bodies which fulfil the events $(\bar{A}_n^z)_{n \in \mathbb{N}}$ is smaller than

$$2 \left(\exp(-ucf_0^{d-\alpha_k-\epsilon}) + \sum_{\ell=0}^{\infty} \exp\left(-uc\{f_0^{\epsilon(\alpha_k-k)/2}\}^{\left(\frac{\min\{d-k,k\}}{\alpha_k-k}-\epsilon\right)^\ell}\right) \right) =: \Gamma(f_0). \quad (3.6)$$

As in Section 2.2.2, f_0 can be chosen large enough to guarantee $\Gamma(f_0) < 1$. To that end, let now $\rho := \rho(u, d, k, \alpha_k, \epsilon) > 1$ be such to ensure $\Gamma(\rho) < 1$. Consider now the event Z_n that no path fulfilling the events $(\bar{A}_i^z)_{i \in \mathbb{N}}$ with $f_0 = \rho^n$ exists. By the above, the probability of this event is $\Gamma(\rho^n)$ and furthermore, by (3.6) we also have

$$\sum_{n=1}^{\infty} \mathbb{P}(Z_n) = \sum_{n=1}^{\infty} \Gamma(\rho^n) < \infty.$$

By Borel-Cantelli, it follows that

$$\mathbb{P}(\liminf_{n \rightarrow \infty} Z_n^c) = 1.$$

Consequently, there exists an almost surely finite $m \in \mathbb{N}$ such that starting the threshold sequence with $f_0 = \rho^m$, there exists almost surely a path that satisfies the events $(\bar{A}_n^z)_{n \in \mathbb{N}}$. Using this to get an infinite path we claim that the paths starting from $\mathbf{0}$ and from \mathbf{x} are connected to vertices that fulfil the condition $D_{z_0}^{(k)}, D_{z_x}^{(k)} \geq \rho^m$ and that both paths (which exists almost surely by the above argument) are connected with each other sufficiently early along each of them, by using a single further vertex, all of which occurs with high probability. From here on out, when requiring that f_0 is large enough, we will implicitly also assume that the above construction is followed.

Connecting $\mathbf{0}$ and \mathbf{x} to infinite paths in almost surely bounded many steps.

We need to ensure that the construction of the path from $\mathbf{0}$ to \mathbf{z}_0 (resp. \mathbf{x} to \mathbf{z}_x) is independent of the path between \mathbf{z}_0 and \mathbf{z}_x , so we use the superposition and thinning properties of the Poisson point process to split it into two independent thinned versions, similarly to how it is done in [35] or [24]. With that in mind, let $b \in (0, 1)$ be an arbitrary number; we colour each vertex of \mathcal{X} black with probability b and red with probability $r := 1 - b$, independently of everything else. We write \mathcal{G}_u^b (resp. \mathcal{G}_u^r) for the graph induced by the black (resp. red) vertices in $\mathcal{G}_u := \mathcal{G}$, where we write u to emphasise the dependence of the model on the density parameter u . Moreover let C_∞^b (resp. C_∞^r) be the unbounded connected component in \mathcal{G}_u^b (resp. \mathcal{G}_u^r). Since we are working in the robust regime of the model, both of these components exist almost surely.

We define $E_0^b(n, s, v)$ to be the event that there exists a vertex \mathbf{z}_0 in the graph \mathcal{G}_u^b with $D_{z_0}^{(k)} > s$ such that $|z_0 - 0| < v$ and \mathbf{z}_0 and $\mathbf{0}$ are connected via at most n further convex bodies. Similarly we define $E_x^b(n, s, v)$ for \mathbf{x} . In addition to that we define for $\mathbf{z}_0 \in \mathcal{X}$ $E_{0,z_0}^b(n, s, v)$ as the event that $E_0^b(n, s, v)$ occurs and the vertex with location z_0 is the vertex that makes it occur. Similarly, we write $E_{x,z_x}^b(n, s, v)$ for $\mathbf{z}_x \in \mathcal{X}$ as the corresponding asked vertex in $E_x^b(n, s, v)$. Moreover we also note that $\{\mathbf{0} \leftrightarrow \mathbf{x}\} \cap \{\mathbf{0}, \mathbf{x} \in C_\infty\}$ converges from below to the event $\{\mathbf{0}, \mathbf{x} \in C_\infty\}$ as $|x|$ goes to infinity due to the uniqueness of the unbounded component (see [9]).

To prove the full claim it suffices to show that for every $s > 0$ there exists almost surely a finite random variable $N(s)$ such that

$$\lim_{b \uparrow 1} \liminf_{s \rightarrow \infty} \liminf_{|x| \rightarrow \infty} \mathbb{P}_{0,x}(\{\mathbf{0}, \mathbf{x} \in C_\infty^b\} \cap E_0^b(N(s), s, |x|/8) \cap E_x^b(N(s), s, |x|/8) \cap F) \geq \theta^2, \quad (3.7)$$

3.3. Proof of the upper bound

where F is the event that there exists a path such that $\mathbf{0}$ and \mathbf{x} are connected in fewer than $(2 + \delta) \log \log |x| / (\log(\min\{d - k, k\}) - \log(\alpha_k - k))$ steps for small $\delta > 0$. We show first

$$\liminf_{s \rightarrow \infty} \liminf_{|x| \rightarrow \infty} \mathbb{P}_{0,x}(\{\mathbf{0}, \mathbf{x} \in C_\infty^b\} \cap E_0^b(N(s), s, |x|/8) \cap E_x^b(N(s), s, |x|/8) \cap F) \geq \theta_b^2,$$

from which (3.7) follows by the following Proposition.

Proposition 3.4. *The function $u \mapsto \theta(u)$ is continuous for the Poisson Boolean model with boxes as grains for $u \neq u_c$.*

Proof of Proposition 3.4. The proof can be adapted to the proof with balls as convex grains as in [51, Theorem 3.9] or [45]. The only thing we have to check is $\mathbb{P}_{0,x}(\{C_x \cap \partial C_0 \neq \emptyset\} \cap \{C_x \cap \text{int}(C_0) = \emptyset\}) = 0$ for all $x \in \mathcal{P}$, which is stated in Lemma A.5 and proven in Section A.6. \square

To show the upper bound of θ_b note that

$$\begin{aligned} & \mathbb{P}_{0,x}(\{\mathbf{0}, \mathbf{x} \in C_\infty^b\} \cap E_0^b(N(s), s, |x|/8) \cap E_x^b(N(s), s, |x|/8) \cap F) \\ &= \mathbb{E}_{0,x} \left[\mathbb{P}_{0,x,z_0,z_x}(\{\mathbf{0}, \mathbf{x} \in C_\infty^b\} \cap E_{0,z_0}^b(N(s), s, |x|/8) \cap E_{x,z_x}^b(N(s), s, |x|/8) \cap F) \right] \\ &\geq \mathbb{P}_{0,x}(\{\mathbf{0}, \mathbf{x} \in C_\infty^b\}) \\ &\quad - \mathbb{P}_{0,x}(\{\mathbf{0} \in C_\infty^b\} \setminus E_0^b(N(s), s, |x|/8)) \\ &\quad - \mathbb{P}_{0,x}(\{\mathbf{x} \in C_\infty^b\} \setminus E_x^b(N(s), s, |x|/8)) \\ &\quad - \mathbb{E}_{0,x} \left[\mathbb{P}_{0,x,z_x,z_0}((E_{0,z_0}^b(N(s), s, |x|/8) \cap E_{x,z_x}^b(N(s), s, |x|/8)) \setminus F) \right]. \end{aligned} \tag{3.8}$$

We now show that the last three summands converge to zero as s and $|x|$ are made large. Due to the translation invariance of the Poisson process, the second and third summands are equal. Considering the limit $s \rightarrow \infty$ and using the same arguments as for the proof in [24, Lemma 3.2] gives that the second and third term converge to 0, since the probability of arbitrary big convex bodies belonging to the unbounded connected component is positive. It remains to consider the last summand of (3.8). For this we need two things. First, we will use the properties of the infinite path that satisfies $(\bar{A}_n^{z_0})_{n \in \mathbb{N}}$ (resp. $(\bar{A}_n^{z_x})_{n \in \mathbb{N}}$), so that we have two growing sequences of convex bodies. Second, we will find a single convex body to ensure that the two infinite paths are connected to each other “early on”.

Reaching sufficiently powerful vertices in fewer than

$\frac{(1+\delta)}{\log\left(\frac{\min\{d-k,k\}}{\alpha_k-k}\right)} \log \log |x-y|$ **many steps, with high probability.** As argued before, we know that an infinite path exists when starting with a convex body which is large enough, namely if its threshold sequence begins with $f_0 > 0$ big enough. We focus now on the infinite path started from \mathbf{z}_0 using that $(\bar{A}_n^{z_0})_{n \in \mathbb{N}}$ holds and denote by n_1 the first index i in the path, for which the corresponding threshold $f_i \geq |x|/8$. For the path starting in \mathbf{z}_0 we denote this convex body with its location by \mathbf{y}_0 (resp. \mathbf{y}_x for the path starting in \mathbf{z}_x). To avoid confusion, note that \mathbf{y}_0 is not the n_1 th vertex of the path started in $\mathbf{0}$, but is instead only the n_1 th vertex *after* \mathbf{z}_0 , which is itself almost surely finitely many steps along the path. The same observation of course holds also for \mathbf{y}_x . Let now, as before, f_0 be large enough. This leads to

$$\begin{aligned} f_{n_1} &\geq |x|/8 \\ \Leftrightarrow f_0^{\left(\frac{\min\{d-k,k\}}{\alpha_k-k} - \epsilon\right)^{n_1}} &\geq |x|/8 \\ \Leftrightarrow n_1 \log\left(\frac{\min\{d-k,k\}}{\alpha_k-k} - \epsilon\right) + \log \log f_0 &\geq \log \log(|x|/8). \end{aligned}$$

Recall that we are interested in an upper bound for the chemical distance. We choose therefore

$$n_1 \geq \left\lceil \frac{\log(\log |x| - \log(8)) - \log \log f_0}{\log\left(\frac{\min\{d-k,k\}}{\alpha_k-k} - \epsilon\right)} \right\rceil.$$

We can assume without loss of generality that $|x|$ is large enough so that the locations of the vertex \mathbf{y}_0 as well as all preceding vertices are in $B_{\frac{3}{8}|x|}(\mathbf{0})$ and by translation invariance the same is true for \mathbf{y}_x and the ball $B_{\frac{3}{8}|x|}(x)$. We can assume without loss of generality that $f_{n_1} = |x|/8$ as we have that $\lceil |x| \rceil / |x|$ converges to 1 as $|x| \rightarrow \infty$. In all other cases we get some (bounded) multiplicative factors in the calculations which do not affect the results.

Before proceeding to the final missing step, let us summarise our work so far. Once (3.7) is established, we have that on the event $\{\mathbf{0}, \mathbf{x} \in C_\infty\}$, one can in at most almost surely finitely many (in fact and crucially, almost surely bounded many) steps connect $\mathbf{0}$ to some vertex \mathbf{z}_0 with high probability as $|x| \rightarrow \infty$. The convex body of this vertex is then sufficiently large that it is almost surely the first vertex of an infinite path satisfying the events $(\bar{A}_n^{z_0})_{n \in \mathbb{N}}$, whose n_1 th vertex \mathbf{y}_0 has the k th side-length larger than $|x|/8$ and the path from \mathbf{z}_0 to \mathbf{y}_0 takes fewer than $(1 + \delta) \log \log |x| / \log\left(\frac{\min\{d-k,k\}}{\alpha_k-k}\right)$ many steps

3.3. Proof of the upper bound

for small $\delta > 0$; the same is true also for the vertex \mathbf{x} . Once we establish that \mathbf{y}_0 and \mathbf{y}_x are connected to the same vertex with an even larger convex body with high probability, (3.7) will be proven and the proof of the upper bound complete. The above construction is outlined in Figure 3.1, showing how the path connecting $\mathbf{0}$ with \mathbf{x} arises.

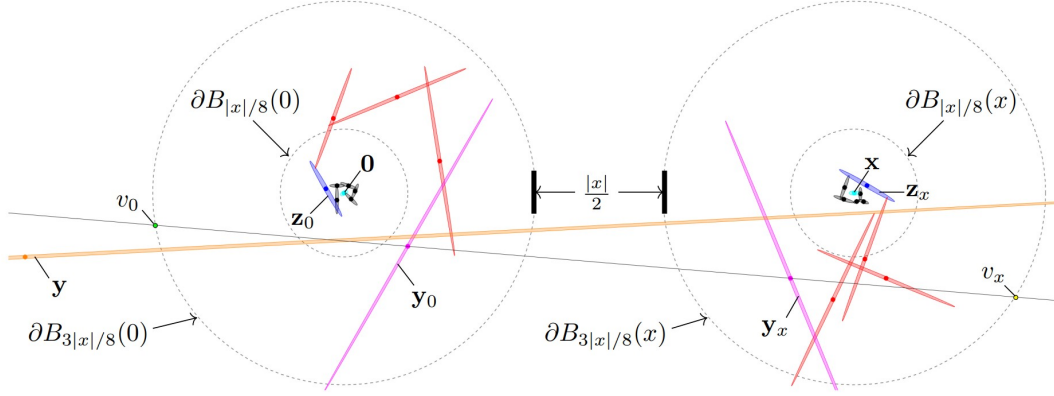


Figure 3.1: In cyan blue $\mathbf{0}$ and \mathbf{x} , in black the path connecting $\mathbf{0}$ with \mathbf{z}_0 (resp. \mathbf{x} with \mathbf{z}_x), in blue \mathbf{z}_0 and \mathbf{z}_x , the path connecting \mathbf{z}_0 with \mathbf{y}_0 in red (resp. \mathbf{z}_x with \mathbf{y}_x), \mathbf{y}_0 and \mathbf{y}_x in pink and in orange the vertex \mathbf{y} connecting \mathbf{y}_0 and \mathbf{y}_x . The dashed gray circles are the boundary of $B_{|x|/8}(0)$, $B_{3|x|/8}(0)$, $B_{|x|/8}(x)$ and $B_{3|x|/8}(x)$. v_0 and v_x as defined in (3.13) and (3.14).

Connecting the two sufficiently powerful vertices through a single connecting vertex with high probability. We now proceed to argue this last step. For that we define $F_{n_1}^{(0,z_0)}$ (resp. $F_{n_1}^{(x,z_x)}$) as the event that there

exists a path of length n_1 in the graph \mathcal{G}_u^r such that starting with \mathbf{z}_0 (resp. \mathbf{z}_x) the path satisfies $\bar{A}_{n_1}^{z_0}$ (resp. $\bar{A}_{n_1}^{z_x}$). In addition to that we define $F_{n_1}^{(0,z_0,y_0)}$ as the event that in $F_{n_1}^{(0,z_0)}$, \mathbf{y}_0 is the n_1 th vertex in the path that implies $\bar{A}_{n_1}^{z_0}$. Analogously we define $F_{n_1}^{(x,z_x,y_x)}$ for \mathbf{y}_x . Moreover let $F^{(0,x,y_0,y_x)}$ be the event that there exists a vertex outside of $B_{\frac{\min\{d-k,k\}}{|x|}\alpha_k - k} - \epsilon(0)$ with a corresponding box that intersects \mathbf{y}_0 and \mathbf{y}_x . Note that under the condition that $0, x, z_0, z_y, y_0, y_x \in \mathcal{P}$ we have that $F_{n_1}^{(0,z_0,y_0)} \cap F_{n_1}^{(x,z_x,y_x)} \cap F^{(0,x,y_0,y_x)} \subseteq F$, conditioned on $E_0^b(D(s), s, |x|/8) \cap E_x^b(D(s), s, |x|/8)$; i.e. the start of the path in $\mathbf{0}$ and \mathbf{x} being successful. From here on we write E_{0,z_0}^b for $E_{0,z_0}^b(D(s), s, |x|/8)$ (resp. E_{x,z_x}^b for $E_{x,z_x}^b(D(s), s, |x|/8)$) to keep the notation concise. We will now focus on the probability in the brackets of the last summand in (3.8). We can

3.3. Proof of the upper bound

rewrite this term to

$$\mathbb{P}_{0,x,z_0,z_x}((E_{0,z_0}^b \cap E_{x,z_x}^b) \setminus F) = \mathbb{P}_{0,x,z_0,z_x}(F^c \mid E_{0,z_0}^b \cap E_{x,z_x}^b) \mathbb{P}_{0,x,z_0,z_x}(E_{0,z_0}^b \cap E_{x,z_x}^b) \quad (3.9)$$

in order to work with the conditional probability given $E_{0,z_0}^b \cap E_{x,z_x}^b$, and use the events defined earlier to bound the last expression from above by using

$$\begin{aligned} & \mathbb{E}_{0,x,z_0,z_x} \left[\mathbb{P}_{0,x,z_0,z_x,y_0,y_x}((F_{n_1}^{(0,z_0,y_0)} \cap F_{n_1}^{(x,z_x,y_x)} \cap F^{(0,x,y_0,y_x)})^c \mid E_{0,z_0}^b \cap E_{x,z_x}^b) \right. \\ & \quad \left. \times \mathbb{P}_{0,x,z_0,z_x,y_0,y_x}(E_{0,z_0}^b \cap E_{x,z_x}^b) \right] \\ & \leq \mathbb{P}_{0,x,z_0,z_x}((F_{n_1}^{(0,z_0)})^c \cup (F_{n_1}^{(x,z_x)})^c \mid E_{0,z_0}^b \cap E_{x,z_x}^b) \quad (3.10) \\ & \quad + \mathbb{E}_{0,x,z_0,z_x} \left[\mathbb{P}_{0,x,z_0,z_x,y_0,y_x}((F_{n_1}^{(0,z_0,y_0)} \cap F_{n_1}^{(x,z_x,y_x)}) \cap (F^{(0,x,y_0,y_x)})^c \mid E_{0,z_0}^b \cap E_{x,z_x}^b) \right. \\ & \quad \left. \times \mathbb{P}_{0,x,z_0,z_x,y_0,y_x}(E_{0,z_0}^b \cap E_{x,z_x}^b) \right]. \end{aligned}$$

The first summand is by our choice of f_0 almost surely equal to 0. In order to show that the last summand in (3.8) converges to zero it suffices to show that the second summand in (3.10) or equivalently

$$\mathbb{E}_{0,x,z_0,z_x} \left[\mathbb{P}_{0,x,z_0,z_x,y_0,y_x}(F_{n_1}^{(0,z_0,y_0)} \cap F_{n_1}^{(x,z_x,y_x)} \cap (F^{(0,x,y_0,y_x)})^c \cap E_{0,z_0}^b \cap E_{x,z_x}^b) \right] \quad (3.11)$$

has a uniform bound over all z_0 and z_x which converges to zero as $|x| \rightarrow \infty$; this implies that integrating (3.9) over z_0 and z_x leads to a term that converges to zero as $|x| \rightarrow \infty$. We focus now on $(F^{(0,x,y_0,y_x)})^c$ and introduce some new terminology to help us with that. Recall that $p_v^{(i)}$ is the orientation of the i th side-length of the box C_v for $\mathbf{v} \in \mathcal{X}$ and $i \in \{1, \dots, d\}$. We say a vertex $\mathbf{v} \in \mathcal{X}$ is *good with respect to* the vertex $\mathbf{w} \in \mathcal{X}$ if it satisfies the following two conditions.

(G1) The vertex \mathbf{v} has *good orientation* relative to the orientation of \mathbf{w} in the sense that for all $i \in \{1, \dots, d\}$ the orientation satisfies

$$p_v^{(i)} \in \{\phi \in \mathbb{S}^{d-1} : \angle(\phi, p_w^{(i)}) \leq \frac{\epsilon}{\log|x|}\}.$$

(G2) The location v of \mathbf{v} has *good position* relative to \mathbf{w} , i.e. it satisfies

$$\begin{aligned} & v \in \{y \in \mathbb{R}^d : |w - y| \geq 2f_{n_1}, \angle(w - y, \pm p_v^{(j)}) > \varphi \text{ for all } 1 \leq j \leq k\} \\ & =: A(w, n_1), \end{aligned}$$

where $\varphi = 2^{-(d+1)}(d+1)^{-1}$.

It is useful at this stage to note that by construction $|y_0 - y_x| \geq 2f_{n_1}$, which is one of the two conditions in (G2). We also observe (and prove later on) that when \mathbf{v} is good relative \mathbf{w} we have that the intersection of the orthogonal projections of C_v and C_w onto a hyperplane perpendicular to $v - w$, has $(d-1)$ -dimensional Lebesgue measure of order $f_{n_1}^k$. In addition to that (G2) gives us roughly that v does not lie “too close” to the affine subspace through w spanned by the k large side-lengths of C_w , where φ is chosen as in the definition (2.4). (G2) also ensures that v has distance at least $2f_{n_1}$ to w . Note that this is similar to the definition of (2.4). Observe also that the restriction in (G1) becomes tighter for large $|x|$, and so for sufficiently large $|x|$ we get that \mathbf{v} being good with respect to \mathbf{w} implies almost surely also the reverse relationship, i.e. \mathbf{w} is good with respect to \mathbf{v} .

Using this (in particular, that $|x|$ is large) we can rewrite $(F^{(0,x,y_0,y_x)})^c$ as

$$\begin{aligned}
 (F^{(0,x,y_0,y_x)})^c &= \left(\{ \bar{A}y \in \mathcal{P} \setminus B_{|x|}^{\frac{\min\{d-k,k\}}{\alpha_k-k} - \epsilon}(0) : C_y \cap C_{y_x} \neq \emptyset \text{ and } C_y \cap C_{y_0} \neq \emptyset \} \right. \\
 &\quad \left. \cap \{ \mathbf{y}_0 \text{ and } \mathbf{y}_x \text{ are good with respect to each other.} \} \right) \\
 &\cup \left(\{ \bar{A}y \in \mathcal{P} \setminus B_{|x|}^{\frac{\min\{d-k,k\}}{\alpha_k-k} - \epsilon}(0) : C_y \cap C_{y_x} \neq \emptyset \text{ and } C_y \cap C_{y_0} \neq \emptyset \} \right. \\
 &\quad \left. \cap \{ \mathbf{y}_0 \text{ and } \mathbf{y}_x \text{ are not good with respect to each other.} \} \right) \\
 &\subseteq \left(\{ \bar{A}y \in \mathcal{P} \setminus B_{|x|}^{\frac{\min\{d-k,k\}}{\alpha_k-k} - \epsilon}(0) : C_y \cap C_{y_x} \neq \emptyset \text{ and } C_y \cap C_{y_0} \neq \emptyset \} \right. \\
 &\quad \left. \cap \{ \mathbf{y}_0 \text{ and } \mathbf{y}_x \text{ are good with respect to each other.} \} \right) \\
 &\cup \{ \mathbf{y}_0 \text{ and } \mathbf{y}_x \text{ are not good with respect to each other.} \} \\
 &=: (E_1^{(y_0,y_x)} \cap E_2^{(y_0,y_x)}) \cup E_3^{(y_0,y_x)}.
 \end{aligned}$$

With this we can bound (3.11) from above by

$$\begin{aligned}
 &\mathbb{P}_{0,x,z_0,z_x,y_0,y_x} \left(E_1^{(y_0,y_x)} \cap E_2^{(y_0,y_x)} \cap F_{n_1}^{(0,z_0,y_0)} \cap F_{n_1}^{(x,z_x,y_x)} \cap E_{0,z_0}^b \cap E_{x,z_x}^b \right) \\
 &\quad + \mathbb{P}_{0,x,z_0,z_x,y_0,y_x} \left(E_3^{(y_0,y_x)} \cap F_{n_1}^{(0,z_0,y_0)} \cap F_{n_1}^{(x,z_x,y_x)} \cap E_{0,z_0}^b \cap E_{x,z_x}^b \right) \\
 &\leq \mathbb{P}_{0,x,z_0,z_x,y_0,y_x} \left(E_1^{(y_0,y_x)} \mid E_2^{(y_0,y_x)} \cap F_{n_1}^{(0,z_0,y_0)} \cap F_{n_1}^{(x,z_x,y_x)} \cap E_{0,z_0}^b \cap E_{x,z_x}^b \right) \\
 &\quad + \mathbb{P}_{0,x,z_0,z_x,y_0,y_x} \left(E_3^{(y_0,y_x)} \cap F_{n_1}^{(0,z_0,y_0)} \cap F_{n_1}^{(x,z_x,y_x)} \cap E_{0,z_0}^b \cap E_{x,z_x}^b \right).
 \end{aligned} \tag{3.12}$$

We will show that this expression has a uniform upper bound over all z_0, z_x, y_0, y_x and that this bound converges to zero as $|x| \rightarrow \infty$. For that we define similarly to Section 2.2.2 the σ -algebra \mathfrak{F}_n^x , generated by the restriction of the

3.3. Proof of the upper bound

(simplified box) Poisson-Boolean base model to the points with locations inside $B_{3f_n}(0) \cup B_{3f_n}(x)$. Using this we have that $E_2^{(y_0, y_x)}$, $F_{n_1}^{(0, z_0, y_0)}$, $F_{n_1}^{(x, z_x, y_x)}$, E_{0, z_0}^b , E_{x, z_x}^b are $\mathfrak{F}_{n_1}^x$ measurable.

Lemma 3.5. *For the events defined as above, we have*

$$\begin{aligned} \mathbb{P}_{0, x, z_0, z_x, y_0, y_x}(E_1^{(y_0, y_x)} | E_2^{(y_0, y_x)} \cap F_{n_1}^{(0, z_0, y_0)} \cap F_{n_1}^{(x, z_x, y_x)} \cap E_{0, z_0}^b \cap E_{x, z_x}^b) \\ \leq \exp(-uc|x|^{\epsilon(\alpha_k - k)/2}). \end{aligned}$$

Proof. We define for $v, w, z \in \mathbb{R}^d$ and $A \subseteq \mathbb{R}^d$ the set $P_{v, w}^z(A)$ as the orthogonal projection of A onto the hyperplane through z perpendicular to $w - v$. In addition to that define

$$v_0 := \frac{y_0 - y_x}{|y_0 - y_x|} \gamma_0(y_0, y_x) + y_0, \quad (3.13)$$

and

$$v_x := \frac{y_x - y_0}{|y_x - y_0|} \gamma_x(y_0, y_x) + y_x \quad (3.14)$$

where $\gamma_0(y_0, y_x), \gamma_x(y_0, y_x) > 0$ are chosen such that $v_0 \in \partial B_{3|x|/8}(0)$ and $v_x \in \partial B_{3|x|/8}(x)$. v_0 and v_x can be found in Figure 3.1.

With this we define

$$K_{v_x} := P_{y_0, y_x}^{v_x}(C_{y_0}) \cap P_{y_0, y_x}^{v_x}(C_{y_x}),$$

that is, the intersection of the orthogonal projections of C_{y_0} and C_{y_x} onto the hyperplane through v_x perpendicular to $y_x - y_0$. An example for K_{v_x} in \mathbb{R}^3 is pictured in Figure 3.2.

Since we are conditioning on the event that \mathbf{y}_0 and \mathbf{y}_x are good with respect to each other, we can control the size of the area of K_{v_x} . Recall that we assume $|x|$ is large enough for the *good with respect to* property to be symmetric, so that K_{v_x} is a $(d-1)$ -dimensional polytope with diameters $D_{K_{v_x}}^{(1)}, \dots, D_{K_{v_x}}^{(d-1)}$ which satisfy $D_{K_{v_x}}^{(i)} \geq \frac{1}{2}\varphi \min\{D_{y_0}^{(i)}, D_{y_x}^{(i)}\}$ for all $i \in \{1, \dots, d-1\}$. Consequently, the $(d-1)$ -dimensional Lebesgue mass of K_{v_x} is at most

$$c \prod_{i=1}^{d-1} \min\{D_{y_0}^{(i)}, D_{y_x}^{(i)}\},$$

where c is a constant that depends only on d and k . Besides, $D_{K_{v_x}}^{(1)}, \dots, D_{K_{v_x}}^{(k)} \geq \frac{1}{2}\varphi f_{n_1}$ and $D_{K_{v_x}}^{(k+1)}, \dots, D_{K_{v_x}}^{(d-1)} \geq \frac{1}{2}\varphi\epsilon$.

3.3. Proof of the upper bound

Using now Lemma A.1 we know that there exists a $(d-1)$ -dimensional box contained in K_{v_x} which is congruent to

$$c \cdot ([0, 2^{-2(d-2)} f_{n_1}]^k \times [0, 2^{-2(d-2)} \epsilon]^{d-1-k} \times \{0\}).$$

We denote by $B_{K_{v_x}}$ the box which satisfies this. This box is in general not unique, so we choose without loss of generality $B_{K_{v_x}}$ using an arbitrary lexicographic ordering of the boxes with respect to their centers, orientations and side-lengths. Note that the set of all possible boxes is closed and as such, a minimal (or maximal) element of can be uniquely chosen. In addition to that we define rot_{y_0, y_x} as the rotation that maps the canonical basis vectors e_1, \dots, e_d of \mathbb{R}^d as follows,

$$\begin{aligned} \text{rot}_{y_0, y_x}(e_1) &= \frac{y_x - y_0}{|y_x - y_0|}, \\ \text{rot}_{y_0, y_x}(e_i) &= v_i, \quad i \in \{2, \dots, d\}, \end{aligned}$$

where v_i is defined as the orientation of the $(i-1)$ st diameter of $B_{K_{v_x}}$, for $i \in \{2, \dots, d\}$. Note that the choice of $(v_i)_{i \in \{2, \dots, d\}}$ is unique up to permutations and mirrorings of the side-lengths of $B_{K_{v_x}}$ (and we pick the first of these according to some arbitrary ordering). We say a vertex $\mathbf{y} \in \mathcal{X}$ with corresponding box that intersects \mathbf{y}_0 and \mathbf{y}_x is *good* if it has the following properties.

(C1) C_y intersects $P_{y_0, y_x}^{v_0}(B_{K_{v_x}})$ and $\frac{1}{3}(B_{K_{v_x}} - v_x) + v_x$.

(C2) The k th side-length of C_y is at least $2(|v_x - v_0| + |y - v_0|)$.

(C3) For the location of \mathbf{y} we have

$$\begin{aligned} y \in I_{y_0, y_x} := \text{rot}_{y_0, y_x} \bigg(& \left\{ y = (y^{(1)}, \dots, y^{(d)}) \in \mathbb{R}^d : y^{(1)} \leq -|x|^{\frac{\min\{d-k, k\}}{\alpha_k - k} - \epsilon}, \right. \\ & y^{(i)} \in [-c_1(|y^{(1)}| + |v_0 - v_x|), c_1(|y^{(1)}| + |v_0 - v_x|)], \\ & y^{(j)} \in [-c_2(|y^{(1)}| + |v_0 - v_x|), c_2(|y^{(1)}| + |v_0 - v_x|)], \\ & \left. i \in \{2, \dots, k+1\}, j \in \{k+2, \dots, d\} \right\} \bigg) + v_0, \end{aligned}$$

where

$$c_1 := \frac{\frac{1}{3} \cdot 2^{-2(d-2)} f_{n_1}}{|v_0 - v_x|}$$

3.3. Proof of the upper bound

and

$$c_2 := \frac{\frac{1}{3} \cdot 2^{-2(d-2)} \epsilon}{|v_0 - v_x|}.$$

(C1) is chosen such that it implies that C_y intersects with C_{y_0} and C_{y_x} . Next, (C2) guarantees that the first k side-lengths of C_y are large enough to result in an intersection with $\frac{1}{3}(B_{K_{v_x}} - v_x) + v_x$ when the orientation of C_y is suitable. (C3) ensures that the argument we will use works for all $k \in \{1, \dots, d-1\}$ and that we do not have to treat the case $k=1$ separately. In particular it, together with (C2), ensures that if C_y intersects $\frac{1}{3}(B_{K_{v_x}} - v_x) + v_x$, it must also intersect $P_{y_0, y_x}^{v_0}(B_{K_{v_x}})$. Figure 3.2 depicts the sets (C1) and (C3) for the 3-dimensional case and Figure 3.3 illustrates the intuition behind the constants c_1 and c_2 .

To keep notation in the following calculations concise, we write $EF_{y_0, y_x}^{z_0, z_x}$ instead of $E_2^{(y_0, y_x)} \cap F_{n_1}^{(0, z_0, y_0)} \cap F_{n_1}^{(x, z_x, y_x)} \cap E_{0, z_0}^b \cap E_{x, z_x}^b$.

$$\begin{aligned} & \mathbb{P}_{0, x, z_0, z_x, y_0, y_x} \left(E_1^{(y_0, y_x)} \mid E_2^{(y_0, y_x)} \cap F_{n_1}^{(0, z_0, y_0)} \cap F_{n_1}^{(x, z_x, y_x)} \cap E_{0, z_0}^b \cap E_{x, z_x}^b \right) \\ & \leq \mathbb{E}_{0, x, z_0, z_x, y_0, y_x} \left[\mathbb{P}_{0, x, z_0, z_x, y_0, y_x} \left[\text{there exists no } \mathbf{y} \in \mathcal{X} \text{ such that} \right. \right. \\ & \quad \left. \left. y \in B_{|x| \frac{\min\{d-k, k\}}{\alpha_k - k} - \epsilon}(0)^c : C_y \cap C_{y_0} \neq \emptyset \text{ and } C_y \cap C_{y_x} \neq \emptyset \mid \mathfrak{F}_{n_1}^x \right] \right. \\ & \quad \left. \times \mathbb{1}_{EF_{y_0, y_x}^{z_0, z_x}} \right] / \mathbb{P}_{0, x, z_0, z_x, y_0, y_x} (EF_{y_0, y_x}^{z_0, z_x}) \\ & \leq \mathbb{E}_{0, x, z_0, z_x, y_0, y_x} \left[\mathbb{P}_{0, x, z_0, z_x, y_0, y_x} \left[\text{there exists no } \mathbf{y} \in \mathcal{X} \text{ such that } y \in I_{y_0, y_x} : \right. \right. \\ & \quad \left. \left. C_y \cap C_{y_0} \neq \emptyset \text{ and } C_y \cap C_{y_x} \neq \emptyset \mid \mathfrak{F}_{n_1}^x \right] \mathbb{1}_{EF_{y_0, y_x}^{z_0, z_x}} \right] \\ & \quad / \mathbb{P}_{0, x, z_0, z_x, y_0, y_x} (EF_{y_0, y_x}^{z_0, z_x}) \\ & = \mathbb{E}_{0, x, z_0, z_x, y_0, y_x} \left[\exp \left(-u \int_{I_{y_0, y_x}} \mathbb{P}_C(C_y \cap C_{y_0} \neq \emptyset \text{ and } C_y \cap C_{y_x} \neq \emptyset) d\lambda(y) \right) \right. \\ & \quad \left. \times \mathbb{1}_{EF_{y_0, y_x}^{z_0, z_x}} \right] / \mathbb{P}_{0, x, z_0, z_x, y_0, y_x} (EF_{y_0, y_x}^{z_0, z_x}). \end{aligned}$$

The last inequality follows since $I_{y_0, y_x} \subseteq B_{|x| \frac{\min\{d-k, k\}}{\alpha_k - k} - \epsilon}(0)^c$. We can continue bounding the previous expression from above by

$$\begin{aligned} & \mathbb{E}_{0, x, z_0, z_x, y_0, y_x} \left[\exp \left(-u \int_{I_{y_0, y_x}} \mathbb{P}_C \left(C_y \cap \left(\frac{1}{3}(B_{K_{v_x}} - v_x) + v_x \right) \neq \emptyset \text{ and} \right. \right. \right. \\ & \quad \left. \left. \left. D_y^{(k)} \geq 2(|v_x - v_0| + |y - v_0|) \right) d\lambda(y) \right) \mathbb{1}_{EF_{y_0, y_x}^{z_0, z_x}} \right] \\ & \quad / \mathbb{P}_{0, x, z_0, z_x, y_0, y_x} (EF_{y_0, y_x}^{z_0, z_x}) \end{aligned}$$

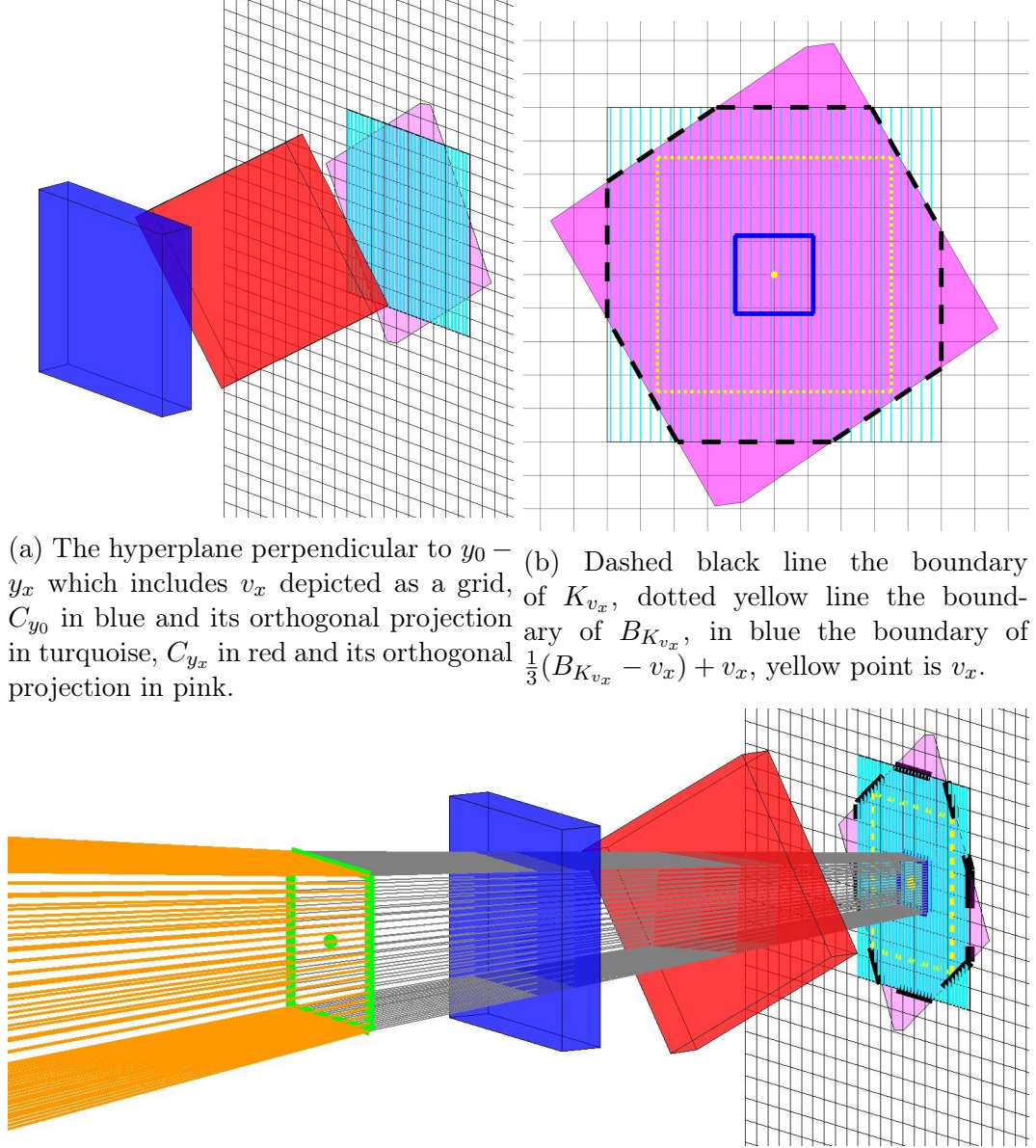
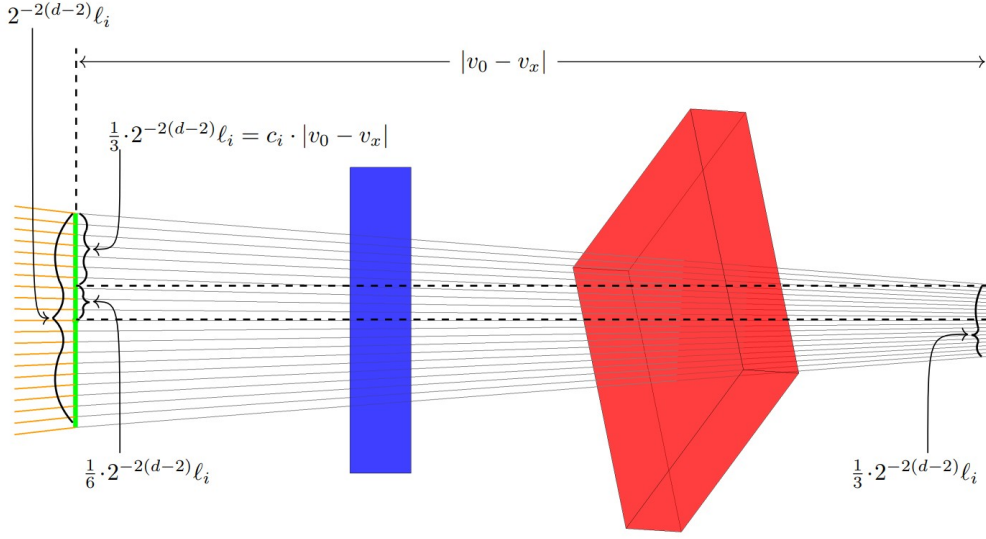


Figure 3.2: Example in \mathbb{R}^3 . Visualisation of the possible defined sets in (C1) and (C3) for the connector \mathbf{y} for \mathbf{y}_0 and \mathbf{y}_x .

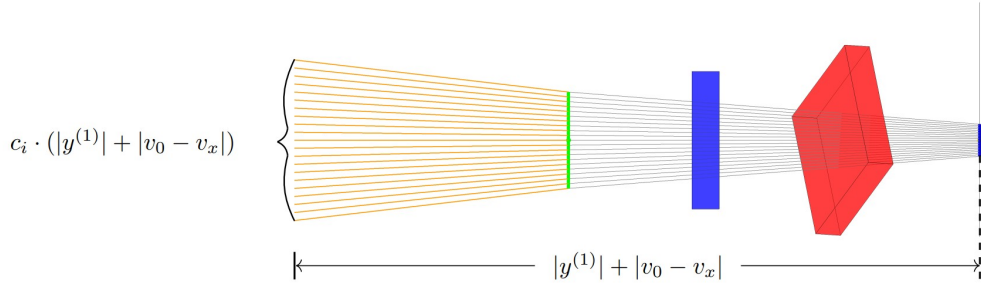
which can be rewritten to

$$\begin{aligned} \mathbb{E}_{0,x,z_0,z_x,y_0,y_x} \left[\exp \left(-u \int_{I_{y_0,y_x}} \mathbb{P}_C(C_y \cap \frac{1}{3}(B_{K_{v_x}} - v_x) + v_x) \neq \emptyset \right. \right. \\ \left. \left. \times \mathbb{P}(D_y^{(k)} \geq 2(|v_x - v_0| + |y - v_0|)) \, d\lambda(y) \right) \mathbb{1}_{EF_{y_0,y_x}^{z_0,z_x}} \right] \\ / \mathbb{P}_{0,x,z_0,z_x,y_0,y_x}(EF_{y_0,y_x}^{z_0,z_x}). \end{aligned}$$

3.3. Proof of the upper bound



(a) Intuition behind the choice of the constants c_1 and c_2 , using the proportion of the side-length of $\frac{1}{3}(B_{K_{v_x}} - v_x) + v_x$ (the blue line on the right side of the picture) and $P_{y_0, y_x}^{v_0}(B_{K_{v_x}})$ (the green line), where $\ell_i = f_{n_1}$ for $i \in \{2, \dots, k+1\}$ and $\ell_i = \epsilon$ for $i > k+1$.



(b) An illustration of the choice of $y^{(i)}$ in I_{y_0, y_x} for $i \in \{2, \dots, d\}$.

Figure 3.3: Illustration of the role of c_1 and c_2 in \mathbb{R}^3 . In the above figures, c_i equals c_1 for $i \in \{2, \dots, k+1\}$ and equals c_2 otherwise. The colour of the lines constructing I_{y_0, y_x} are grey as before; similarly the colours for the boundary of I_{y_0, y_x} , C_{y_0} , C_{y_x} , $P_{y_0, y_x}^{v_0}(B_{K_{v_x}})$ and $\frac{1}{3}(B_{K_{v_x}} - v_x) + v_x$ are the same as in Figure 3.2.

In order to bound the integrand we use translation and rotation invariance of the Lebesgue measure, Potter bounds and the size of the set of orientations of C_y that results in an intersection with $\frac{1}{3}(B_{K_{v_x}} - v_x) + v_x$ which yields

$$\begin{aligned}
 & \mathbb{P}_C(\text{rot}_{y_0, y_x}^{-1}(C_y - v_0) \cap \text{rot}_{y_0, y_x}^{-1}(\frac{1}{3}(B_{K_{v_x}} - v_x) + v_x - v_0)) \neq \emptyset \\
 & \quad |D_y^{(k)}| \geq 2(|v_x - v_0| + |y|) \\
 & \times \mathbb{P}(D_y^{(k)} \geq 2(|v_x - v_0| + |y|)) \\
 & \geq c \frac{f_{n_1}^{\min\{d-k, k\}}}{(|v_x - v_0| + |y|)^{d-k}} (|v_x - v_0| + |y|)^{-\alpha_k - \varepsilon}
 \end{aligned}$$

3.3. Proof of the upper bound

and use this lower bound going forward. Using now that $|v_x - v_0| \in (|x|/4, 2|x|)$, $|y| > cf_{n_1+1}$, $|x|/8 = f_{n_1}$ and the norm equivalence in \mathbb{R}^d we can bound the last term from below by

$$c \frac{|x|^{\min\{d-k, k\}}}{|y|_1^{d-k}} |y|_1^{-\alpha_k - \varepsilon} = c |x|^{\min\{d-k, k\}} |y|_1^{-\alpha_k - \varepsilon - d + k}$$

where $|\cdot|_1$ is again the 1-norm. Putting it all together, we can therefore bound

$$\mathbb{P}_{0,x,z_0,z_x,y_0,y_x} \left(E_1^{(y_0,y_x)} \mid E_2^{(y_0,y_x)} \cap F_{n_1}^{(0,z_0,y_0)} \cap F_{n_1}^{(x,z_x,y_x)} \cap E_{0,z_0}^b \cap E_{x,z_x}^b \right)$$

from above by

$$\mathbb{E}_{0,x,z_0,z_x,y_0,y_x} \left[\exp \left(-uc \int_{I_{0,x}} |x|^{\min\{d-k, k\}} |y|_1^{-\alpha_k - \varepsilon - d + k} d\lambda(x) \right) \mathbb{1}_{E_{y_0,y_x}^{z_0,z_x}} \right] \quad (3.15)$$

$$/ \mathbb{P}_{0,x,z_0,z_x,y_0,y_x} (E_{y_0,y_x}^{z_0,z_x}).$$

We focus now at the integral. Note that we use in the rest of this section, compared to Section 2.2.4, another notation for integrals in order to get the calculation more readable. More precisely the order of the terms in the integral, as the boundaries of the integrals are more complicated, are different.

Using now the definition of $I_{0,x}$ we get

$$\begin{aligned} & \int_{I_{0,x}} |x|^{\min\{d-k, k\}} |y|_1^{-\alpha_k - \varepsilon - d + k} d\lambda(x) \\ & \geq \int_{|x|^{\frac{\min\{d-k, k\}}{\alpha_k - k} - \varepsilon}}^{\infty} dy^{(1)} \int_{-c_1(y^{(1)} + |v_0 - v_x|)}^{c_1(y^{(1)} + |v_0 - v_x|)} dy^{(2)} \dots \int_{-c_1(y^{(1)} + |v_0 - v_x|)}^{c_1(y^{(1)} + |v_0 - v_x|)} dy^{(k+1)} \int_{-c_2(y^{(1)} + |v_0 - v_x|)}^{c_2(y^{(1)} + |v_0 - v_x|)} dy^{(k+2)} \\ & \quad \dots \int_{-c_2(y^{(1)} + |v_0 - v_x|)}^{c_2(y^{(1)} + |v_0 - v_x|)} |x|^{\min\{d-k, k\}} |y|_1^{-\alpha_k - \varepsilon - d + k} dy^{(d)}, \end{aligned}$$

where we highlight the change of integration range when going from $k+1$ to $k+2$. Using $y^{(1)} + |v_0 - v_x| \geq \frac{1}{2}y^{(1)}$ we can bound this from below by

$$\begin{aligned} & \int_{|x|^{\frac{\min\{d-k, k\}}{\alpha_k - k} - \varepsilon}}^{\infty} dy^{(1)} \int_{-\frac{c_1}{2}y^{(1)}}^{\frac{c_1}{2}y^{(1)}} dy^{(2)} \dots \int_{-\frac{c_1}{2}y^{(1)}}^{\frac{c_1}{2}y^{(1)}} dy^{(k+1)} \int_{-\frac{c_2}{2}y^{(1)}}^{\frac{c_2}{2}y^{(1)}} dy^{(k+2)} \\ & \quad \dots \int_{-\frac{c_2}{2}y^{(1)}}^{\frac{c_2}{2}y^{(1)}} |x|^{\min\{d-k, k\}} |y|_1^{-\alpha_k - \varepsilon - d + k} dy^{(d)} \\ & \geq c \int_{|x|^{\frac{\min\{d-k, k\}}{\alpha_k - k} - \varepsilon}}^{\infty} |x|^{\min\{d-k, k\}} (|y^{(1)}| + k|\frac{c_1}{2}y^{(1)}| + (d-k-1)|\frac{c_2}{2}y^{(1)}|)^{-\alpha_k - \varepsilon + k - 1} dy^{(1)} \end{aligned}$$

3.3. Proof of the upper bound

$$\begin{aligned}
&\geq c \int_{|x|^{\frac{\min\{d-k,k\}}{\alpha_k-k}-\epsilon}}^{\infty} |x|^{\min\{d-k,k\}} |y^{(1)}|^{-\alpha_k-\epsilon+k-1} dy^{(1)} \\
&\geq c |x|^{\min\{d-k,k\}} \left(|x|^{\frac{\min\{d-k,k\}}{\alpha_k-k}-\epsilon} \right)^{-\alpha_k-\epsilon+k}.
\end{aligned} \tag{3.16}$$

In the first inequality we integrated over the last $d-1$ coordinates of y . The second inequality is given by using definitions of c_1 and c_2 . Integrating over the first coordinate of y then gives the final inequality. Continuing the calculation of (3.15), substituting in the bound from (3.16), we get

$$\begin{aligned}
&\mathbb{E}_{0,x,z_0,z_x,y_0,y_x} \left[\exp \left(-uc |x|^{\min\{d-k,k\}} \left(|x|^{\frac{\min\{d-k,k\}}{\alpha_k-k}-\epsilon} \right)^{-\alpha_k-\epsilon+k} \right) \mathbb{1}_{E_{y_0,y_x}^{z_0,z_x}} \right] \\
&\quad / \mathbb{P}_{0,x,z_0,z_x,y_0,y_x} (E_{y_0,y_x}^{z_0,z_x}) \\
&\leq \exp \left(-uc |x|^{-\epsilon \frac{\min\{d-k,k\}}{\alpha_k-k} + \epsilon(\alpha_k + \epsilon - k)} \right) \\
&\leq \exp \left(-uc |x|^{\epsilon(\alpha_k - k)/2} \right),
\end{aligned}$$

where the last inequality follows using that for $0 < \epsilon < (\alpha_k - k)^2 \epsilon / (2 \min\{d-k, k\})$ (recall that we can choose ϵ appearing in the Potter bounds arbitrarily small) we have

$$-\epsilon \frac{\min\{d-k, k\}}{\alpha_k - k} + \epsilon(\alpha_k + \epsilon - k) > \frac{\epsilon}{2}(\alpha_k - k) > 0.$$

as in Section 2.2.2. \square

With this, we have proven that the first term of (3.12) converges to zero as $|x|$ becomes large. It remains to prove the same for the second term, which we do with the following lemma.

Lemma 3.6. *We have*

$$\begin{aligned}
&\mathbb{P}_{0,x,z_0,z_x,y_0,y_x} \left(E_3^{(y_0,y_x)} \cap F_{n_1}^{(0,z_0,y_0)} \cap F_{n_1}^{(x,z_x,y_x)} \cap E_{0,z_0}^b \cap E_{x,z_x}^b \right) \\
&\leq \exp(-uc |x|^{\epsilon(\alpha_k - k) - \delta})
\end{aligned}$$

for $0 < \delta < \epsilon(\alpha_k - k)$ and $|x|$ large enough.

Proof. Let $\tilde{E}_3^{(y_0,y_x)}$ be the event defined in such a way that

$$\tilde{E}_3^{(y_0,y_x)} \cap F_{n_1}^{(0,z_0,y_0)} \cap F_{n_1}^{(x,z_x,y_x)} \cap E_{0,z_0}^b \cap E_{x,z_x}^b = E_3^{(y_0,y_x)} \cap F_{n_1-1}^{(0,z_0)} \cap F_{n_1-1}^{(x,z_x)} \cap E_{0,z_0}^b \cap E_{x,z_x}^b$$

holds, i.e. the vertices \mathbf{y}_0 and \mathbf{y}_x are good with respect to each other and \mathbf{y}_0

(resp. \mathbf{y}_x) can be used to extend the path of length $n_1 - 1$ starting in \mathbf{z}_0 (resp. \mathbf{z}_x) so that the extended path implies the event $F_{n_1}^{(0,z_0,y_0)}$ (resp. $F_{n_1}^{(x,z_x,y_x)}$). We have

$$\begin{aligned} \mathbb{P}_{0,x,z_0,z_x,y_0,y_x} & \left(E_3^{(y_0,y_x)} \cap F_{n_1}^{(0,z_0,y_0)} \cap F_{n_1}^{(x,z_x,y_x)} \cap E_{0,z_0}^b \cap E_{x,z_x}^b \right) \\ &= \mathbb{P}_{0,x,z_0,z_x,y_0,y_x} \left(\tilde{E}_3^{(y_0,y_x)} \cap F_{n_1-1}^{(0,z_0)} \cap F_{n_1-1}^{(x,z_x)} \cap E_{0,z_0}^b \cap E_{x,z_x}^b \right) \\ &\leq \mathbb{P}_{0,x,z_0,z_x,y_0,y_x} \left(\tilde{E}_3^{(y_0,y_x)} \mid F_{n_1-1}^{(0,z_0)} \cap F_{n_1-1}^{(x,z_x)} \cap E_{0,z_0}^b \cap E_{x,z_x}^b \right). \end{aligned}$$

To bound this probability from above recall that in general, for vertices of paths we consider, for every $n \in \mathbb{N}$ and suitable $z \in \mathbb{R}^d$, i.e. $z \in O_{n+1}(\mathbf{x}_n)$, using a similar argument as for Section 2.2.2, we can obtain the following inequality

$$\begin{aligned} \mathbb{P}_C \left((z + C) \cap Q_{f_n}^*(x_n, x) \neq \emptyset \mid D_C^{(k)} \geq 2^{2(d-1)+\epsilon} f_{n+1} \right) & \mathbb{P}_C(D_C^{(k)} \geq 2^{2(d-1)+\epsilon} f_{n+1}) \\ & \geq c \frac{f_n^{\min\{d-k,k\}}}{f_{n+1}^{d-k}} f_{n+1}^{-\alpha_k+\epsilon}. \end{aligned} \quad (3.17)$$

Setting $n = n_1 - 1$, the right hand side of this inequality is a lower bound for the probability that a vertex with given location in $O_{n+1}(\mathbf{x}_n)$ is the n_1 th vertex in the growing path as required for \mathbf{y}_0 (resp. \mathbf{y}_x) to satisfy $F_{n_1}^{(0,z_0,y_0)}$ (resp. $F_{n_1}^{(x,z_x,y_x)}$) under the condition $F_{n_1-1}^{(0,z_0)} \cap F_{n_1-1}^{(x,z_x)} \cap E_{0,z_0}^b \cap E_{x,z_x}^b$. In addition to that note that \mathbf{y}_0 (resp. \mathbf{y}_x) has location in $O_0 := B_{3|x|/8}(0) \setminus B_{|x|/8}(0)$ (resp. $O_x := B_{3|x|/8}(x) \setminus B_{|x|/8}(x)$). Hence y_0 and y_x lie in disjoint areas.

Writing from here on $F_{n_1-1}^{(0,z_0)} \cap F_{n_1-1}^{(x,z_x)} \cap E_{0,z_0}^b \cap E_{x,z_x}^b$ as $G_{n_1-1}^{(0,x,z_0,z_x)}$ and using properties of the Poisson point process we calculate

$$\begin{aligned} & \mathbb{P}_{0,x,z_0,z_x,y_0,y_x} \left(\tilde{E}_3^{(y_0,y_x)} \mid F_{n_1-1}^{(0,z_0,y_0)} \cap F_{n_1-1}^{(x,z_x,y_x)} \cap E_{0,z_0}^b \cap E_{x,z_x}^b \right) \\ &= \mathbb{E}_{0,x,z_0,z_x,y_0,y_x} \left[\mathbb{P}_{0,x,z_0,z_x,y_0,y_x} \left[\nexists \mathbf{v}, \mathbf{w} \in \mathcal{X} \text{ that extend } F_{n_1-1}^{(0,z_0)} \text{ and } F_{n_1-1}^{(x,z_x)} \text{ such} \right. \right. \\ & \quad \left. \left. \text{that } \mathbf{v} \text{ and } \mathbf{w} \text{ are good with respect to each other. } \mid \mathfrak{F}_{n_1-1}^x \right] \right. \\ & \quad \left. \times \mathbb{1}_{G_{n_1-1}^{(0,x,z_0,z_x)}} \right] / \mathbb{P}_{0,x,z_0,z_x,y_0,y_x} (G_{n_1-1}^{(0,x,z_0,z_x)}) \\ &\leq \mathbb{E}_{0,x,z_0,z_x,y_0,y_x} \left[\exp \left(-uc \int_S d\mathbb{P}_{p_v} \int_{O_0} d\lambda(w) \int_{O_x \cap A(w,n_1)} \mathbb{P}_{v,w,p_v} \left(\angle(p_w^{(i)}, p_v^{(i)}) \leq \frac{\epsilon}{\log|x|}, \right. \right. \right. \\ & \quad \left. \left. \left. \forall i \in \{1, \dots, d\} \right) \right) \frac{f_{n_1-1}^{2 \min\{d-k,k\}}}{f_{n_1}^{2(d-k)}} f_{n_1}^{-2(\alpha_k-\epsilon)} d\lambda(v) \right] \\ & \quad \times \mathbb{1}_{G_{n_1-1}^{(0,x,z_0,z_x)}} \Big] / \mathbb{P}_{0,x,z_0,z_x,y_0,y_x} (G_{n_1-1}^{(0,x,z_0,z_x)}), \end{aligned}$$

where S is the set of all possible orientations of C (see below for a more

3.3. Proof of the upper bound

precise definition) and we used (3.17) to thin out the Poisson point process in the inequality. Note that the bound in (3.17) only holds for pairs of vertices for which $v \in O_{n_1}(\mathbf{x}_{n_1-1})$ (and similarly for w). Since we are restricting ourselves to O_0 and O_x , this assumption is satisfied. In particular, since O_0 and O_x are bounded, there exists a constant $c > 0$ for which (3.17) holds for all vertices with locations inside O_0 and O_x . Furthermore, in line with our notation, p_v in the index of \mathbb{P} signifies that we conditioned on p_v .

To continue, define

$$S := \bigtimes_{i=1}^{d-1} \mathbb{S}^{d-i}$$

to be the set of all possible orientations of C . Here, \mathbb{S}^{d-i} is the set of possible orientations for $p_C^{(i)}$, which is the orientation of the i th side of C , for $i \in \{1, \dots, d-1\}$, relative to all preceding orientations. Note that the orientation of $p_C^{(d)}$ is completely determined (up to mirroring) when the orientations of $p_C^{(1)}, \dots, p_C^{(d-1)}$ are known; also observe that given all preceding orientations, $p_C^{(i)}$ is distributed uniformly on \mathbb{S}^{d-i} . We write \mathbb{P}_{p_C} for the law of the vector $(p_C^{(1)}, \dots, p_C^{(d)})$ and \mathbb{P}_{p_v} when C is attached to a specific location $v \in \mathcal{P}$.

To bound $\mathbb{P}_{0,x}(\tilde{E}_3 \mid F_{n_1-1}^{(0)} \cap F_{n_1-1}^{(x)} \cap E_0^b \cap E_x^b)$ from above we calculate

$$\begin{aligned} & \int_S d\mathbb{P}_{p_v} \int_{O_0} d\lambda(w) \int_{O_x \cap A(w, n_1)} \frac{f_{n_1-1}^{2 \min\{d-k, k\}}}{f_{n_1}^{2(d-k)}} f_{n_1}^{-2(\alpha_k - \varepsilon)} \\ & \quad \times \mathbb{P}_{v, w, p_v}(\angle(p_w^{(i)}, p_v^{(i)}) \leq \frac{\epsilon}{\log|x|}, \forall i \in \{1, \dots, d\}) d\lambda(v) \\ & \geq c \int_S d\mathbb{P}_{p_v} \int_{O_0} d\lambda(w) \int_{O_x \cap A(w, n_1)} \frac{f_{n_1-1}^{2 \min\{d-k, k\}}}{f_{n_1}^{2(d-k)}} f_{n_1}^{-2(\alpha_k - \varepsilon)} \log(|x|)^{-(d-1)!} d\lambda(v) \\ & \geq c f_{n_1}^{2d} \frac{f_{n_1-1}^{2 \min\{d-k, k\}}}{f_{n_1}^{2(d-k)}} f_{n_1}^{-2(\alpha_k - \varepsilon)} \log(|x|)^{-(d-1)!}. \end{aligned}$$

The first inequality holds since the set of allowed orientations for $p_w^{(i)}$ for fixed $p_v^{(i)}$ has volume of order $\log(|x|)^{-(d-1)!}$, which can be shown by induction. Intuitively, looking at the sets that are given for the orientations of the sides of C , we first consider the longest side and determine the rotational area which is allowed so that it has suitable orientation; this is a set of size proportional to $\log(|x|)^{-d+1}$. Fixing this first orientation, it remains to consider the remaining $d-1$ sides. For the orientation of the second side we have a restriction of the rotational area which is proportional to $\log(|x|)^{-(d-2)}$ and so on, until we are looking at the second to last side, where we have a rotational area proportional to $\log(|x|)^{-1}$ left. Altogether this leads to the exponent $-(d-1)!$. For the final

3.3. Proof of the upper bound

inequality above we use that the volume of O_0 resp. $O_x \cap A(w, n_1)$ for fixed $w \in \mathbb{R}^d$ is of order $f_{n_1}^d$ and that \mathbb{P}_{p_v} is uniform on S .

Choosing again $0 < \varepsilon < (\alpha_k - k)^2 \varepsilon / (2 \min\{d - k, k\})$, the last expression can be bounded from below by

$$f_{n_1}^{\varepsilon(\alpha_k - k)} \log(|x|)^{-(d-1)!} \geq c|x|^{\varepsilon(\alpha_k - k) - \delta},$$

with $\delta > 0$ small enough such for the exponent of $|x|$ to be positive.

Together we get

$$\mathbb{P}_{0,x,z_0,z_x,y_0,y_x} \left(E_3^{(y_0,y_x)} \cap F_{n_1}^{(0,z_0,y_0)} \cap F_{n_1}^{(x,z_x,y_x)} \cap E_{0,z_0}^b \cap E_{x,z_x}^b \right) \leq \exp(-uc|x|^{\varepsilon(\alpha_k - k) - \delta}).$$

□

Note that the upper bounds from Lemma 3.5 and Lemma 3.6 do not depend on z_0, z_x, y_0 and y_x . Consequently, integrating over these locations and using these uniform bounds gives an upper bound for the last term of (3.8). This implies that the chemical distance for fixed $k \in M$ is given by $\frac{2+\delta}{\log\left(\frac{\min\{d-k,k\}}{\alpha_k-k}\right)} \log \log |x|$ with high probability as $|x| \rightarrow \infty$.

Finally, we get the claimed upper bound as follows. Recall that k is such that $\alpha_k \in (k, \min\{2k, d\})$, i.e. $k \in \mathcal{M}$. Furthermore, we have proven that the upper bound holds for the “smallest” Poisson Boolean model with convex grains. This gives us also an upper bound for the chemical distance for every other Poisson Boolean base model with $\alpha_k \in (k, \min\{d, 2k\})$, for any and therefore every $k \in \mathcal{M}$. Together, we get that $\text{dist}(\mathbf{0}, \mathbf{x})$ is, under the condition that $0, x \in \mathcal{P}$ and $\mathbf{0} \leftrightarrow \mathbf{x}$, for every $\delta > 0$, bounded from above by

$$\min \left\{ \frac{2+\delta}{\log\left(\frac{\min\{d-k,k\}}{\alpha_k-k}\right)} \log \log |x| : k \in M \right\} = \frac{2+\delta}{\log\left(\frac{\min\{d-\kappa,\kappa\}}{\alpha_\kappa-\kappa}\right)} \log \log |x|,$$

with high probability as $|x| \rightarrow \infty$.

Remark 3.7. For the case where there exists some $k \in \{1, \dots, d\}$ such that $\alpha_k \leq k$ this model dominates (in the standard, almost sure coupling sense; see Remark 3.3) all other models where we replace α_k by $k + \rho$ for $\rho > 0$ in the “smallest” box model as in the proof of the upper bound. Looking at the smaller model we have already shown that the upper bound for the chemical distance is given by $(2+\delta)/\log\left(\frac{\min\{d-k,k\}}{\rho}\right) \log \log |x|$. With $\rho \downarrow 0$ we get that the factor $(2+\delta)/\log\left(\frac{\min\{d-k,k\}}{\rho}\right)$ is getting arbitrary small. With this we get

3.3. Proof of the upper bound

that $\text{dist}(\mathbf{x}, \mathbf{y})$ grows in the bigger model faster than $c \log \log |x - y|$ for all $c > 0$.

Chapter 4

Examples

In this chapter, we discuss a few examples. We investigate ellipses with long and short axes, where the long axes are almost surely the same and regularly varying, while the short axes are fixed, of size 1. We therefore have that the long diameters are strongly positive correlated. Another example is the case where we consider ellipses whose axes are generated by independent random variables. The diameters are then determined by the ordering of these random variables according to size. Furthermore, we consider a case where we have different strong positive correlation. Here, the axes are not almost surely the same, but are determined by a single random variable to different powers. In addition, we investigate right triangles. The location of the vertex is then uniformly chosen as one of the corners.

Moreover, we will also discuss an example in which we observe that we obtain robustness by applying the second part of Theorem 2.2, but non-robustness when we keep the parameters and change the correlation structure.

Ellipsoids with long and short axes

We sample a random radius $R > 1$ from a distribution which has a tail distribution that is regularly varying with index $-\alpha$. For integers $0 \leq m \leq d$ we define a random ellipsoid K with centre in the origin and $d - m$ long axes of length R and m short axes of length one. We let C be the random convex set obtained by rotating K about its centre by an independent uniform angle $\vartheta \in S^{d-1}$. Then

- C is sparse if $\alpha \geq d - m$.
- C is robust if $\alpha < \min\{2(d - m), d\}$.
- C is non-robust if $\alpha > \min\{2(d - m), d\}$.

3.3. Proof of the upper bound

Observe that in the case $m = 0$ the ellipsoid C is a ball of random radius and in this case there exists no grain distribution that is both robust and sparse, as observed earlier by Gou  re [22]. The case $m = 1$, $d = 2$ corresponds to the case studied by Teixeira and Ungaretti [53] and we recover their result. Note that in all dimensions $d \geq 2$ whenever $0 < m < d$ there exists α such that C is both robust and sparse.

As stated in Proposition 2.1 it is known that the model is dense if the volume of the convex body has infinite expectation. This is equivalent to requiring that R^{d-m} has infinite expectation which is guaranteed if $\alpha < d - m$.

For the grain distribution being robust we look at the first part of Theorem 2.2. The statement in this theorem is equivalent to $\alpha < \min\{2(d - m), d\}$. This is clear by looking at the tail indices of the distribution of the diameters. Let $k \leq d - m$. We have for $x > 0$ and $k \leq d - m$ that

$$\mathbb{P}(D^{(k)} \geq x) = \mathbb{P}(R \geq x),$$

i.e. $D^{(k)}$ has a regularly varying tail distribution with index $-\alpha$. For $k > d - m$ we have $D^{(k)} = 1$ almost surely. So $D^{(k)}$ has a tail distribution with index $-\infty$ for $k > d - m$. If we are now asking for $\alpha_k < \min\{2k, d\}$ for some $k \in \{1, \dots, d\}$ one can see that this is the same as requiring $\alpha < 2(d - m)$ if $d - m \leq m$ or $\alpha < d$ if $d - m > d/2$. This is equivalent to $\alpha < \min\{2(d - m), d\}$.

The last criterion, i.e. the criteria on non-robustness is given by Theorem 2.3. The conditions in this theorem, namely that the second moment of the volume exists or that the diameter, i.e. $D^{(1)}$ is in \mathcal{L}^d , gives us $\alpha > 2(d - m)$ and therefore also that the second moment of the volume is finite and $\alpha > d$ to ensure $D^{(1)} \in \mathcal{L}^d$. In other words, we require $\alpha > \min\{2(d - m), d\}$. Note that this inequality being satisfied also implies the condition on the α_k for $k \in \{1, \dots, d\}$ as required in Theorem 2.3. Ignoring the boundary cases, we see that our criterion is sharp.

With Theorem 3.1 we can state also something about the chemical distance. If we have that $\mathcal{M} \neq \emptyset$, i.e. $\alpha \in (d - m, \min\{2(d - m), d\})$, the first condition from Theorem 3.1 on the parameters holds and we get

$$\lim_{|x-y| \rightarrow \infty} \mathbb{P}_{x,y} \left(\frac{2 - \delta}{\log \left(\frac{\min\{m, d-m\}}{\alpha_{d-m-d+m}} \right)} \leq \frac{\text{dist}(\mathbf{x}, \mathbf{y})}{\log \log |x - y|} \leq \frac{2 + \delta}{\log \left(\frac{\min\{m, d-m\}}{\alpha_{d-m-d+m}} \right)} \middle| x \leftrightarrow y \right) = 1,$$

for $x, y \in \mathcal{P}$ and small $\delta > 0$. In particular this theorem improves both the

upper and lower bounds shown in [34], where Hilário and Ungaretti considered the special case, namely $d = 2$ and $m = 1$ with ellipses such that the diameters fulfil $\mathbb{P}(D^{(1)} \geq r) = cr^{-\alpha}$ for $c > 0$, $\alpha \in (1, 2)$ and $D^{(2)} = 1$ almost surely.

Ellipsoids with independent axes

We sample d independent random radii $R_1, \dots, R_d \geq 1$ from distributions which have regularly varying tail distributions with index $-\beta_i$. We define a random ellipsoid $K \subset \mathbb{R}^d$ with axes of length R_1, \dots, R_d and let C be the random convex set obtained by rotating K about its centre by an independent uniform angle $\vartheta \in S^{d-1}$. Then

- C is sparse if $\beta_i > 1$ for all $1 \leq i \leq d$.
- C is robust if there exists $1 \leq i \leq d$ such that $\beta_i < 2$.
- C is non-robust if $\beta_1 > d$.

Note that the criteria are not sharp in this example. In this setting we assume without loss of generality that $\beta_i \leq \beta_{i+1}$ for all $i \in \{1, \dots, d-1\}$. We are now interested in the tail indices of the diameters $D^{(1)}, \dots, D^{(d)}$. For $x > 0$ we have

$$\mathbb{P}(D^{(1)} \geq x) = 1 - \mathbb{P}(D^{(1)} < x) = 1 - \prod_{k=1}^d (1 - \mathbb{P}(R_k \geq x))$$

by using the independence of the radii. Using now the calculation rule of regularly varying functions (see for example [3]) we have that $D^{(1)}$ is regularly varying with index $-\beta_1$. Using again the independence of the radii and considering the event $\{D^{(k)} \geq x\}$ leads us to the tail indices of the other diameters; more precisely $D^{(k)}$ is regularly varying with index $-\sum_{i=1}^k \beta_i$. Using Proposition 2.1 we get that the grain distribution is sparse if $\text{Vol}(C) \in \mathcal{L}^1$. In our case we have due to independence

$$\mathbb{E}[\text{Vol}(C)] = \prod_{i=1}^d \mathbb{E}[R_i],$$

which is finite if $\min_{i=1}^d \beta_i > 1$.

The first criterion of Theorem 2.2 gives the condition for the $\alpha_k := \sum_{i=1}^k \beta_i$ to ensure robustness. This can be equivalently stated as

- (i) There exists $1 \leq k \leq d$ such that $\alpha_k < \min\{2k, d\}$.

(ii) There exists $1 \leq i \leq d$ such that $\beta_i < 2$.

(ii) follows from (i) due to the fact that if $\beta_i > 2$ for all i then we have $\alpha_k = \sum_{i=1}^k \beta_i > 2k$ for every $k \in \{1, \dots, d\}$. The other direction is also true. If $\alpha_k \geq \min\{2k, d\}$ for every $k \in \{1, \dots, d\}$ we have in particular that $\beta_1 = \alpha_1 \geq 2$. Due to $\beta_{i+1} \geq \beta_i$ we have $\beta_i \geq 2$ for every $i \in \{1, \dots, d\}$.

The second (trivial) criterion from Theorem 2.3 gives us that $\beta_1 > d$ implies the grain distribution is non-robust.

We consider now the chemical distance in this example for the robust but sparse case. For that we assume for $1 \leq i \leq d$ that $\beta_i < 2$ and additionally that $\min_{1 \leq i \leq d} \beta_i > 1$ to guarantee that $\alpha_k > k$ for all $1 \leq k \leq d$ and therefore also $\text{Vol}(X) \in \mathcal{L}^1$. Define now as in Theorem 3.1 $\mathcal{M} := \{s \in \{1, \dots, d-1\} : \sum_{i=1}^s \beta_i \in (s, \min\{2s, d\})\}$ and recall the definition of κ . We get then that

$$\mathbb{P}_{x,y} \left(\frac{2-\delta}{\log \frac{\min\{\kappa, d-\kappa\}}{-\kappa + \sum_{i=1}^{\kappa} \beta_i}} \leq \frac{\text{dist}(\mathbf{x}, \mathbf{y})}{\log \log |x-y|} \leq \frac{2+\delta}{\log \frac{\min\{\kappa, d-\kappa\}}{-\kappa + \sum_{i=1}^{\kappa} \beta_i}} \mid x \leftrightarrow y \right) \xrightarrow{|x-y| \rightarrow \infty} 1.$$

for $x, y \in \mathcal{P}$ while $\delta > 0$.

Ellipsoids with strongly dependent axes

Let $0 \leq \beta_1 \leq \dots \leq \beta_d$ and pick $U \in (0, 1)$ uniformly at random. We define a random ellipsoid $K \subset \mathbb{R}^d$ with axes of length $U^{-\beta_1}, \dots, U^{-\beta_d}$ and let C be the random convex set obtained by rotating K about its centre (or indeed any inner point) by an independent uniform angle $\vartheta \in S^{d-1}$. Then

- C is sparse if $\sum_{i=1}^d \beta_i < 1$,
- C is robust if there exists $1 \leq k \leq \lfloor d/2 \rfloor$ such that $\beta_{d-k+1} > \frac{1 - \sum_{j=1+k}^{d-k} \beta_{d-j+1}}{2k}$ or if there exists $k > \lfloor d/2 \rfloor$ such that $\beta_{d-k+1} > \frac{1}{d}$,
- C is non-robust if $\frac{1}{d} > \beta_d$ for every $1 \leq k \leq d$.

In this model we have ellipsoids with axes of length $U^{-\beta_k}$ with $k \in \{1, \dots, d\}$, U uniformly distributed on $(0, 1)$, and $0 \leq \beta_1 \leq \dots \leq \beta_d$. For $x > 1$ we get that

$$\mathbb{P}(U^{-\beta_k} \geq x) = \mathbb{P}(U < x^{-1/\beta_k}) = x^{-\frac{1}{\beta_k}},$$

i.e. the diameter $D^{(k)}$ has regularly varying tail distribution with index $-\frac{1}{\beta_{d-k+1}}$ for $k \in \{1, \dots, d\}$. By the criterion of Proposition 2.1 we see that the model

3.3. Proof of the upper bound

is sparse if $\sum_{i=1}^d \beta_i < 1$. This is true due to the fact that $\text{Vol}(C)$ has regularly varying tail distribution with index $(\sum_{i=1}^d \beta_i)^{-1}$. The specific criteria for robustness of Theorem 2.2, i.e. the second part of the theorem, leads to the conditions on the β_k for $k \in \{1, \dots, d\}$ to results in robustness. For that note that $\gamma_k = \frac{\beta_{d-k-1}}{\beta_d}$. Putting these equations in the specific conditions of the robustness of Theorem 2.2 leads to the following criteria.

(i) For $k \leq \lfloor d/2 \rfloor$ we have

$$\alpha < 2k\gamma_k + \sum_{j=k+1}^{d-k} \gamma_j = 2k \frac{\beta_{d-k+1}}{\beta_d} + \sum_{j=k+1}^{d-k} \frac{\beta_{d-j+1}}{\beta_d},$$

$$\text{which is equivalent to } \beta_{d-k+1} > \frac{1 - \frac{1}{\beta_{d-k+1}} \sum_{j=k+1}^{d-k} \beta_{d-j+1}}{2k}.$$

(ii) For $k > \lfloor d/2 \rfloor$ we have that $\alpha_1 < d\gamma_k = \frac{\beta_{d-k+1}}{\beta_d}$ which is the same as $\beta_{d-k+1} > \frac{1}{d}$.

Furthermore, the criterion for non-robustness is given by $\frac{1}{d} > \beta_d$ by using the second part of Theorem 2.3.

We focus now here in the setting $\mathcal{M} \neq \emptyset$ with $\beta_{d-k+1}^{-1} > k$ for all $k \in \{1, \dots, d\}$, while we define $\mathcal{M} := \{s \in \{1, \dots, d-1\} : \beta_{d-k+1}^{-1} \in (k, \min\{2k, d\})\}$ and κ as in Theorem 3.1. For that we get by Theorem 3.1

$$\mathbb{P}_{x,y} \left(\frac{2 - \delta}{\log \frac{\min\{\kappa, d-\kappa\}}{\beta_{d-\kappa+1}^{-1} - \kappa}} \leq \frac{\text{dist}(\mathbf{x}, \mathbf{y})}{\log \log |x - y|} \leq \frac{2 + \delta}{\log \frac{\min\{\kappa, d-\kappa\}}{\beta_{d-\kappa+1}^{-1} - \kappa}} \middle| x \leftrightarrow y \right) \xrightarrow{|x-y| \rightarrow \infty} 1,$$

for $x, y \in \mathcal{P}$ while $\delta > 0$.

Random triangles

Let $R > 1$ be random with regularly varying tail of index $-\alpha$, for $\alpha > 0$. Take the *right* triangle $K \subset \mathbb{R}^2$ such that R is the length of the hypotenuse and $\text{Vol}(K) = \frac{1}{4}R^{1+\beta}$, for some $\beta \in (0, 1)$. Note that this describes the triangle uniquely up to symmetries. Now choose the origin uniformly as one of the corners of K and let C be the random set obtained by a uniform rotation via this point. Then

- C is sparse if $\alpha > 1 + \beta$,
- C is robust if $\alpha < 2$,

- C is non-robust if $\alpha > 2$.

By our triangle construction $D^{(1)}$ is the length of the hypotenuse, i.e. $D^{(1)} = R$ is regularly varying with tail index $-\alpha =: -\alpha_1$. As the volume of a triangle is half of the product of one side and the corresponding height and the height orthogonal to the hypotenuse is the second diameter, we get

$$\lambda(C) = \frac{1}{4}R^{1+\beta} = \frac{1}{2}D^{(1)}D^{(2)},$$

so that $D^{(2)} = \frac{1}{2}R^\beta$. Our proposition states that the model is sparse if $\lambda(C) \in \mathcal{L}^1$. In this example this is the case whenever $\alpha > \beta + 1$. To obtain robustness, it suffices that $D^{(1)} \notin \mathcal{L}^2$, for which $\alpha < 2$ is sufficient, and that there exists $k \in \{1, 2\}$ such that $\alpha_k < \min\{2k, d\}$, which also holds if $\alpha < 2$ as $\alpha_1 = \alpha$. To obtain non-robustness, it suffices that the second moment of the volume is finite and the condition of the tail indices is fulfilled, which holds if $\alpha > 2 + 2\beta$, or that the second moment of the diameter is finite, which holds if $\alpha > 2$. This leads to non-robustness if $\alpha > 2$. Considering now the robust case we focus on $\alpha < 2$ and $\mathcal{M} \neq \emptyset$ so that $\alpha \in (1, 2)$ to ensure the model is sparse. Theorem 3.1 gives us

$$\mathbb{P}_{x,y} \left(\frac{2-\delta}{\log \frac{1}{\alpha-1}} \leq \frac{\text{dist}(\mathbf{x}, \mathbf{y})}{\log \log |x-y|} \leq \frac{2+\delta}{\log \frac{1}{\alpha-1}} \mid x \leftrightarrow y \right) \xrightarrow{|x-y| \rightarrow \infty} 1.$$

for $x, y \in \mathcal{P}$ and $\delta > 0$ small.

An example where correlations of the diameters determine robustness

Our next example shows that the existence of a grain distribution where higher order information about the diameter distributions is crucial to determine whether it is robust or not. This shows that outside of the universal criteria for robustness, further information can be important to ensure the grain distribution is robust, which leads us to conjecture that our universal criterion is in fact best possible.

The example is as follows. Let $\alpha_1 \in (2, 2 + \gamma_2)$ for some $\gamma_2 \in (0, 1/2)$. We consider the following Poisson Boolean model with $d = 3$. Let D be a regularly varying random variable with index $-\alpha_1$ and the diameters of C are given as follows. For each realisation of C and independently of everything else, with probability $\frac{1}{2}$, we set $D^{(1)} = D$ and $D^{(2)} = D^{(3)} = \epsilon$ and otherwise

set $D^{(1)} = D^{(2)} = D^{\gamma_2}$ and $D^{(3)} = \epsilon$. Then, $D^{(1)}$ is regularly varying with index $-\alpha_1$ and $D^{(2)}$ regularly varying with index $-\alpha_1/\gamma_2$ and the grain distribution is non-robust. If we instead set $D^{(1)} = D$, $D^{(2)} = D^{\gamma_2}$ and $D^{(3)} = \epsilon$ almost surely we get that the resulting grain distribution is robust. The second case can be seen quickly as this was shown in Section 2.2.3 while we have that the strongly positive correlated model can be rewritten so that the model has the structure of the one in Section 2.2.3 (see Remark 2.2.2). We have for this kind of correlation that the resulting grain distribution is robust if there exists some $k \leq \lfloor 3/2 \rfloor$ such that $\alpha_k < 2k + \frac{1}{\gamma_k} \sum_{j=k+1}^{d-k} \gamma_j$. Our choice of parameters satisfies this requirement, since

$$\alpha_1 < 2 \cdot 1 + \frac{1}{\gamma_1} \sum_{j=1+1}^{3-1} \gamma_j = 2 + \gamma_2.$$

We consider now the other case in this example. Let therefore D be a regularly varying random variable with index $-\alpha_1$. Set, independently of everything else and with probability $\frac{1}{2}$, the diameters to be D, ϵ, ϵ and otherwise set the diameters to be $D^{\gamma_2}, D^{\gamma_2}, \epsilon$. Due to properties of regularly varying functions, this leads to the claimed marginal distributions of the diameters, namely $D^{(1)}$ is regularly varying with index $-\alpha_1$ and $D^{(2)}$ regularly varying with index $-\alpha_1/\gamma_2$. Note that $D^{(3)}$ is as in the previous case regularly varying with index $-\infty$ as it is almost surely constant.

For this explicit choice of the diameters and parameters, we show in the following that the grain distribution is non-robust. We do this following the same construction as in the proof from Section 2.2.4. Since it is now possible for either the first or second diameter to be too large, the step in (2.13) has to account for this, leading to

$$\begin{aligned} \mathbb{P}_{0,x,y} \left(\begin{array}{l} \mathbf{0} \sim \mathbf{x}, \mathbf{x} \sim \mathbf{y}, \\ \mathbf{0} \not\sim \mathbf{y}, 0 \notin 2\bar{R}_y \end{array} \right) \\ \leq \frac{1}{2} \mathbb{P}_{0,x,y} \left(\begin{array}{l} \bar{D}_x \geq \max(\text{dist}(\bar{R}_0, x), \text{dist}(\bar{R}_y, x)), \\ \bar{R}_0 \cap \bar{R}_x \neq \emptyset, \bar{R}_x \cap \bar{R}_y \neq \emptyset, \mathbf{0} \not\sim \mathbf{y}, 0 \notin 2\bar{R}_y \end{array} \right). \end{aligned} \quad (4.1)$$

$$+ \frac{1}{2} \mathbb{P}_{0,x,y} \left(\begin{array}{l} \bar{D}_x^{\gamma_2} \geq \max(\text{dist}(\bar{R}_0, x), \text{dist}(\bar{R}_y, x)), \\ \bar{R}_0 \cap \bar{R}_x \neq \emptyset, \bar{R}_x \cap \bar{R}_y \neq \emptyset, \mathbf{0} \not\sim \mathbf{y}, 0 \notin 2\bar{R}_y \end{array} \right). \quad (4.2)$$

where \bar{D}_x is defined as in Section 2.2.4 \bar{D} . The above bound arises since two distinct cases can lead to the diameters being sufficiently large for an intersection - we are either in the first case where C has one large diameter

and two small ones, or in the second where two of the diameters are large. By construction, both of these cases can occur only when the matching case of C occurs, which happens with probability $\frac{1}{2}$. The first summand, except for the factor $\frac{1}{2}$ is a special case of the case $k = 1$ of Theorem 2.3. The second summand, again other than the factor $\frac{1}{2}$, is a special case of the case $k = 2$ from Theorem 2.3. We get by using the same calculation as in Section 2.2.4, the condition that $\alpha_1 > 2$, $\alpha_2 > 4$ and that the second moment of the volume is finite in order to get non-robustness. Our grain distribution satisfies all these condition and in particular also the moment condition since

$$\mathbb{E}[\text{Vol}(C)] \leq \frac{1}{2}\mathbb{E}[D] + \frac{1}{2}\mathbb{E}[D^{2\gamma_2}],$$

which is finite due to choice of parameters.

Remark 4.0.1. We have chosen $d = 3$ in the above case for clarity and conciseness. A similar argument can however be done for any $d \geq 2$ and an arbitrary choice of $k \in \{1, \dots, d - 1\}$ for appropriately tuned tail exponents, by considering the perfectly correlated case which yields a robust grain distribution, and the bivariate case which is instead non-robust.

Chapter 5

Possible future work

In this chapter we consider some ideas for possible future work. For that, we briefly summarise what we have shown so far. On the one hand, we have proven that there exists conditions (universal or specific) that lead to a grain distribution being dense, robust or non-robust. The criterion for density is universal. For robustness we have shown a universal criterion and also a specific one that applies to certain correlations for the diameters. The non-robustness criterion refers to a special class of models belonging to Poisson Boolean models with regularly varying diameters, but we could also apply the proof to other examples. Furthermore, we have a result concerning the chemical distance for models that satisfy the universal conditions for robustness, but $\alpha_k > k$ for all $k \in \{1, \dots, d\}$, so that we can guarantee sparseness. The order here is $\log \log$. For all other ranges, we have shown that the order cannot be $\log \log$.

The following list includes questions that arose during this research.

- We have seen that there exists a universal result concerning density and robustness. During this work we were not able to get any universal criteria for the non-robustness. As we have seen in the last example in Chapter 4, it is possible that correlations between the diameters are crucial to determine whether a grain distribution is robust or non-robust. One possible future work could therefore be to get more conditions on volumes or some more information about correlation structures to get a universal result on non-robustness beyond the trivial case $D^{(1)} \in \mathcal{L}^d$ from [22]. Perhaps the use of copulas could lead to insight on the topic.
- A further interesting work could be to focus on the parameters regimes which were not covered in the first part of Theorem 3.1. In it we get the exact behaviour of the chemical distance for the case $\mathcal{M} \neq \emptyset$ with $\alpha_k > k$ for all $k \in \{1, \dots, d\}$. In all other cases we argue that the found

order of the behaviour of the chemical distance does not hold. One could therefore work on the correct behaviour of the chemical distance for all other parameter regimes. In our work we do not get more information about these other parameters as the proofs rely on the structure of the proof for the universal criteria on robustness.

- In our model we work here with a “hard” Poisson Boolean model. There exist also so-called *soft* versions of Poisson Boolean model with balls as convex grains. In these versions of the model, additional randomness is attached to the existence of edges. For each pair of vertices further random variable is sampled which influences the connection probability between this pair. This can be thought of as blow-up of the spheres of the two vertices of the pair by using this random variable. This soft version of the Poisson Boolean model was introduced in [27] and one can find more research on it in for example [37].

Further research opportunities lies in looking at some soft version of our model by attaching an additional random variable to every pair of vertices to modify the connection probability and get some other conditions for density, robustness and non-robustness. In connection with this, the chemical distance could be also interesting.

- In this work we are dealing with rotation invariant distributions of the convex grains, i.e. we have that the convex bodies are rotated uniformly. One could introduce some external field such as in the Ising model. Just briefly: The Ising model is a model which is of interest in the field of statistical mechanics. It is a model on \mathbb{Z}^d where the vertices get some spin (values ± 1) and one introduces an external field that influences the magnetic properties. An introduction on this model can be found for example in [52, 29].

We could also change just the choice of rotation for the convex grains by having for example some preference for the first diameter to be oriented in some given direction. This choice of rotation can be found for example in the work of Broman [7]. There the author investigates stick percolation and choose two different types of rotation, and looks at the asymptotic behaviour of the critical intensity parameter. He shows that in the uniform rotation case that $\lambda_c(L) \sim L^{-2}$, where L as the length of the stick. For the case that all sticks are aligned in the same direction he proves $\lambda_c(L) \sim L^{-1}$.

- In this work we deal with criteria on when we can observe a grain distribution being dense, robust or non-robust. For non-robustness we have that there exists some critical intensity which determines supercritical behaviour and subcritical behaviour. One could focus on this critical intensity and look at different features. For example, one could look at the asymptotic behaviour of it depending on the dimension as Meester et al. do for the random connection models [44] or the dependence on other model parameters.
- One interesting feature could also be the degree distribution for our explicit model. One could try to calculate the exact distribution or on bounds on them to see the dependence on the tail parameters $\alpha_1, \dots, \alpha_d$.

Appendix A

Further calculation

A.1 Existence of a box inside a convex body K

The next lemma is a tool that is used throughout this thesis. It states that for convex bodies with given diameters there exists a box with side-lengths which are of the same order as the diameters of the convex body. To prove this note that the smallest convex bodies that have diameters of size $D^{(1)}, \dots, D^{(d)}$ are the convex hulls of the endpoints of all of the diameters, that is, the d -dimensional convex polytopes with $2d$ vertices. We will, from here on out, refer to these endpoints as the polytope *corners* in order to avoid ambiguity with the vertices of \mathcal{K} . We will also use corners to refer to the vertices of boxes for the same reason.

Lemma A.1. *Let $K \subset \mathbb{R}^d$ be an arbitrary convex polytope with $2d$ corners and diameters $0 < l_d \leq \dots \leq l_1 < \infty$. Then there exists a box $B := B(K) \subset K$ which is congruent to*

$$\bigtimes_{i=1}^d [0, 2^{-2(d-1)} l_i].$$

Proof. We consider first the case $d = 2$. In this case, it is clear that the line segment of length l_1 connecting two of the polytope corners divides the polytope into two triangles. Both triangles have a hypotenuse of length l_1 . We denote by \tilde{l}_2 (resp. \hat{l}_2) the height relative to the hypotenuse of the first (resp. second) triangle. The maximum of both is at least $\frac{l_2}{2}$ since together they equal l_2 . Looking now at the bigger of the two triangles and using that triangles are convex, it is clear that there exists a box B of side-lengths at least $\frac{l_2}{4}$ and $\frac{l_1}{2}$

that is contained in this triangle and therefore also in K (see Figure A.1). It can be quickly verified that if this is not possible, then l_1 would not have been the first diameter.

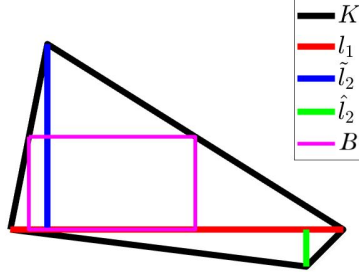


Figure A.1: $l_2 = \tilde{l}_2 + \hat{l}_2$. $\tilde{l}_2 = \max\{\tilde{l}_2, \hat{l}_2\} \geq l_2/2$. B with side-lengths at least $l_1/4$ and $l_2/4$.

Assume now that the claim is true for a fixed integer $d \geq 2$. We consider now the induction step for $d+1$. Due to the rotation invariance of the volume in Euclidean space, we assume that l_1, \dots, l_{d+1} have orientations e_1, \dots, e_{d+1} corresponding to the canonical basis of \mathbb{R}^{d+1} . We know that in the subspace spanned by the directions of the first d diameters, i.e. spanned by e_1, \dots, e_d , there exists a d -dimensional box of side-lengths $2^{-2(d-1)}l_1, \dots, 2^{-2(d-1)}l_d$ which we denote by B_d . Due to translation invariance, we assume without loss of generality that $B_d = \times_{i=1}^d [-2^{-2d+1}l_i, 2^{-2d+1}l_i] \times \{0\}$. Looking now at the two corners of the polytope which give rise to the $(d+1)$ st diameter with length l_{d+1} , it is true that at least one of them has distance greater or equal $l_{d+1}/2$ from $\mathbb{R}^d \times \{0\}$, similar to the $d=2$ case above. We focus on the corner which satisfies this and denote it by p . Note that just like in the case $d=2$, p has to lie “above” a d -dimensional box congruent to $\times_{i=1}^d [0, l_i] \times \{0\}$ that includes in its boundary the orthogonal projections of the first $2d$ corners of K onto $\mathbb{R}^d \times \{0\}$, since otherwise at least for one l_i for $i \in \{1, \dots, d\}$ could not be the i th diameter. We next construct a box which is included in K using that without loss of generality the $(d+1)$ st coordinate of p equals $l_{d+1}/2$.

Looking at the maximal distance of B_d to p in the direction e_i for $i \in \{1, \dots, d\}$, it is clear that this distance is at most $(1 - 2^{-2(d-1)})l_i$, since l_1, \dots, l_d are the sizes of the first d diameters and K is a polytope. A visualisation in 3 dimensions is given in Figure A.2. We claim that a box which is congruent to $B := \times_{i=1}^{d+1} [0, 2^{-2d}l_i]$ exists inside of K . To find it, we have to consider two different cases. The first one is that $p^{(i)} \in [-2^{-2d+1}l_i, 2^{-2d+1}l_i]$ for all $i \in \{1, \dots, d\}$, i.e. the orthogonal projection of p onto $\mathbb{R}^d \times \{0\}$ is contained

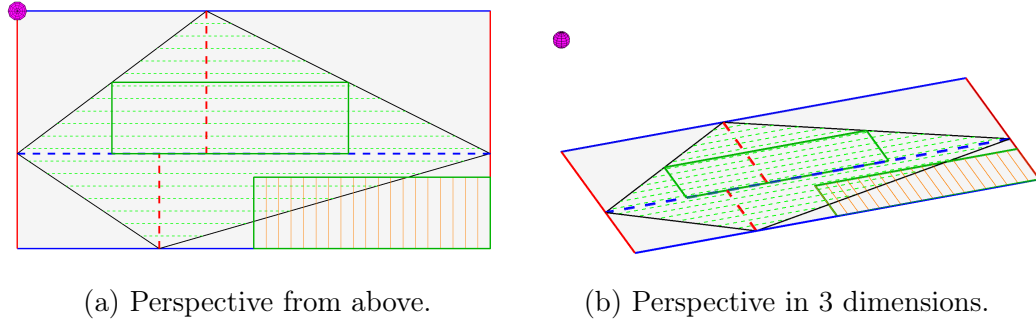


Figure A.2: Visualisation of the maximal distance of B_d and p in the directions e_i for $i \in \{1, \dots, d\}$ for the case $d = 2$. The blue and red solid lines represent an upper bound for the polytope with diameters l_1 and l_2 . The black lines and hatched green area denote the polytope given by the first $2d$ corners and the diameters of length l_1, \dots, l_d . The green rectangle in this convex set is B_2 while the rectangle with green boundary and hatched orange is B_2 shifted such that it has the maximal distance to p , which is given as the pink point.

in B_d . Note that the convex hull of B_d and p is a hyperpyramid (see Figure A.3). Considering now the connection lines of the corners of B_d and p and choosing the midpoints of these lines we obtain that the convex hull of these midpoints and their orthogonal projections onto $\mathbb{R}^d \times \{0\}$ determine a $(d + 1)$ -dimensional box, which we denote by \tilde{B} . This box is congruent to $\times_{i=1}^d [0, 2^{-2d+1}l_i] \times [0, l_{d+1}/4]$ using the self-similarity property of hyperpyramids. Since this box contains a smaller box which is congruent to the sought after box B , we are done with this case. A visualisation of this step for $d+1 = 3$ is given in Figure A.3.

In the second case we are dealing with p such that the orthogonal projection of it onto $\mathbb{R}^d \times \{0\}$ does not lie in B_d , see Figure A.4. As we are interested in finding a box which is congruent to the sought after box B , it suffices to look for a minimal box and show that this is a suitable choice. We assume therefore as in the previous case, that p has distance $l_{d+1}/2$ to $\mathbb{R}^d \times \{0\}$.

We consider now the worst case scenario for the location of p , i.e. that it has the maximal distance to the base B_d in each direction e_i , $i \in \{1, \dots, d\}$, which is $(1 - 2^{-2(d-1)})l_i$ as discussed above. For that to be the case, p has to lie in

$$N := \{x \in \mathbb{R}^{d+1} : (\pm(1 - 2^{-2d+1})l_1, \dots, \pm(1 - 2^{-2d+1})l_d, l_{d+1}/2)\}.$$

We will determine now a new vertex which will be used to construct the sought after box.

Let $y \in B_d$ be such that it has maximal distance to p . The coordinates

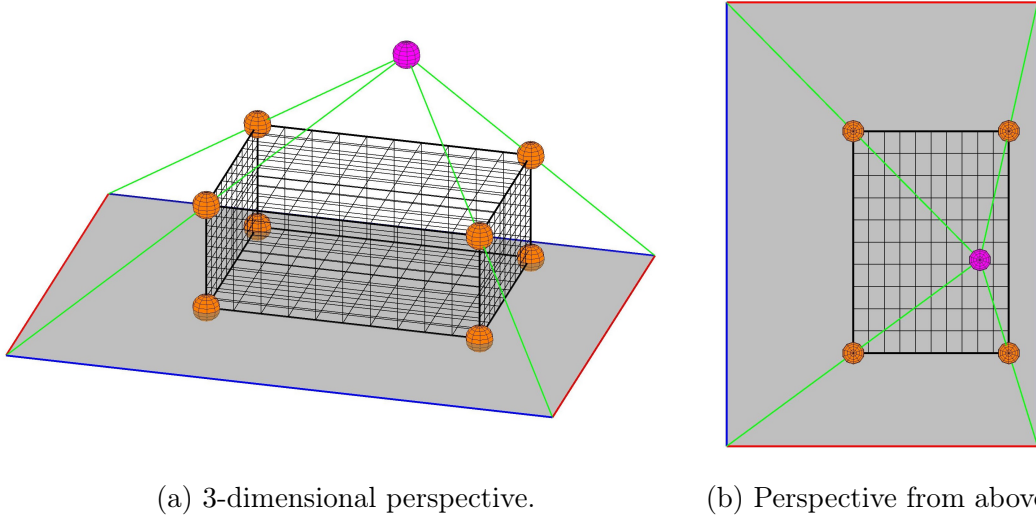


Figure A.3: Example for the induction step for the first case of Lemma A.1 from $d = 2$ to $d + 1 = 3$ from different perspectives. B_2 is in gray, p is the pink point, in green are the connection lines of p and the corners of B_2 , the orange points as the midpoints of these lines and the orthogonal projection of the midpoints, and \tilde{B} is the box represented by the black mesh.

of such a vertex y fulfil $y^{(i)} = \mp 2^{-2d+1}l_i$ for all $i \in \{1, \dots, d\}$ and $y^{(d+1)} = 0$. Due to the symmetry of B_d we can without loss of generality look at $p = ((1 - 2^{-2d+1})l_1, \dots, (1 - 2^{-2d+1})l_d, l_{d+1}/2) \in N$ and consequently set $y := (-2^{-2d+1}l_1, \dots, -2^{-2d+1}l_d, 0) \in B_d$. Consider now the point

$$z := 2^{-2(d-1)}(p - y) + y = (2^{-2d+1}l_1, \dots, 2^{-2d+1}l_d, 2^{-2d+1}l_{d+1})$$

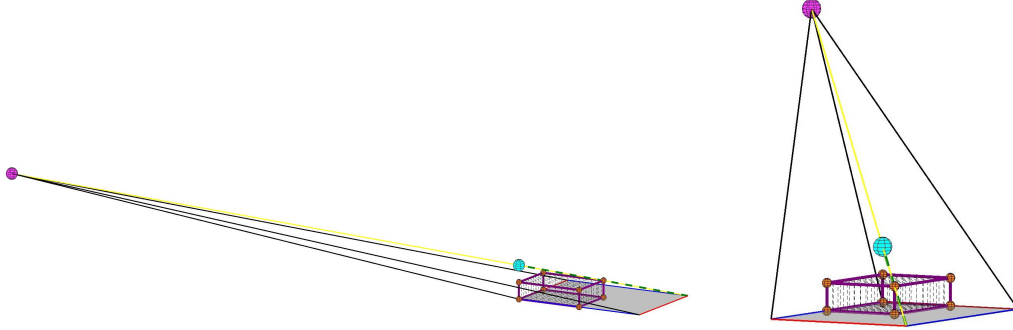
which lies in the convex hull of B_d and p , and in particular lies “above” B_d (as indicated in the example of Figure A.4). We claim even more, namely that the convex hull of z and B_d is a minimal hyperpyramid which is also included in K , whereby it is minimal in the sense that its volume is minimal across for all choices of p . To see the latter, note that we are considering the worst case location of p , but that there exists an actual corner of the polytope that has the same distance from $\mathbb{R}^d \times \{0\}$ as p . If one were to construct the point z (call it \tilde{z}) for this corner, one would immediately have that \tilde{z} lies in K and that the distance of \tilde{z} to $\mathbb{R}^d \times \{0\}$ is not smaller than that of z (since z has the minimal possible distance for a vertex constructed in this way).

With z taking the role of p we are back in the first case and using convexity and the midpoints of the connection lines from z to the corners of B_d gives us

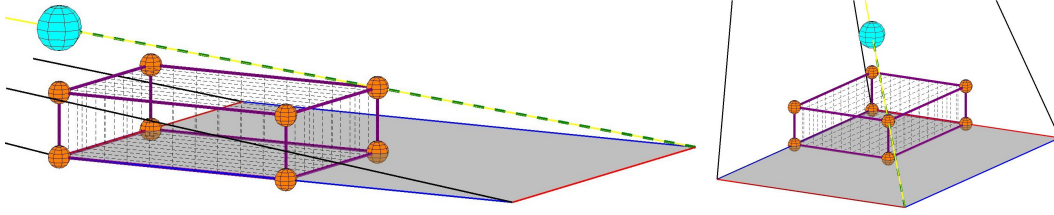
the desired box. The midpoints and their orthogonal projections are given by

$$\tilde{N} := \{x \in \mathbb{R}^{d+1} : x^{(i)} \in \{0, 2^{-2d+1}l_i\}, \forall i \in \{1, \dots, d\}, x^{(d+1)} \in \{0, 2^{-2d}\}\}.$$

The resulting box, denoted as B , has side-lengths $2^{-2d}l_1, \dots, 2^{-2d}l_d$ which concludes the proof.



(a) Induction step from $d = 2$ to $d = 3$ of the second case of p .



(b) Induction step zoomed in from $d = 2$ to $d = 3$ of the second case for p .

Figure A.4: Example for the described induction step of Lemma A.1 from $d = 2$ to $d + 1 = 3$ of the second case for p . B_2 in gray, p the pink point, in turquoise $z = (2^{-2d+1}l_1, \dots, 2^{-2d+1}l_d, 2^{-2d+1}l_{d+1})$, yellow the connection line of p and y , in green the connection line of z and y , the orange points as \tilde{N} and in purple the boundary of B . The hyperpyramid is given as the convex hull of the turquoise point and B_2 . The boundary of B_2 is indicated via the red and blue lines.

We note that it is possible for one of the two hyperpyramids can be degenerate, that is, have 0 volume. This however does not affect the proof, since we always work with the larger of the two when choosing the corner p . \square

A.2 Results are independent of the choice of diameters

The next lemma shows that the results of this thesis are independent from the choice of diameters given the indices of the regularly varying diameters are always the same, it does not matter in what order we chose the diameters, if the sequence of diameters is not unique.

Lemma A.2. *Let $C \subset \mathbb{R}^d$ be a random convex body such that there exists a ball of radius $\epsilon > 0$ which is included in C . We assume that the diameters of C are given by $D^{(1)}, \dots, D^{(d)}$ and that $D^{(k)}$ has regularly varying distribution with index $-\alpha_k$ for some positive α_k for all $k \in \{1, \dots, d\}$. We assume that $\alpha_1 \leq \dots \leq \alpha_d$. Let $\tilde{D}^{(1)}, \dots, \tilde{D}^{(d)}$ be another choice of diameters of C . Then $\tilde{D}^{(1)}, \dots, \tilde{D}^{(d)}$ also have regularly varying distribution with the same indices $-\alpha_1 \geq -\alpha_2 \geq \dots \geq -\alpha_d$.*

Proof. Looking at the definition of the first diameter it is clear that $D^{(1)} = \tilde{D}^{(1)}$ almost surely. Otherwise one of them can not be the first diameter of C . In addition to that we know that there exists rectangles R_1 and \tilde{R}_1 which are congruent to

$$\bigtimes_{i=1}^d [0, D^{(i)}] \text{ and } \bigtimes_{i=1}^d [0, \tilde{D}^{(i)}]$$

and fulfil $C \subset R_1$ and $C \subset \tilde{R}_1$ almost surely. Using Lemma A.1 we have that there exists also rectangles R_2 and \tilde{R}_2 which are congruent to

$$\bigtimes_{i=1}^d [0, 2^{-2(d-1)} D^{(i)}] \text{ and } \bigtimes_{i=1}^d [0, 2^{-2(d-1)} \tilde{D}^{(i)}]$$

and satisfy $R_2, \tilde{R}_2 \subset C$. To prove the claim note that a rectangle with side-lengths $l_1 \geq l_2 \geq \dots \geq l_d$ includes an d -dimensional ellipsoid with axes of length l_1, \dots, l_d . Note also that the intersection of an ellipsoid with a hyperplane, which includes the center of the ellipsoid, is a $(d-1)$ -dimensional ellipsoid [43]. Fix now an arbitrary hyperplane that includes the center of the ellipsoid and let $l'_1 \geq l'_2 \geq \dots \geq l'_{d-1}$ be the axes of the $(d-1)$ -dimensional ellipsoid resulting as the intersection of the d -dimensional ellipsoid with the hyperplane. We have that $l'_i \geq l_{i+1}$ for all $i \in \{1, \dots, d-1\}$. In other words

the smallest intersection is to choose a hyperplane that is perpendicular to the orientation of the biggest axis. Furthermore we know that

$$P_{H_{p_C^{(1)}}}(R_1) \supset P_{H_{p_C^{(1)}}}(\tilde{R}_2),$$

while $p_C^{(1)}$ is the orientation of $D^{(1)}$. We also have that $P_{H_{p_C^{(1)}}}(\tilde{R}_2)$ includes the orthogonal projection of an ellipsoid with axes $2^{-2(d-1)}\tilde{D}^{(1)}, \dots, 2^{-2(d-1)}\tilde{D}^{(d)}$ onto $H_{p_C^{(1)}}$. Using now all of these properties we have that this orthogonal projection includes an $(d-1)$ -dimensional ellipsoid with axes of length $2^{-2(d-1)}\tilde{D}^{(2)}, \dots, 2^{-2(d-1)}\tilde{D}^{(d)}$. With Lemma A.1 there exists some $(d-1)$ -dimensional rectangle of side-length $c_1\tilde{D}^{(1)}, \dots, c_1\tilde{D}^{(d)}$ for suitable $c_1 > 0$ which only depends on the dimension. So we get that

$$D^{(2)} \geq c_1\tilde{D}^{(2)}$$

almost surely. Conversely the same argumentation leads to the existence of some finite $\tilde{c}_1 > 0$ such that

$$\tilde{D}^{(2)} \geq \tilde{c}_1 D^{(2)}.$$

Doing this procedure now for $P_{H_{p_C^{(1)}}}(R_1)$ and $P_{H_{p_C^{(1)}}}(\tilde{R}_2)$ resp. $P_{H_{p_C^{(1)}}}(R_2)$ and $P_{H_{p_C^{(1)}}}(\tilde{R}_2)$ we get the existence for two constants $c_2, \tilde{c}_2 \in (0, \infty)$ such that

$$D^{(3)} \geq c_2\tilde{D}^{(3)}$$

and

$$\tilde{D}^{(3)} \geq \tilde{c}_2 D^{(3)}.$$

This can be done iteratively. We get the existence of constants $c_1, \dots, c_{d-1}, \tilde{c}_1, \dots, \tilde{c}_{d-1} \in (0, \infty)$ such that for all $i \in \{1, \dots, d\}$

$$D^{(i)} \geq c_{i-1}\tilde{D}^{(i)} \geq c_{i-1}\tilde{c}_{i-1}D^{(i)}$$

almost surely. Due to the properties of regularly varying functions this shows the claim. \square

A.3 Proof of the inequality of (2.8)

In this section, we consider the key inequality (2.8) that is used in the proof of the universal criteria of robustness, i.e. the first part of Theorem 2.2.

Lemma A.3. *With the definitions from Chapter 2 we get for $k \in \{1, \dots, d-1\}$ that the following holds*

$$\begin{aligned} \mathbb{P}_C((x+C) \cap Q_{f_n}^*(x_n, x) \neq \emptyset \mid D_C^{(k)} \geq 2^{2(d-1)+\epsilon} f_{n+1}) & \mathbb{P}_C(D_C^{(k)} \geq 2^{2(d-1)+\epsilon} f_{n+1}) \\ & \geq c \frac{f_n^{\min\{d-k, k\}}}{f_{n+1}^{d-k}} f_{n+1}^{-(\alpha_k + \epsilon)} \end{aligned}$$

for some constant $c \in (0, \infty)$ that depends only on d, k, ϵ and ϵ .

Proof. First, we note that the condition in the first term ensures that the first k diameters of C are large enough so that $C \cap O_n(\mathbf{x}_n)$ can occur. The reason for this is, on the one hand, that the box, which is almost surely included in C according to Lemma A.1, is large enough so that the convex body can intersect with C_{x_n} if the orientation is suitable. On the other hand, the sequence $(f_n)_{n \in \mathbb{N}}$ grows super-exponentially, which means that the distance $|x_{n+1} - x_n|$ is of the order of f_{n+1} . We have therefore that $|x_{n+1} - x_n| \gg f_n$.

Looking now at the second factor on the left side of the inequality we can use Potter bounds to get the lower bound which gives us the second factor on the right side of the inequality. What now needs to be considered is the set of all orientations that lead to an intersection or rather a lower bound of the size of this set of orientation to prove the whole inequality, i.e. we have to show that

$$\begin{aligned} \mathbb{P}_C((x+C) \cap Q_{f_n}^*(x_n, x) \neq \emptyset \mid D_C^{(k)} \geq 2^{2(d-1)+\epsilon} f_{n+1}) \\ \geq c \frac{f_n^{\min\{d-k, k\}}}{f_{n+1}^{d-k}}. \end{aligned}$$

Recall that we are looking at fix k and ask for $D^{(k)}$ to be large enough and do not look at $D^{(j)}$ for $j \leq k$, as we know that this diameters are almost surely bigger than $D^{(k)}$. For all other diameters we assume them to be equal ϵ as we are just interested in a lower bound.

We prove the claim in the following by induction over d .

Base case $d = 2$: The only case to consider here is $d - k = k = 1$. Under the condition that $D^{(1)} \geq 2^{2+\epsilon} f_{n+1}$, we can assume, in order to estimate the intersection probability from below, that the second diameter has size ϵ . We now consider the box centered at x_n with side-lengths f_n and ϵ . As $x \in O_n(x_n)$ we have that the orthogonal projection of C_{x_n} onto a hyperplane perpendicular to $x_n - x$ includes a 1-dimensional box (given via Lemma A.1), i.e. a line which has at least length cf_n , while $c \in (0, \infty)$ only depending on φ from (2.4). This means for the orientation of $D_x^{(1)}$ that the set of all possible orientations that results in an intersection is of order cf_n/f_{n+1} for suitable $c \in (0, \infty)$ by using inequalities of trigonometrical functions for small angles. As $\min\{d - k, k\} = 1$ we prove the base case.

Induction step $d \mapsto d + 1$: For the induction step, we have to look at two different cases. The first one is $k \in \{1, \dots, d - 1\}$ and the second one $k = d$.

We first starts with $k \in \{1, \dots, d - 1\}$. Note that only the size of the orthogonal projection of C_{x_n} onto a hyperplane perpendicular to $x_n - x$ is relevant as we have that first k diameters of \mathbf{x} are large enough to result in an intersection and we think of all other diameters being fix equal ϵ in order to get a lower bound for the intersection probability. We assume without loss of generality, in order to simplify notation, that the $(d - 1)$ -dimensional box which is included in $B_{f_n}^*(\mathbf{x}_n, x)$, due to Lemma A.1 is centered in the origin. Note that we can assume that this box has k side-lengths of size cf_n and all others of side-length $c\epsilon$ for some c only depending again on d and φ , as again we are interested in a lower bound. This assumption is possible due to translation invariance of the Lebesgue measure. And with the same reason we assume that

$$\frac{1}{2} \left(\{0\} \times \bigtimes_{j=1}^k [-cf_n, cf_n] \times \bigtimes_{i=k+1}^d [-c\epsilon, c\epsilon] \right) =: B_{B^*}$$

and $x = (|x|, 0, \dots, 0)$. Note that $|x|$ is of order f_{n+1} as $|x_n - x|$ is of order f_{n+1} . Defining \tilde{B}_{B^*} as

$$\tilde{B}_{B^*} := \frac{1}{2} \left(\{0\} \times \bigtimes_{j=1}^k [-cf_n, cf_n] \times \bigtimes_{i=k+1}^{d-1} [-c\epsilon, c\epsilon] \times \mathbb{R} \right)$$

we want to focus on

$$\mathbb{P}_C((x + C) \cap \tilde{B}_{B^*} \neq \emptyset \mid D_C^{(k)} \geq 2^{2(d-1)+\epsilon} f_{n+1}),$$

i.e. the probability that C_x is well oriented in the sense that the orthogonal projection of C_x onto the hyperplane perpendicular to $e_{d+1} := (0, \dots, 0, 1) \in \mathbb{R}^{d+1}$, intersects with the orthogonal projection of B_{B^*} onto the same hyperplane. In this event we have one restriction fewer as in the original conditional probability (see first factor of (2.8)), i.e. this event reduces to an intersection problem in d dimensions as we have uniformly rotation of the convex bodies. Using induction hypotheses leads to

$$\mathbb{P}_C((x + C) \cap \tilde{B}_{B^*} \neq \emptyset \mid D_C^{(k)} \geq 2^{2(d-1)+\epsilon} f_{n+1}) \geq c \frac{f_n^{\min\{d-k, k\}}}{f_{n+1}^{d-k}}.$$

To get now the requested lower bound for the probability stated in this lemma, note that for all orientations of the diameters that results in some intersection with \tilde{B}_{B^*} , not all are suitable to results in an intersection with B_{B^*} . To get a lower bound for that we get the additional factor $c\epsilon/f_{n+1}$ as the proportion of the set of all orientations to that C_x results in an intersection with B_{B^*} from all other orientations that results in an intersections with \tilde{B}_{B^*} .

We can now consider the case $k = d$. Let H_x be the hyperplane defined as

$$H_x := x + \{y \in \mathbb{R}^{d+1} : \langle y, p_x^{(d+1)} \rangle = 0\},$$

i.e. the hyperplane that includes x and is perpendicular to the orientation $p_x^{(d+1)}$. Recall that $p_x^{(d+1)}$ is the orientation of the $(d+1)$ st diameter of C_x . Note that the probability that C_x intersects with B_{B^*} (similar defined as in the case $k \in \{1, \dots, d-1\}$), under the condition that the first d diameters of C_x are big enough, is smaller than the probability H_x intersects with B_{B^*} as $D_x^{(d+1)} > 0$.

Let now $T_{-x} : \mathbb{R}^{d+1} \rightarrow \mathbb{R}^{d+1}$ be the translation by $-x$, i.e.

$$T_{-x}(M) = \{y \in \mathbb{R}^d : y - x \in M\},$$

i.e. the translation by $-x$ so that $0 \in T_{-x}(H_x)$ and $-x \in T_{-x}(B_{B^*})$. This does not effect the probability again due to translation invariance of the Lebesgue measure. We have therefore

$$T_{-x}(H_x) = \{x \in \mathbb{R}^d : \langle y, p_x^{(d+1)} \rangle = 0\}.$$

Again we assume without loss of generality that $x = (|x|, 0, \dots, 0)$. As the distance of $y \in \mathbb{R}^{d+1}$ to $T_{-x}(H_x)$ is given as $|\langle y, p_x^{(d+1)} \rangle|$ we have to look at all

possible orientations of $p_x^{(d+1)}$ such that this distance is smaller than cf_n . As we choose without loss of generality that $x = (|x|, 0, \dots, 0)$, we have that the following inequality should be satisfied

$$|\langle -x, p_x^{(d+1)} \rangle| = |x|(p_x^{(d+1)})_{(1)} < cf_n$$

as we denote by $(p_x^{(d+1)})_{(1)}$ the first coordinate of $p_x^{(d+1)}$. Recall that $|x| \asymp f_{n+1}$ and we get therefore the condition

$$(p_x^{(d+1)})_{(1)} < cf_n/f_{n+1}.$$

Due to the rotation invariance of the distribution of C we have that the orientation of C is uniformly distributed. We therefore get that the probability of having this restriction on $p_x^{(d+1)}$ is of order f_n/f_{n+1} as this is the order of the proportion of all $y = (y^{(1)}, \dots, y^{(d)}) \in \mathbb{S}^d$ which satisfy $y^{(1)} < cf_n/f_{n+1}$. This leads to the required inequality and we are done with the proof. Note that the fundamental properties of hyperplanes including distances of points to them can be found for example in [15]. \square

Remark A.3.1. Note that the whole calculation can be done similar to get (2.9) in the proof of the specific criteria robustness of part (b) from Theorem 2.2.

A.4 Intersection probability for $\mathcal{A}_1(\mathbf{0}, \mathbf{y})$ - $\mathcal{A}_5(\mathbf{0}, \mathbf{y})$

In this section we prove a lemma that is crucial for the inequalities for the intersection probabilities in $\mathcal{A}_1(\mathbf{0}, \mathbf{y})$ - $\mathcal{A}_5(\mathbf{0}, \mathbf{y})$. This lemma includes a result of an upper bound of the probability that a random box intersects a box with fixed side-lengths. Recall that in $\mathcal{A}_1(\mathbf{0}, \mathbf{y})$ - $\mathcal{A}_5(\mathbf{0}, \mathbf{y})$ the location of the connector \mathbf{x} for $\mathbf{0}$ and \mathbf{y} is chosen in such a way that we reduce the intersection probability by a suitable intersection of C_x with some special box, that is either the box concerning to $\mathbf{0}$ or \mathbf{y} or a box that can be constructed with the help of side-lengths of these two boxes. For more details look again at Section 2.2.4.

This is the reason why the following lemma is useful to bound the intersection probability from above.

Lemma A.4. *Let \bar{R}_0 be a box that is congruent to*

$$\bigtimes_{i=1}^d [-j_0^{(i)}, j_0^{(i)}]$$

while $j_0 \in \mathbb{N}^d$ with $j_0^{(i)} \geq j_0^{(i+1)}$ for $i \in \{1, \dots, d-1\}$. Denote \bar{R}_x as the box which is centered in x with diameters $\bar{D}^{(1)}, \dots, \bar{D}^{(d)}$ as defined in Section 2.2.4. Let $M \in (0, \infty)$ be a constant and we assume that $D^{(i)} = D^{(k)}$ for all $i \in \{1, \dots, k-1\}$ and $D^{(\ell)} \leq M$ almost surely for all $\ell \in \{k+1, \dots, d\}$. In addition to that we assume without loss of generality that $x = (|x|, 0, \dots, 0)$ and furthermore that $x \notin \bar{R}_0$. We are therefore looking at the generalisation of the ellipses model [53] as described in Theorem 2.3. For that we have for large $|x|$

$$\mathbb{P}(\bar{R}_x \cap \bar{R}_0 \neq \emptyset) \leq c|x|^{-(\alpha_k - \varepsilon)} \prod_{s=1}^{d-k} \frac{j_0^{(s)}}{|x|}.$$

Proof. The proof is quite similar to the proof of Lemma A.3. We therefore only point out what has to be change to get the upper bound. We have

$$\mathbb{P}(\bar{R}_x \cap \bar{R}_0 \neq \emptyset) = \mathbb{P}(\bar{R}_x \cap \bar{R}_0 \neq \emptyset \mid \bar{D}_x^{(k)} \geq \text{dist}(\bar{R}_0, x)) \mathbb{P}(\bar{D}_x^{(k)} \geq \text{dist}(\bar{R}_0, x)).$$

For the calculations it is important that $|x|$ is big so that $\text{dist}(\bar{R}_0, \bar{R}_x) \asymp |x|$. We therefore get the first factor of the inequality, stated in this lemma, due to Potter bounds. Note that as $D^{(k)}$ is regularly varying with index $-\alpha_k$ the Potter bounds also apply here. In addition to that we know that $D^{(j)} \leq M$ for $j \in \{k+1, \dots, d\}$ almost surely. We therefore bound the box \bar{R}_x from above by replacing $\bar{D}^{(j)}$ by $\lceil M \rceil$. We assume that the box \bar{R}_0 is oriented in such a way that the orientation of the smallest diameter is the same as the orientation of $(x-0)/|x|$ to get an upper bound for the intersection probability. Similar as in the proof of Lemma A.3 we look at the orthogonal projection of \bar{R}_0 onto a hyperplane perpendicular to x . For that we can bound the probability from above by the probability of the intersection between \bar{R}_x and a $(d-1)$ -dimensional box with diameters of size $j_0^{(1)}, \dots, j_0^{(d-1)}$. We can therefore show, via repeating the calculations in the proof of Lemma A.3 that the set of

orientations of \bar{R}_x that results in an intersection can be bound from above by

$$c \frac{(j_0^{(1)} + \lceil M \rceil)^{\min\{d-k, k\}} \lceil M \rceil^{\max\{0, d-k, k\}}}{|x|^{d-k}} \leq c \prod_{s=1}^{d-k} \frac{j_0^{(s)}}{|x|},$$

while we used the definition of the model so that $\bar{D}^{(1)} = \bar{D}^{(k)}$ for $j \in \{1, \dots, k-1\}$ and $\bar{D}^{(\ell)} = \bar{D}^{(d)} \leq \lceil M \rceil$. In addition to that we get on the left side of this inequality the term with $\lceil M \rceil$ as the size of the small diameters of \bar{R}_x is crucial for the set of orientations. But as this $M \in (0, \infty)$ is deterministic we can hide this M in the upper bound by some constant factor c that now depends also in M . \square

Note that we assume in the lemma that $x \notin \bar{R}_0$ as this is the important part for the calculations in $\mathcal{A}_1(\mathbf{0}, \mathbf{y})$ - $\mathcal{A}_5(\mathbf{0}, \mathbf{y})$. In addition to that, we have that in the calculation in Section 2.2.4 instead of $|x|$ the term $|x| + |y|$ in the upper bound of the intersection probability. To see this additional $+|y|$ one transfer this to the explicit situations in the individual parts of the calculations and note that the distance of \bar{R}_x and \bar{R}_0 but also the distance from \bar{R}_x and \bar{R}_y (from Section 2.2.4) are crucial. This leads to this extra term $+|y|$.

A.5 Intersection probability for $\mathcal{A}_6(\mathbf{0}, \mathbf{y})$ - $\mathcal{A}_8(\mathbf{0}, \mathbf{y})$

In this section we prove the upper bound of the connection probability that is used in Section 2.2.4 in $\mathcal{A}_6(\mathbf{0}, \mathbf{y})$, $\mathcal{A}_7(\mathbf{0}, \mathbf{y})$ and $\mathcal{A}_8(\mathbf{0}, \mathbf{y})$.

Lemma A.5. *Let \bar{R}_0 and \bar{R}_y be boxes which are congruent to*

$$\bigtimes_{i=1}^d [-j_0^{(i)}, j_0^{(i)}] \text{ resp. } \bigtimes_{i=1}^d [-j_y^{(i)}, j_y^{(i)}]$$

while $j_0, j_y \in \mathbb{N}^d$ with $j_0^{(i)} \geq j_0^{(i+1)}$ and $j_y^{(i)} \geq j_y^{(i+1)}$ for $i \in \{1, \dots, d-1\}$. Denote \bar{R}_x as the box which is centered in x with diameters $\bar{D}^{(1)}, \dots, \bar{D}^{(d)}$ as defined in Section 2.2.4. We assume that $D^{(i)} = D^{(k)}$ for all $j \in \{1, \dots, k-1\}$ and $D^{(\ell)} \leq M$ almost surely for all $\ell \in \{k+1, \dots, d\}$. In addition to that we assume that without loss of generality that $x = (|x|, 0, \dots, 0)$ and $y = (|y|, 0, \dots, 0)$. We are therefore looking at the generalisation of the ellipses model of [53] as described in Theorem 2.3.

For that we have for large $|x|, |y|$

$$\mathbb{P}(\bar{R}_x \cap \bar{R}_0 \neq \emptyset, \bar{R}_x \cap \bar{R}_y \neq \emptyset) \leq c(|x| + |y|)^{-(\alpha_k - \varepsilon)} \prod_{s=1}^{d-k} \frac{j_0^{(s)} j_y^{(s)}}{(|x| + |y|)^2}.$$

Proof. In order to proof the claim we use as in the proof of the inequality (2.8) conditional probability that the diameters are big enough i.e.

$$\begin{aligned} \mathbb{P}(\bar{R}_x \cap \bar{R}_0 \neq \emptyset, \bar{R}_x \cap \bar{R}_y \neq \emptyset) &\leq c\mathbb{P}(\bar{D}^{(k)} \geq \max\{|x|, |x - y|, |y|\}) \\ &\times \mathbb{P}\left(\begin{array}{c} \bar{R}_x \cap \bar{R}_0 \neq \emptyset, \\ \bar{R}_x \cap \bar{R}_y \neq \emptyset \end{array} \middle| \bar{D}^{(k)} \geq \max\{|x|, |x - y|, |y|\}\right). \end{aligned}$$

Note that the max term is given as the diameters of \bar{R}_x should be big enough to reach \bar{R}_0 and \bar{R}_y but also, due to convexity of the box, to bridge the distance between \bar{R}_0 and \bar{R}_y . As we are interested in the case that \bar{R}_x is the connector between \bar{R}_0 and \bar{R}_y and that \bar{R}_0 and \bar{R}_y do not intersect with each other, we can use that the distance are proportional to $|x|, |x - y|$ and $|y|$ for the distance of \bar{R}_x to \bar{R}_0 and \bar{R}_y and the distance of \bar{R}_0 to \bar{R}_y . Due to the Potter bounds and the fact that $\max\{|x|, |x - y|, |y|\} \asymp |x| + |y|$ we get that the first factor of the inequality, i.e.

$$\mathbb{P}(\bar{D}^{(k)} \leq \max\{|x|, |x - y|, |y|\}) \leq c(|x| + |y|)^{-(\alpha_k - \varepsilon)}.$$

Note again that the Potter bounds holds also for $\bar{D}^{(k)}$. It remains to prove the following

$$\mathbb{P}(\bar{R}_x \cap \bar{R}_0 \neq \emptyset, \bar{R}_x \cap \bar{R}_y \neq \emptyset \mid \bar{D} \geq \max\{|x|, |x - y|, |y|\}) \leq c \prod_{s=1}^{d-k} \frac{j_0^{(s)} j_y^{(s)}}{(|x| + |y|)^2}.$$

We already now from Lemma A.4 that the probability of $\bar{R}_x \cap \bar{R}_0 \neq \emptyset$ under the condition that the k th diameter of \bar{R}_x is big enough can be bound from above by

$$c \prod_{s=1}^{d-k} \frac{j_0^{(s)}}{|x| + |y|}.$$

We must now consider what is necessary for \bar{R}_x to intersect \bar{R}_y . If we are looking all possible orientations of \bar{R}_x so that an intersection with \bar{R}_0 is possible, we know that if $\bar{R}_x \cap \bar{R}_0 \neq \emptyset$ is occurs, we have to restrict all these possible orientations so that this leads to an intersection with \bar{R}_y . This

proportion of the orientations of \bar{R}_x can be bounded from above by

$$c \prod_{s=1}^{d-k} \frac{j_y^{(s)}}{|x| + |y|}.$$

Intuitively speaking, this can be achieved by again using the inequalities for trigonometrical functions and considering that if one of the axes is rotated so that $\bar{R}_x \cap \bar{R}_0 \neq \emptyset$ you only have $d - 1$ axes available to achieve \bar{R}_y . This reduces the whole problem to a $(d - 1)$ -dimensional problem, whereby we only have $k - 1$ large diameters available. Overall, Lemma A.4 then provides the above factor and thus the required inequality is obtained. \square

A.6 Continuity of the percolation probability

In this section we want to prove the key lemma that is necessary to prove the continuity of the percolation probability in the Poisson Boolean model with *boxes* as convex grains stated in Proposition 3.4. For that we denote in the following for $K \subset \mathbb{R}^d$ the interior of K as $\text{int}(K)$ and the boundary of K as ∂K .

Lemma A.6. *For every $x \in \mathcal{P}$ we have*

$$\mathbb{P}_{0,x}(\{C_x \cap \partial C_0 \neq \emptyset\} \cap \{C_x \cap \text{int}(C_0) = \emptyset\}) = 0.$$

Proof. Let \mathbb{P}_{C_0, D_x} be the probability measure under the condition that C_0 and the size of the diameters of C_x are fixed i.e. the only random part is the rotation of C_x . We will argue the claim by using contradiction. Let rot_{C_0} be the rotation for which

$$C_0 = \text{rot}_{C_0} \left(\bigtimes_{i=1}^d [-2^{-2d+1} D^{(i)}, 2^{-2d+1} D^{(i)}] \right).$$

Define the δ -reduction of C_0 as

$$C_0^\delta := \text{rot}_{C_0} \left(\bigtimes_{i=1}^d [-2^{-2d+1} D^{(i)} + \delta, 2^{-2d+1} D^{(i)} - \delta] \right),$$

and set $C_0^\delta = \emptyset$ if $\delta > \epsilon 2^{-2d+1}$. It holds that

$$\text{int}(C_0) = \bigcup_{m \in \mathbb{N}} C_0^{1/m}.$$

Moreover we also have

$$\text{int}(C_0) = \bigcup_{m \in \mathbb{N}} \text{int}(C_0^{1/m}).$$

Furthermore, it holds that

$$\partial C_0 = \lim_{m \rightarrow \infty} \partial C_0^{1/m}.$$

Assume now, incorrectly, that

$$\mathbb{P}_{C_0, D_x}(\{C_x \cap \partial C_0 \neq \emptyset\} \cap \{C_x \cap \text{int}(C_0) = \emptyset\}) > 0. \quad (\text{A.1})$$

Using the preceding observations, we can obtain

$$\begin{aligned} \mathbb{P}_{C_0, D_x}(C_x \cap \text{int}(C_0) \neq \emptyset) &= \lim_{m \rightarrow \infty} \mathbb{P}_{C_0, D_x}(C_x \cap C_0^{1/m} \neq \emptyset) \\ &= \lim_{m \rightarrow \infty} \mathbb{P}_{C_0, D_x}(C_x \cap \text{int}(C_0^{1/m}) \neq \emptyset) \\ &\quad + \lim_{m \rightarrow \infty} \mathbb{P}_{C_0, D_x}(\{C_x \cap \partial C_0^{1/m} \neq \emptyset\} \\ &\quad \cap \{C_x \cap \text{int}(C_0^{1/m}) = \emptyset\}) \\ &> \mathbb{P}_{C_0, D_x}(C_x \cap \text{int}(C_0) \neq \emptyset), \end{aligned}$$

where the inequality follows from (A.1) and the third observation above. Since this yields

$$\mathbb{P}_{C_0, D_x}(C_x \cap \text{int}(C_0) \neq \emptyset) > \mathbb{P}_{C_0, D_x}(C_x \cap \text{int}(C_0) \neq \emptyset),$$

which is a contradiction, we must have that

$$\mathbb{P}_{C_0, D_x}(\{C_x \cap \partial C_0 \neq \emptyset\} \cap \{C_x \cap \text{int}(C_0) = \emptyset\}) = 0.$$

Integrating this over all possible C_0 and D_x leads then to the stated claim. \square

Appendix B

List of Notation

Basic notation

\mathbb{N}	Natural numbers
\mathbb{N}^d	Set of all d -dimensional vectors with natural numbers as entries
\mathbb{R}	Real numbers
\mathbb{R}^d	d -dimensional Euclidean space
\mathbb{Z}^d	Integer lattice
\mathbb{S}^k	k -dimensional unit sphere
$\mathcal{B}(\mathbb{R}^d)$	Borel- σ -algebra of \mathbb{R}^d
$H_{p_K^{(i)}}, H_v, H$	Hyperplanes
K	Convex set $K \subset \mathbb{R}^d$
e_1, \dots, e_d	Canonical vectors in \mathbb{R}^d
φ, ϑ	Angles
$R, R_x, \bar{R}, \bar{R}_x$	Rectangles
\mathcal{C}^d	Space of convex bodies in \mathbb{R}^d with the Hausdorff metric
$\text{conv}(A)$	Convex hull of $A \subset \mathbb{R}^d$
$\text{diam}(K)$	Classical Euclidean diameter of a set $K \subset \mathbb{R}^d$
$\text{Dist}(A, B)$	Hausdorff distance between $A, B \subset \mathbb{R}^d$
$\angle(x, y)$	The angle between vectors $x, y \in \mathbb{R}^d$
$P_H(B)$	Orthogonal projection of a set $B \subset \mathbb{R}^d$ onto a hyperplane H
$P_{v,w}^z(A)$	Orthogonal projection onto hyperplane that includes z and is perpendicular to $v-w$
rot_ϑ	Rotation concerning $\vartheta \in \mathbb{S}^{d-1}$

$\text{rot}_{x,y}$	Special kind of rotation defined by $x, y \in \mathbb{R}^d$
$\mathbb{1}_A$	indicator function
$a + K$	Set K shifted via $a \in \mathbb{R}^d$, i.e. $\{x \in \mathbb{R}^d \mid x = (a + y), \text{ for } y \in K\}$
rK	Blow-up of a set K by a factor $r > 0$, i.e. $rK := \{rx : x \in K\}$
T_x	Translation in \mathbb{R}^d concerning $x \in \mathbb{R}^d$
$ x - y $	Euclidean distance for $x, y \in \mathbb{R}^d$, i.e. $\sqrt{\sum_{i=1}^d x^{(i)} - y^{(i)} ^2}$, while $ a $ is the absolute value for $a \in \mathbb{R}$
$ x _1$	1-norm, i.e. $\sum_{i=1}^d x^{(i)} $
$\rho_{x,y}$	Orientation of the vector $x - y$
$\bar{L}, \lceil x \rceil$	Rounding up of $L \in \mathbb{R}$ resp. of $x \in \mathbb{R}$
$B_r(x)$	Ball of radius $r > 0$ around $x \in \mathbb{R}^d$, i.e. $\{y \in \mathbb{R}^d \mid x - y < r\}$
$\text{Vol}(C)$	Volume/ d -dimensional Lebesgue measure of the set C
λ	d -dimensional Lebesgue measure
λ_{d-1}	$(d - 1)$ -dimensional Lebesgue measure

Measures, random objects

\mathcal{X}	Poisson point process corresponding to the Poisson-Boolean model on \mathcal{S}
\mathcal{S}	$\mathbb{R}^d \times (\mathcal{C}^d \times \mathbb{R}^d)$
\mathcal{P}	Poisson point process of the locations
\mathcal{P}_0	Palm version of a Poisson point process
u	Intensity of the underlying Poisson point process of the locations
\mathbb{P}	Probability measure
\mathbb{P}_A	Law of \mathcal{X} under the condition $A \in \mathcal{P}$ with $A = \{x_1, \dots, x_n\} \subset \mathbb{R}^d$, i.e. the palm version
\mathbb{E}	Expectation corresponding to \mathbb{P}
\mathbb{E}_x	Expectation under \mathbb{P}_x for $x \in \mathcal{P}$
C	Random convex body with rotation invariant distribution

\tilde{C}_x	i.i.d. copy of C for $x \in \mathcal{P}$
C_x	Convex body shifted via its location, i.e. $C_x := x + \tilde{C}_x$
\mathbb{P}_C	Law of C
\mathcal{C}	Union of convex bodies, i.e. $\bigcup_{x \in \mathcal{P}} C_x$
$D_C^{(1)}, \dots, D_C^{(d)}$	Diameters of a convex body C
$D_x^{(1)}, \dots, D_x^{(d)}$	Diameters of C_x
$p_C^{(1)}, \dots, p_C^{(d)}$	Orientations of $D_C^{(1)}, \dots, D_C^{(d)}$
$p_x^{(1)}, \dots, p_x^{(d)}$	Orientations of $D_x^{(1)}, \dots, D_x^{(d)}$

Graph theory

$\mathcal{G} = (\mathcal{P}, \mathcal{E})$	Graph \mathcal{G} with vertex set \mathcal{P} and edge set \mathcal{E}
$\mathcal{G} = (\mathcal{V}, \mathcal{E})$	Graph \mathcal{G} with vertex set \mathcal{V} and edge set \mathcal{E}
$\mathcal{G}_u^b, \mathcal{G}_u^r$	Graph with underlying vertex intensity ub resp. ur
$C_\infty, C_\infty^b, C_\infty^r$	Unbounded connected component of \mathcal{G} resp. \mathcal{G}_u^b resp. \mathcal{G}_u^r
$\mathbf{x} \sim \mathbf{y}$	Vertices \mathbf{x} and \mathbf{y} are connected by an edge
$x \stackrel{n}{\sim} y$	Vertices \mathbf{x} and \mathbf{y} are connected via a path of length $n \in \mathbb{N}$
$\mathbf{x} \leftrightarrow \mathbf{y}$	Vertices \mathbf{x} and \mathbf{y} are connected via a path
$\text{dist}(\mathbf{x}, \mathbf{y})$	Chemical distance of two vertices \mathbf{x}, \mathbf{y}
$\theta, \theta_u, \theta_b$	Percolation probability

Others

$\alpha, \alpha_i, \gamma_i, \beta_i$	Model parameters
ϵ	Radius of the ball that is almost surely included in C
ε	Constant appearing from Potter bounds
\mathcal{M}	$\{k \in \{1, \dots, d-1\} : \alpha_k \in (k, \min\{2k, d\})\}$
κ	$\operatorname{argmax}_{s \in \mathcal{M}} \frac{\min\{d-s, s\}}{\alpha_s - s}$
$(f_n)_{n \in \mathbb{N}}, (\tilde{f}_n)_{n \in \mathbb{N}}$	Threshold sequences (on page 25, on page 32)
$(A_n)_{n \in \mathbb{N}}, (\bar{A}_n^x)_{n \in \mathbb{N}}, (\underline{A}_n^x)_{n \in \mathbb{N}}$	Sequences of events (on page 27, on page 57)

Bibliography

- [1] Aizenman, M., H. Kesten, und C. M. Newman. “Uniqueness of the Infinite Cluster and Continuity of Connectivity Functions for Short and Long Range Percolation.” *Communications in Mathematical Physics* 111.4 (1987): 505–531.
- [2] Antal, P., und A. Pisztora. “On the Chemical Distance for Supercritical Bernoulli Percolation.” *The Annals of Probability* 24.2 (1996): 1036–1048.
- [3] Bingham, N. H., C. M. Goldie, und J. L. Teugels. “Regular Variation.” Vol. 27. *Cambridge University Press* (1989).
- [4] Biskup, M. “On the Scaling of the Chemical Distance in Long-Range Percolation Models.” *Annals of Probability* 32.4 (2004): 2938–2977.
- [5] Bringmann, K., R. Keusch, und J. Lengler. “Sampling Geometric Inhomogeneous Random Graphs in Linear Time.” *Leibniz International Proceedings in Informatics* 87 (2017): 20:1–20:15.
- [6] Broadbent, S. R., und J. M. Hammersley. “Percolation Processes: I. Crystals and Mazes.” *Mathematical Proceedings of the Cambridge Philosophical Society* 53.3 (1957): 629–641.
- [7] Broman, E. I. “Higher-Dimensional Stick Percolation.” *Journal of Statistical Physics* 186.1 (2022): 1–32.
- [8] Černý, J., und S. Popov. “On the Internal Distance in the Interlacement Set.” *Electronic Journal of Probability* 17 (2012): Paper No.47, 1–27.
- [9] Chebunin, M., und G. Last. “On the Uniqueness of the Infinite Cluster and the Cluster Density in the Poisson Driven Random Connection Model.” arXiv:2403.17762 (2024).
- [10] Duminil-Copin, H. “Introduction to Bernoulli Percolation.” Lecture Notes (2018).

- [11] Damron, M., J. Hanson, und P. Sosoe. “On the Chemical Distance in Critical Percolation.” *Annals of Probability* 45.4 (2017): 1006–1034.
- [12] Dereich, S., C. Mönch, und P. Mörters. “Typical Distances in Ultra-small Random Networks.” *Advances in Applied Probability* 44.2 (2012): 583–601.
- [13] Durrett, R. “Random Graph Dynamics.” Vol. 20. *Cambridge University Press* (2010).
- [14] Drewitz, A., B. Ráth, und A. Sapozhnikov. “On Chemical Distances and Shape Theorems in Percolation Models with Long-Range Correlations.” *Journal of Mathematical Physics* 55.8 (2014): 083701.
- [15] Fischer, G. “Lineare Algebra: Eine Einführung für Studienanfänger.” 14th ed., *Vieweg* (2003).
- [16] Franceschetti, M., M. D. Penrose, und T. Rosoman. “Strict Inequalities of Critical Values in Continuum Percolation.” *Journal of Statistical Physics* 142.2 (2011): 460–486.
- [17] Freyer, A., und E. Lucas. “Interpolating Between Volume and Lattice Point Enumerator with Successive Minima.” *Monatshefte für Mathematik* 198.4 (2022): 717–740.
- [18] Garet, O., und R. Marchand. “Asymptotic Shape for the Chemical Distance and First-Passage Percolation on the Infinite Bernoulli Cluster.” *ESAIM: Probability and Statistics* 8 (2004): 169–199.
- [19] Garet, O., und R. Marchand. “Large Deviations for the Chemical Distance in Supercritical Bernoulli Percolation.” *The Annals of Probability* 35.3 (2007): 833–866.
- [20] Gilbert, E. N. “Random Plane Networks.” *SIAM Journal on Applied Mathematics* 9.4 (1961): 533–543.
- [21] Gomes, P. A., A. Pereira, und R. Sanchis. “Upper Bounds for Critical Probabilities in Bernoulli Percolation Models.” arXiv:2106.10388 (2021).
- [22] Gouéré, J. B. “Subcritical Regimes in the Poisson Boolean Model of Continuum Percolation.” *The Annals of Probability* 36.4 (2008): 1209–1220.

- [23] Gouéré, J. B., und F. Labey. “Percolation in the Boolean Model with Convex Grains in High Dimension.” *Electronic Journal of Probability* 28 (2023): 1–57.
- [24] Gracar, P., A. Grauer, und P. Mörters. “Chemical Distance in Geometric Random Graphs with Long Edges and Scale-Free Degree Distribution.” *Communications in Mathematical Physics* 395.2 (2022): 859–906.
- [25] Gracar, P., M. Korfhage, und P. Mörters. “Robustness in the Poisson Boolean Model with Convex Grains.” arXiv:2410.13366 (2024).
- [26] Gracar, P., und M. Korfhage. “Chemical Distance in the Poisson Boolean Model with Regularly Varying Diameters.” arXiv:2503.18577 (2025).
- [27] Gracar, P., L. Lühtrath, und C. Mönch. “Finiteness of the Percolation Threshold for Inhomogeneous Long-Range Models in One Dimension.” arXiv:2203.11966 (2022).
- [28] Gracar, P., L. Lühtrath, und P. Mörters. “Percolation Phase Transition in Weight-Dependent Random Connection Models.” *Advances in Applied Probability* 53.4 (2021): 1090–1114.
- [29] Grimmett, G. “Percolation.” *Springer*, Berlin Heidelberg (1999).
- [30] Grimmett, G. R., und J. M. Marstrand. “The Supercritical Phase of Percolation Is Well Behaved.” *Proceedings of the Royal Society of London. Series A* 430.1879 (1990): 439–457.
- [31] Hall, P. “On Continuum Percolation.” *The Annals of Probability* 13.4 (1985): 1250–1266.
- [32] Hao, N., und M. Heydenreich. “Graph Distances in Scale-Free Percolation: The Logarithmic Case.” *Journal of Applied Probability* 60.1 (2023): 295–313.
- [33] Hara, T., und G. Slade. “Mean-Field Critical Behaviour for Percolation in High Dimensions.” *Communications in Mathematical Physics* 128.2 (1990): 333–391.
- [34] Hilário, M., und D. Ungaretti. “Euclidean and Chemical Distances in Ellipses Percolation.” arXiv:2103.09786 (2021).

- [35] Hirsch, C., und C. Mönoch. “Distances and Large Deviations in the Spatial Preferential Attachment Model.” *Bernoulli* 26.2 (2020): 927–947.
- [36] Hug, D., G. Last, und W. Weil. “Boolean Models.” arXiv:2308.05861 (2023).
- [37] Jahnel, B., L. Lühtrath, und M. Ortgiese. “Cluster Sizes in Subcritical Soft Boolean Models.” arXiv:2404.13730 (2024).
- [38] Kendall, M. G. “A Course in the Geometry of N Dimensions.” *Courier Corporation* (2004).
- [39] Kulik, R., und P. Soulier. “Heavy-Tailed Time Series.” *Springer* (2020).
- [40] Last, G., und M. Penrose. “Lectures on the Poisson Process.” *Cambridge University Press* (2017).
- [41] Last, G., M. D. Penrose, und S. Zuyev. “On the Capacity Functional of the Infinite Cluster of a Boolean Model.” *Annals of Applied Probability* 27.3 (2017): 1678–1801.
- [42] Last, G., F. Nestmann, und M. Schulte. “The Random Connection Model and Functions of Edge-Marked Poisson Processes: Second Order Properties and Normal Approximation.” *Annals of Applied Probability* 31.1 (2021): 128–168.
- [43] Lee, S. N., und M. H. Shih. “A Volume Problem for an N-Dimensional Ellipsoid Intersecting with a Hyperplane.” *Linear Algebra and Its Applications* 132 (1990): 93–102.
- [44] Meester, R., M. D. Penrose, und A. Sarkar. “The Random Connection Model in High Dimensions.” *Statistics & Probability Letters* 35.2 (1997): 145–153.
- [45] Meester, R., und R. Roy. “Continuum Percolation.” Vol. 119. *Cambridge University Press* (1996).
- [46] Milgram, S. “The Small-World Problem.” *Psychology Today* 1 (1967): 61–67.
- [47] Penrose, M. D. “On a Continuum Percolation Model.” *Advances in Applied Probability* 23.3 (1991): 536–556.

- [48] Reitzner, M., M. Schulte, und C. Thäle. “Limit Theory for the Gilbert Graph.” *Advances in Applied Mathematics* 88 (2017): 26–61.
- [49] Roy, R. “Percolation of Poisson Sticks on the Plane.” *Probability Theory and Related Fields* 89.4 (1991): 503–517.
- [50] Roy, R., und H. Tanemura. “Critical Intensities of Boolean Models with Different Underlying Convex Shapes.” *Advances in Applied Probability* 34 (2002): 48–57.
- [51] Sarkar, A. “Continuity and Convergence of the Percolation Function in Continuum Percolation.” *Journal of Applied Probability* 34.2 (1997): 363–371.
- [52] Simon, B. “The Statistical Mechanics of Lattice Gases.” Vol. I. *Princeton University Press* (1993).
- [53] Teixeira, A., und D. Ungaretti. “Ellipses Percolation.” *Journal of Statistical Physics* 168 (2017): 369–393.